THESIS

PRESENTED TO
THE BORDEAUX SEGALEN UNIVERSITY

PRESENTED BY: **JEINNY KARINA VARGAS SANCHEZ**
ENC-NETWORK
ERASMUS MUNDUS PROGRAM

THESIS SUBMITTED
FOR THE DEGREE OF DOCTOR OF PHILOSOPHY
BORDEAUX UNIVERSITY 2

HEALTH AND LIFE SCIENCES DOCTORAL SCHOOL OF BORDEAUX
MENTION: Science, Technology, Health
SPECIALTY: Neuroscience

IN VIVO PEPTIDE BIOMARKER SCREENING FOR MOLECULAR IMAGING IN EAE NEUROINFLAMMATION

THESIS DIRECTED BY

PI: KLAUS G. PETRY, PhD
INSERM U. 1049
UNIVERSITE BORDEAUX SEGALEN (FRANCE)

CO-PI: ELGA DE VRIES, PROFESSOR
BLOOD BRAIN BARRIER AND NEUROINFLAMMATION RESEARCH GROUP
VU. UNIVERSITY MEDICAL CENTER, AMSTERDAM (NL)

THESIS EXAMINED The December 6th, 2013.

BY THE EXAMINATION COMMITTEE COMPOSED OF

Mrs. DUPPLA-COUFFINHAL Cécile	Research director, INSERM U. 441	Jury President
Mrs. ANDRIEUX Karine	Professor, Paris Descartes University	Reporter
Mr. HUNOT Stephane	Research director, ICM-Institute	Reporter
Mr. PETRY Klaus G.	Research director, INSERM U. 1049	Thesis Director

THÈSE

PRÉSENTÉE à

L' UNIVERSITE BORDEAUX SEGALEN

PRÉSENTÉE PAR: **JEINNY KARINA VARGAS SANCHEZ**
ENC-NETWORK
ERASMUS MUNDUS PROGRAM

THESE SOUMISE
POUR LE DEGRE DE DOCTORAT
UNIVERSITE BORDEAUX 2

ECOLE DOCTORALE SCIENCES DE LA VIE ET DE LA SANTÉ
MENTION: Sciences, Technologie, Santé
SPÉCIALITÉ: Neurosciences

IDENTIFICATION *in vivo* DE BIOMARQUEURS PEPTIDIQUES POUR L'IMAGERIE MOLÉCULAIRE DANS LE MODELE EAE DE NEUROINFLAMMATION

THÈSE DIRIGÉE PAR
PI: KLAUS G. PETRY, DOCTEUR
INSERM U. 1049
UNIVERSITE BORDEAUX SEGALEN (FRANCE)

CO-PI: ELGA DE VRIES, PROFESSEUR
GROUPE DE RECHERCHE DE LA BARRIERE HEMATO-ENCEPHALIQUE ET DE LA NEUROINFLAMMATION
VU. UNIVERSITY MEDICAL CENTER, AMSTERDAM (NL)

Présentée et soutenue le 6 Décembre, 2013

DEVANT LE JURY COMPOSE DE:

Mme. DUPPLA-COUFFINHAL Cécile	Directeur de recherche INSERM U. 441	Présidente du Jury
Mme. ANDRIEUX Karine	Professeur, Université Paris Descartes	Rapporteur
M. HUNOT Stephane	Directeur de recherche, Institute-ICM	Rapporteur
M. PETRY Klaus G.	Directeur de recherche, INSERM U. 1049	Directeur de thèse

ACKNOWLEDGMENT

To the Erasmus Mundus Joint Doctorate (EMJD) program for the opportunity to continue my formation as a researcher in a PhD program and to award to me the scholarship to realize my PhD here in Europa.

To ENC-Network program specially to the scientific director Arjen BRUSSAARD and the general manager Maaike LEUSDEN from Neuroscience Campus Amsterdam, also to Christophe MULLE scientific coordinator and Laurie FRANCOIS project manager from Bordeaux Segalen University and Bordeaux Neuroscience Institute for their excellent mission to achieve through transdisciplinary approaches to allow the formation of new generations of neuroscientists across Europe, giving the opportunity to young researchers from around the world to be enrolled in this program.

To the Bordeaux Segalen University (France) and VU university medical center (Amsterdam, NL), for having me as a pupil enrolled in the PhD program.

Specially thanks to the Mrs. Delphine PERRIN and her team for their excellent administrative job of the student management in the doctoral school of Bordeaux University.

To the president of the jury Mrs. DUPPLA-COUFFINHAL Cécile and the jury members Mrs. ANDRIEUX Karine and Mr. HUNOT Stephane who examined in so enriching and constructive my performance in the development of this project.

Especially thanks to Dr. PETRY Klaus G in Bordeaux Segalen University, as a director of this thesis during three years of constant work.

Also, thanks to the Professor Elga DE VRIES in VU University medical center who received me in her lab as co-director to cooperate in the development of this project.

Sincere thanks to the Dr. Claudine BOIZIAU for her excellent and professional direction in my complete training as a researcher, throughout the development of this project and especially for her excellent work as a teacher and friend.

To the Dr. Antoine VEKRIS in Bordeaux Segalen University who formed me and trained me in molecular biology and especially thanks for your help and arduous work in the bioinformatic analysis of the large data packet results obtained in this project, and also thanks to Dr. Macha NIKOLSKI from Bioinformatics Center of Bordeaux (CBiB) for the supporting scientific in the analysis Bioinformatics.

To the Dr. Elodie MORDELET in Bordeaux Segalen University and the technical support of Susanne van DER POL in VU university medical center who trained me in immunohistochemistry and also helped me in the better development of the immunohistochemistry assays.

To Nadège CASSAGNO in Bordeaux Segalen University for her technical support, who trained to me in the histology culture of hCMEC/D3 cells and also who prepared the cells required for the development of this project.

To the CGFB- Functional Genomic Center of Bordeaux for its arduous work of high-throughput sequencing by Next generation sequencing with the samples obtained in this project and Specially thanks to Christophe HUBERT for his work in the sequencing of this sample.

To the Plateforme Protéome Bordeaux and specially thanks to Marc BONNEU, Stephane CHAIGNEPAIN and Stephane CLAVEROL not only for their excellent direction and work in the mass spectrometry analysis, but also for their valuable scientific contribution in the development of this project.

To the Dr. Florence OTTONES, Pr. Vincent DOUSSET, Pr. Bruno BROCHET, Dr. Thomas TOURDIAS, Justine AUSSUDRE, Sylvie AUSSUDRE, Mathilde DELOIRE, Delphine HAMEL and some others for their support, scientific, technical and administrative throughout the development of this project.

And finally infinite thanks to my MOTHER for her support to help me to maintain courage until the end of this project.

SUMMARY

In neurodegenerative disorders like multiple sclerosis, neuroinflammation modifies the blood brain barrier (BBB) status by causing complex cellular and molecular alterations. The characterization of such molecular changes by an *in vivo* labeling approach is most challenging to generate reliable *in vivo* targeting tools and biomarkers. *In vivo* strategies to define such markers are, however, difficult due to the plethora of the accessible target molecules, the vicinity of diseased target expression among healthy tissue and the potentially structural alterations of target molecules when studied by histopathology.

The aim of this work is to streamline the biomarker discovery of pathological molecular tissue alterations by *in vivo* selection of phage displayed peptide repertoires that are further submitted to physical DNA subtraction « PhiSSH » of sequences encoding common peptides in both repertoires (HEALTHY and PATHOLOGY). The strategy of Subtraction allows thus the enrichment of clones specific for one repertoire and is of particular interest for complex repertoires produced by *in vivo* selection.

We present the application of this strategy in the multiple sclerosis rat model, Experimental Autoimmune Encephalomyelitis (EAE) pathology, where target lesions are disseminated in the central nervous system (CNS). Therefore, the repertoire of ligands selected in EAE rats is composed of a mix of ligands specific for inflammatory lesions and of ligands which were selected against non-pathological (healthy) tissue. Two phage display selections were performed in parallel, in EAE and in healthy rats. From these repertoires, a third one was obtained by the subtraction of healthy specific ligands from the EAE repertoire. The efficiency of the subtraction was monitored by massive sequencing of the three repertoires, «EAE», «HEALTHY» and «SUBTRACTION».

More than 95% of the clones common to EAE and Healthy repertoires were shown to be absent from the Subtraction repertoire. A set of randomly chosen clones and synthesized peptides from the EAE and subtraction repertoires were tested for differential labeling of a) diseased and healthy animal tissues and b) an *in*

vitro BBB model, in (Interleukin-1β) IL-1β challenged and resting control state culture human cells (hCMEC/D3). One of the phage clones and 4 chemically synthesized peptides showed specific binding to brain endothelial cells (EC) in neuro-inflammatory conditions.

Using a strategy of crosslinking of an EAE specific phage clone on protein targets expressed by IL-1ß activated ECs followed by mass spectrometry, we propose hypothetically Galectin-1 as a possible target of this phage.

PhiSSH will be useful for *in vivo* screening of small peptide combinatorial libraries for the discovery of biomarkers specific of molecular and cellular alterations untangled with healthy tissues, as in most pathologies presenting neuroinflammatory activity.

RESUME

Dans les maladies neurodégénératives comme la sclérose en plaques, la neuro-inflammation modifie l'activité de la barrière hémato-encéphalique (BHE) par des altérations cellulaires et moléculaires complexes. La caractérisation de tels changements moléculaires par une approche d'étiquetage *in vivo* justifie la recherche d'outils de ciblage *in vivo* fiables et de biomarqueurs. Les stratégies pour définir *in vivo* ces marqueurs sont cependant compliquées par la pléthore de molécules cibles accessibles, par l'intrication des régions atteintes au sein du tissu sain et par les altérations structurales potentielles des molécules cibles étudiées par histopathologie.

Le but de ce travail est de rationaliser la découverte de biomarqueurs des altérations moléculaires dans les tissus par une stratégie de sélection *in vivo* de répertoires de phages présentant des peptides à leur extrémité (phage display), les ligands présents dans les deux répertoires (sain et pathologique) étant ensuite soustraits physiquement. Cette stratégie de soustraction « PhiSSH » permettant d'enrichir un répertoire en ligands spécifiques est d'un intérêt majeur dans le cas de répertoires complexes tels ceux obtenus dans des sélections *in vivo.*

Nous présentons l'application de cette stratégie dans le modèle de rat de la sclérose en plaques, l'Encéphalomyélite Autoimmune Expérimentale (EAE), où les lésions disséminées dans le système nerveux central engendrent la sélection d'une grande quantité de clones s'associant au tissu sain, par comparaison avec les rats témoins en bonne santé. L'efficacité de la technique de soustraction a été contrôlée par séquençage massif des trois repertoires, «EAE», «SAIN», et «SOUSTRACTION».

Plus de 95 % des clones communs aux répertoires EAE et contrôle sont absents du répertoire de la soustraction. Un ensemble de clones de phages et des peptides synthétisés chimiquement dessinés après l'analyse bioinformatique du répertoire de soustraction ont été testés a) sur des tissus de rats EAE et sains et b) sur des cellules humaines en culture (hCMEC/D3) constituant un modèle de BHE, dans des conditions inflammatoires, (activation IL-1ß) ou non activées. Un des

clones et quatre peptide testés ont montré une association spécifique sur les cellules endothéliales de BHE dans des conditions neuro-inflammatoires.

Pour identifier la cible d'un phage spécifique des lésions neuro-inflammatoires, nous avons mis en œuvre un procédé de création de liaison covalente entre ce phage et les protéines exprimées par des cellules de BHE cultivées en présence d' IL-1ß, puis effectué une analyse par spectométrie de masse. La galectine-1 est apparue comme une cible potential de ce phage.

La découverte de biomarqueurs spécifiques de modifications moléculaires et cellulaires de régions inflammatoires disséminées dans les tissus sains, comme c'est le cas dans la plupart des pathologies présentant une activité neuro–inflammatoire, sera facilitée par l'utilisation de la stratégie de soustraction PhiSSH décrite dans ce document.

CONTENTS

List of Figures

List of Tables

List of annexes

ABBREVIATIONS

AA	Arachidonic acid
ACs	Astrocytes
AD	Alzheimer's disease
AP-2	Adaptor complex
APCs	Antigen presenting cells
BBB	Blood brain barrier
BL	Basal lamina
BM	Membrane compounds
cAMP	Cyclic adenosine monophosphate
CAMs	Cell adhesion molecules
CAV	Caveolin proteins
CNS	Central nervous system
CT	Computed X-ray tomography
CXCL	Chemokine (C-X-C motif) ligand
EAE	Experimental autoimmune encephalomyelitis
EC	Endothelial cells
ECM	Extracellular matrix
G-CSF	Granulocyte colony-stimulating factor
GLUT	Glucose transporters
GM-CSF	Granulocyte monocyte-colony stimulating factor
ICAM	Intercellular adhesion molecules
ICS	Clinically isolated syndrome
IFN-γ	Interferon gamma
IL-1ß	Interleukin-1 ß
JAMs	Junctional adhesion molecules
LFA-1	Lymphocyte function-associated antigen 1
MAG	Myelin-associated glycoprotein
MBP	Myelin basic protein
MCP-1	Monocyte chemo attractant protein-1
MHC	Major histocompatibility complex
MIP-1	Macrophage inflammatory protein-1
MOG	Myelin oligodendrocyte glycoprotein
MPIOs	Micron-sized particles of iron oxide

MRI	Magnetic resonance imaging
MS	Multiple sclerosis
NO	Nitric oxide
NOS	Nitric oxide synthase
NGS	Next generation sequencing
NVU	Neurovascular unit
OVA	Ovalbumin
PCs	The pericytes
PD	Parkinson's disease
PDGFb	Platelet-derived growth factor subunit B
PET	Positron emission tomography
PKA	Protein kinase A
PKC	Protein kinase C
PLC	Phospholipase C
PLP	Proteolipid protein
PLP	Proteolipid protein
PPMS	Primary progressive MS
PVM	Perivascular macrophages
ROS	Reactive oxygen species
RRMS	Relapsing-remitting MS
SIP	Sphingosine-1 phosphate
SLC	Solute carriers transporters
SPECT	Single-photon emission computed tomography
SPIOs	Small particles of iron oxide
SPMS	Secondary progressive MS
TGFβ	Transforming growth factor
TJs	Tight junctions
TNF	Factor de necrosis tumoral
VCAM-1	Vascular cell adhesion molecule-1
VEGF	Vascular endothelial growth factor
VLA	Very late antigen
WM	White matter
WT	Wild type
ZO	Zonula occludens proteins

0. OVERVIEW OF THE RESEARCH TOPIC

The present work aims to identify molecular alterations of the neurovascular unit (NVU) in neuroinflammation conditions as it is observed in the experimental model of multiple sclerosis. The study is mainly focused on the ECs forming the BBB and their molecular alterations during the neuroinflammation process. The *in vivo* application of phage displayed peptide ligands was used to screen molecular alterations in neuroinflammation and was further developed by generating the physical DNA subtraction of phage displayed peptide repertoires selected from EAE pathology against healthy controls. The *in vitro* BBB model allowed further investigation of neuroinflammation induced molecular alterations of the BBB. I will thus introduce first the topics of the BBB, second the relevance of the BBB studies in multiple sclerosis (MS) based on the Experimental Autoimmune Encephalomyelitis animal model (EAE) and third the technical approach of phage display that was used to select potential biomarkers of neuroinflammatory conditions.

1. INTRODUCTION

BBB is formed by tight junctions (TJs) between the capillary ECs. It is the principal barrier separating the parenchyma of the CNS from blood circulation. The main function of the BBB is to maintain a system isolated from the free flow of the blood hydrophilic components into the brain parenchyma, by regulating the entry of toxins, macromolecules, ions and immune cells, that alter the normal homeostasis and neural functions.

For reasons that are still not well understood, immune cells infiltrating into the brain parenchyma may insult the BBB. This event has been associated with down regulation of tight junction components and up regulation of major histocompatibility complex (MHC), cell adhesion molecules (CAMs) and chemokines by BBB ECs, therefore facilitating the leukocyte extravasation from the blood into the brain parenchyma. Thereby it has been described that during brain insults such as trauma, stroke, ischemia, etc., the microglial cells and perivascular cells become activated as antigen presenting cells APCs, which induce changes in the BBB endothelial cells (ECs), altering the barrier integrity. Most of the investigations have been aimed at understanding how the BBB interacts with the surrounding environment in healthy and disease conditions.

In diseases such as multiple sclerosis (MS), which is characterized by demyelination and axonal damage of the CNS, the immune cells (T lymphocytes, monocytes, dendritic cells and NK cells) in the blood circulation, are major actors in the pathological process. The mechanisms inducing the T lymphocyte activation for specific recognition of brain components and their extravasation across the BBB are however, still not completely understood.

Experimental animal models of MS, have thus been developed in which the BBB responds to a variety of factors that can alter the normal structure, function and permeability of the barrier. Such experimental tools are important to develop new therapeutic strategies.

EAE animal model mimics several aspects of MS by displaying the invasive process of infiltrating immune cells into the brain parenchyma as well as many of the immunological alterations and the neurological handicap of MS disease.

MS, but also many other neurodegenerative disorders of the CNS, neuroinflammation modifies the BBB activity by causing complex cellular and molecular alterations. The characterization of such molecular changes by an *in vivo* labeling approach is most challenging to generate reliable *in vivo* targeting tools and biomarkers. Those strategies to define such markers are, however, hampered by the plethora of the accessible target molecules, the vicinity of diseased target expression among healthy tissue and the potentially structural alterations of target molecules when studied by histopathology.

Therefore, it has become necessary to develop new tools to identify pathological molecular tissue alterations. In this way the use of phage display selection has emerged to identify *in vivo* protein ligands and recognition sites. In order to develop these selective markers that bind *in vivo* to differentially expressed targets at the BBB surface during acute neuroinflammation an EAE rat model of MS, we screened a phage-displayed peptide library of randomized peptides of 12 amino acids. We identified several peptides that target the BBB ECs at the level of CNS tissue inflammation. The identified peptide ligands were also tested in an *in vitro* BBB cell culture model, which is exposed to activation conditions *vs* controls to reveal the specific binding.

1.1. Blood Brain Barrier

The CNS is protected from changes in the blood because of the presence of the BBB and the blood–cerebrospinal fluid barrier (BCSFB) (**Abbott et al., 2010; Weksler et al., 2005**). The BBB is mainly formed by ECs of micro vessels bathing the neural tissue, and BCSFB by choroid plexus epithelial cells into the brain ventricular system and arachnoid membrane enveloping the brain (**Abbott et al., 2010; Engelhardt and Sorokin, 2009**). In both cases, the barriers are sustained by TJs between ECs of the BBB or between epithelial cells of the BCSFB (**Engelhardt and Ransohoff, 2012**).

The formation of TJs at BBB ECs in addition to low pinocytic activity enables the BBB to control or even prevent the paracellular flux into the brain parenchyma of either molecular (ions, macromolecules, polar substances neurotoxins and neurotransmitters) and cellular agents (immune cells) that could affect the homeostasis of neural microenvironment (**Abbott et al., 2010; Luissint et al., 2012**). However, BBB ECs can be permeable to hydrophilic nutrients via specific transporters to ensure the constant supply of these molecules and maintain the normal neural functions (**Engelhardt and Sorokin, 2009**).

The BBB ECs are, on their abluminal side, surrounded by pericytes (PCs) embedded in the basal membrane, the end feet of astrocytic glial cells, microglia and neuronal terminals (**Fig. 1**). All together these elements constitute the NVU, maintain the function and development of BBB by regulating the expression and formation of the TJ proteins and specific transporter proteins in the endothelial membrane (**Luissint et al., 2012**).

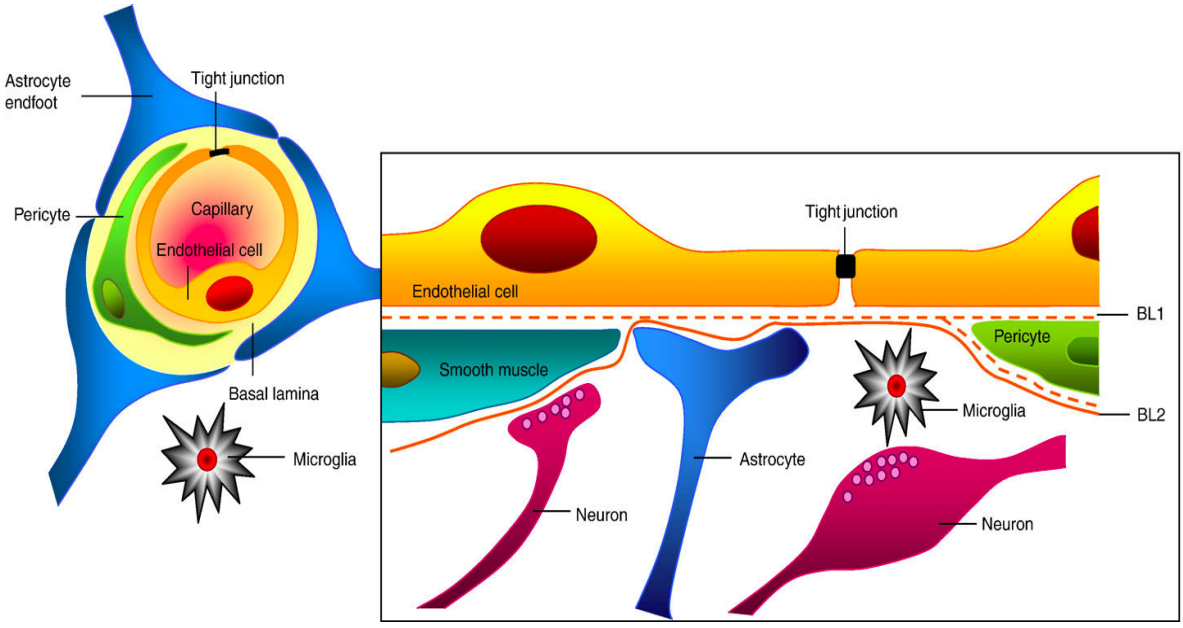

Fig. 1. The microenvironment of BBB: The BBB is a complex system formed by ECs connected by TJs to control the paracellular diffusion across them. Pericytes are embedded along the basement membrane forming the extracellular matrix (ECM) (basal lamina-1, (BL1)) of capillary endothelium. The feet of astrocytes (ACs) surround the capillaries lying on their own ECM (BL2). The neuronal axons secrete arteriolar smooth muscle vasoactive neurotransmitters and peptides to regulate the BBB permeability. All the cells in association with the BBB maintain the barrier properties. **Based on Abbott et al., 2006**.

1.2. Tight Junctions

BBB ECs are linked by an intercellular junctional complex forming TJs. They are composed of integral membrane proteins (occludin, claudins) and junctional adhesion molecules (JAMs), which through their C-terminal region are connected directly with cytoplasmic proteins such as zonula occludens proteins (ZO-1, ZO-2, ZO-3) (**Wolburg et al., 2002**). Altogether, this complex of proteins scaffolding sustains the direct interaction between TJs proteins and the actin cytoskeleton (**Luissint et al., 2012; Ebnet et al., 2003**) (**Fig. 2**).

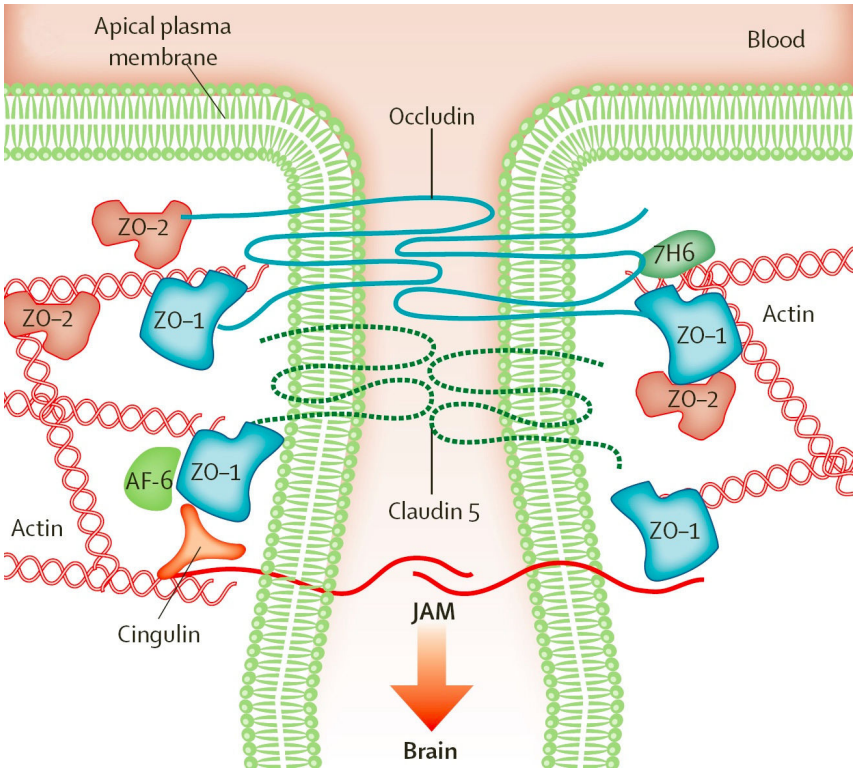

Fig. 2. Tight Junctions: Claudins, Occludin and JAMs proteins form the TJs between BBB ECs. TJ proteins are associated with ZO scaffold proteins on the cytoskeleton actin strands. **Based on Neuwelt et al., 2008**.

Claudins interacts for the assembly of the BBB. Members 3 and 5 are specifically expressed in the brain forming TJs of the capillary ECs and their depletion in mice and cultured human brain ECs induces the disruption of the BBB (**Nitta et al., 2003; Ohtsuki et al., 2007; Luissint et al., 2012**). In contrast, occludin-deficient mice are capable to develop TJs suggesting that occludin is not essential to maintain the integrity of the BBB (**Engelhardt and Sorokin, 2009; Luissint et al., 2012**).

The association of ZO-1, ZO-2, and ZO-3 proteins with claudins and occludins allows activating the interaction with several signalling proteins downstream to modulate the cytoskeleton organization and finally the TJ stability (**Huber et al., 2001**).

Extracellular factors can also affect the stability of the BBB. For example, vascular endothelial growth factor (VEGF) induces barrier disruption by direct effect on TJ molecules or on downstream associated proteins. As shown by different reports, the occludin phosphorylation induced by VEGF-R binding, was directly related to TJ opening and increased permeability of the capillary brain barrier during angiogenesis (**Murakami et al., 2009**).

In this framework, all the changes to which the TJ molecules may be exposed from extra or intracellular milieu can affect directly the actin cytoskeleton organization and finally will be reflected by changes in the BBB permeability and possible cellular extravasation affecting the BBB integrity and brain function.

1.3. Transport at Blood Brain Barrier

BBB ECs express a wide transport system to allow the entry of nutrients into the brain parenchyma, to regulate the ion exchange, maintaining the brain homeostasis and to expel toxins that can affect the brain function (**Chen and Liu, 2012**).

The transport systems include solute carriers (nutrient transport), ATP binding transporters (ABC transporters), ion pumps (ATPase), ion channels and water channels and families of drug efflux transport proteins (drugs, toxins, metabolites or dietary toxins).

1.3.1. Solute carrier transporters

The superfamily of solute carrier transporters (SLC) consists of 43 subfamilies of transporter proteins. They act as ion-coupled transporters, facilitated transporters or exchangers (**Wolburg and Lippoldt, 2002**).

Glucose, amino acids, nucleosides, fatty acids, minerals and vitamins are distributed into the brain through (SLC) transporters. The glucose, for example being the principal energy source of the brain is transported by two types of glucose transporters (GLUT) Na^+ independent and Na^+ dependent classified in the solute carrier family (SLC2/GLUT and SLC5/ SGLT) (**Nies, 2007**).

Amino acids are also transported through brain endothelium by carriers SLC families, which are Na^+ independent Na^+ dependent and Na^+/Cl^- dependent, establishing selective differences between neutral, cationic or anionic amino acids (**Nies, 2007**). In addition, peptides being important neuromodulators and even regulating the BBB permeability are also transported by another family of proton dependent SLCs. This facilitates the transport of short peptides and probably peptide mimicking antibiotics, enzyme, and antiviral drug among others (**Nies, 2007**).

The purine and pyrimidine nucleosides and nucleotides are signaling molecules modulating brain vascular functions by interaction with specific brain receptors. Considering that brain cells are incapable to synthesize themselves the nucleosides, these have to be transported into the brain by a specialized transport system (**Parkinson et al., 2011**). The nucleosides are transported bidirectionally by chemical gradients or unidirectionally by Na^+ independent and Na^+ dependent transporters, which form part of the SLC family (SLC28 and SLC29) (**Nies, 2007**).

Due to the negative charge of the BBB, the transport of anionic molecules is restricted; thereby BBB ECs expresses organic anion transporting polypeptides (OATP1A2, SLCO1A2), organic anion transporters (OAT3, SLC22A8) and organic cation/carnitine transporters (OCTN2, SLC22A3) (**Gao et al., 2000; Kusuhara and Sugiyama, 2005**).

1.3.2. ABC Transporters

ABC transporters are a superfamily comprising actually 49 members known, which are classified into seven subfamilies including ABCA, ABCB, ABCC, ABCD, ABCE, ABCF, and ABCG (**Hediger et al., 2004; Dean et al., 2001; Borst and Elferink, 2002**). They use the energy of ATP hydrolysis to activate the transport of

substrates (metabolites, peptides, lipids, cholesterol, drugs and xenobiotics) across the membrane against high concentration gradients (**Löscher and Potschka, 2005; Schinkel and Jonker, 2003**). There are at least 10 members expressed in BBB ECs, which has the main function to restrict the entry of toxins into the brain parenchyma. Thus the BBB presents a specialized drug efflux system of ABC transporters.

P-glycoprotein ABCB1 /P-gp transporters are encoded by Multidrug resistance (MDR) genes. They are the most important drug efflux pumps at BBB, restricting the drug delivery into the CNS. Thus, several studies have shown elevated brain levels of drugs in mdr1 knock-out mice (**Schinkel and Jonker, 2003**). MDR transporters are recognized by their efficient action subtracting more than 50% of drugs through the BBB.

Besides multidrug resistance proteins (MRP, ABCC) represent another subfamily of ABC transporters, which is estimated to subtract about 20% of drug candidates, including anionic to neutral drugs (**Löscher and Potschka, 2005**).

1.3.3. Endocytosis

Although it is well known that vesicular transport or endocytic transport system is restricted through BBB ECs, several reports have shown endocytic pathways allowing the transport of peptides and proteins across the BBB by adsorptive-mediated endocytosis (AME), receptor mediated endocytosis (RME) or transcytosis.

AME is a nonspecific process dependent on the charge, but not on the size of the components to be transported. It is triggered by electrostatic interactions between the positively charged components to be transported and the negatively charged endothelial cell membranes, activating the formation of endocytic vesicles via clarthrin-mediated way. For example Albumin, IgG and histones are transported by AME (**Drin G al., 2002; Xiao and Gan, 2013**).

In contrast RME is a specific process that can take up macromolecules across specific receptors. Thereby peptides and proteins such as insulin, transferrin, and β-amyloid peptides are translocated across the BBB via insulin receptor (IR), transferrin receptor (TfR) and low-density lipoprotein receptor (LDLR) respectively

(**Shibata et al., 2000; Xiao and Gan, 2013**).

Compounds of high molecular weight are translocated also by receptor-mediated transcytosis such as transferrin, insulin and IgA. The receptors-ligands are internalized via clathrin coated vesicles linked to adaptor complex AP-2 in one (luminal) side of the cell membrane and then transcytosed to the other side where the ligands are exported and the receptors are sent back to the luminal surface of the membrane (**Traub, 2003; Kim and Hersh, 2004**).

Endocytosis can also occur by caveolae invaginations in the plasma membrane. The formation of caveolae depends of three caveolin proteins (CAV-1, 2, and 3). CAV-1 and -2 have been detected in the traffic of molecules across BBB (**Virgintino et al., 2002; Gumbleton et al., 2000**).

Several receptors such as MDR-1 P-gp, insulin-like growth factor receptor (IGFR), nitric oxide synthase (NOS), protein kinase C, etc. have been reported to interact with caveolae. In this way it was shown that P-gp contains a Cav-1 binding motif where caveolins have the role to regulate molecular translocation across MDR-1 P-gp transporters (**Jodoin et al., 2003**).

1.4. Molecular components on the BBB abluminal side

BBB ECs rest on a BL (basal lamina) forming the extracellular matrix (ECM), in which the perivascular cells are embedded. The BL consists of a mesh of molecular complex, which stabilizes the communication between ECs and their cellular microenvironment (pericytes and astrocyte end-feet) surrounding the brain parenchyma (**Roberts et al., 2012**). This communication contributes to the reciprocal organization, stability, and differentiation of the BBB and the perivascular cells (**Yurchenco and Patton, 2009**).

The best-characterized basement membrane compounds (BM) forming the ECM include laminins, collagen IV, nidogen, heparan sulfate proteoglycans, agrin and percalan. They establish links with the actin cytoskeleton of ECs by binding to integrins and dystroglycans (**Roberts et al., 2012**) (**Fig. 3**).

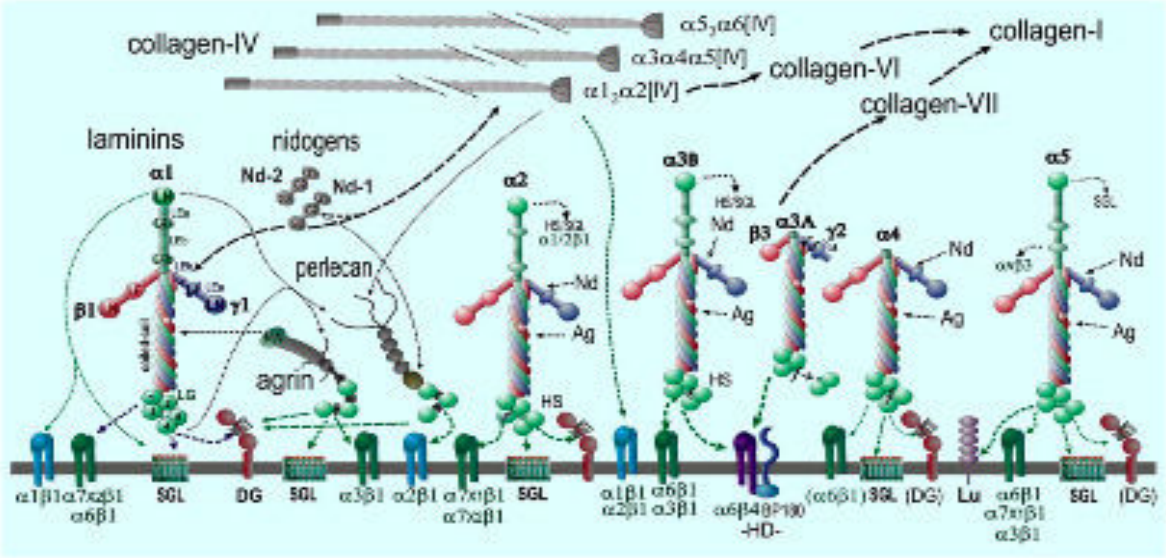

Fig. 3. Basement Membrane Components: Laminins formed by three subunits, collagen type IV heterotrimeric protein formed by **α**12**α**2 [IV], **α**32**α**4 [IV] and **α**52**α**6 [IV] chains. Two nidogen isoforms (Nd1, Nd2), heparan sulphate proteoglycan agrin (Ag) and perlecan (perl). They interact with integrins, **α**-dystroglycan (**α**DG), hemidesmosomal (HD) BP180, sulfated glycolipids (SGL). **Based on Yurchenco et al., 2009**.

The direct interaction between the BM components and the intracellular environment influences also their direct response to changes in the perivascular milieu, through endothelial cell membrane downstream signaling pathways (**Armulik et al., 2010**). For example Agrin and dystroglycan/dystrophin-glycoprotein complex in the BM of BBB are linked to the astrocyte actin cytoskeleton having an effect on the development of the BBB (**Engelhardt, 2011**).

Furthermore the interaction b1-integrin/collagen was shown to maintain claudin-5 localization and thereby the BBB integrity. Also β1-Integrin downstream signaling events mediate association claudin-5 with endothelial actin cytoskeleton to regulate the BBB stability (**Osada et al., 2011; Del Zoppo et al., 2006**).

1.5. Communication between BBB ECs and cellular microenvironment

Development and maintenance of BBB integrity depend on the communication between ECs, surrounding perivascular space and brain parenchyma. Such communication includes actors such as perivascular cells (pericytes, ACs, perivascular macrophage, microglial cells and neurons), which form the NVU. Indeed, the BBB can be regulated in response to different molecular factors

released from surrounding perivascular cells, but also the ECs can have an effect on the development and differentiation of perivascular cells (**Liebner et al., 2011**).

1.5.1. The pericytes

Pericytes (PCs) are contractile cells with a prominent round nucleus and extensions wrapping the ECs. The interconnection between ECs and PCs is mediated by N-cadherin, fibronectin, connexin and various integrins (**Winkler et al., 2011**). In the CNS, PCs are embedded in the BM of BBB ECs where they play an important role in BBB development and sustain (**Krueger and Bechmann, 2010**). PCs are able to induce the formation of a functional BBB during embryogenesis before ACs appears (**Daneman et al., 2010**).

PCs can help the BBB to prevent the flow of harmful components from the blood circulation into the brain parenchyma. Thus, they can contract to open or close the passage of particles (**Dore-Duffy and Cleary, 2011**). It is possible because endothelin-1 receptors are activated on brain PCs to raise the intracellular calcium concentration followed by cellular constriction. This process can be mediated by microfilaments of a smooth muscle-specific isoform of actin (**a**-SMA) and another contraction-related proteins such as tropomyosin and desmin expressed in PCs (**Dalkara et al., 2011**).

PCs express platelet-derived growth factor subunit B (PDGFb) receptors, which are activated by BBB ECs PDGFb released. This interaction is important to ensure the recruitment of PCs on the blood vessels abluminal side and to regulate the BBB permeability. Activation of S1P1 receptor on ECs by sphingosine-1 phosphate (SIP), which is expressed in PCs, may in turn induce N-cadherin and VE-cadherin expression. These cadherins form additional junctional complex between ECs strengthening the BBB functionality (**Krueger and Bechmann, 2010**).

1.5.2. Perivascular Macrophages

The PVM are distinct from brain parenchyma microglia. They are located on endothelial basement membrane of BBB. The PVM are confused also with PCs because both have prolonged cell body but PVM are thinner. Unlike PVM, PCs are

involved in blood flow regulation, while are phagocytic cells in normal physiological situations like the absence of inflammation. PVM can be replaced by monocyte migration derived from bone marrow every 2 to 3 months. They have the ability to recognize, phagocytose, degrade and carry pathogens for presentation to T cells and induce the release of immune mediators. Therefore, they form part of the first innate immune defenses in the brain (**Bechmann et al., 2001; Fabriek et al., 2005**).

Thus PVM expresses pathogen recognition receptors such as CD14, which binds to lipopolysaccharide (LPS) and for presenting to toll-like receptors (TLR). Although TLR and CD14 are co-expressed at the same time, TLR is down regulated in healthy CNS. To support the antigen presentation, PVM express also high levels of CD45 (Leukocyte common antigen LCA), CD40 and major histocompatibility complex (MHC) II and I (**Fabriek et al., 2005**).

1.5.3. Astrocytes

Astrocytes **(ACs)** are classified into two main subtypes of protoplasmic and fibrous ACs. The protoplasmic ones are located within the gray matter, while the fibrous ones are found all throughout white matter. Fibrous AC has long fibers whose feet are connected physically with the capillary walls. Thus a limit is formed between the blood flow and the brain parenchyma (**Sofroniew and Vinters, 2010**). In this context, ACs has been documented to produce regulators of the blood flow, such as prostaglandins (PGE), nitric oxide (NO), and arachidonic acid (AA) (**Gordon et al., 2007; Ladecola et al., 2007**).

ACs are also essential to maintain ionic homeostasis by regulating the pH, input substrates and neurotransmitters into neurons via Na^+/H^+ exchanger, K^+ channels and vacuolar type proton ATPase. Furthermore ACs controls the gradient osmotic pressure in the brain by means the water channel protein aquaporin (AQP), in particular AQP4 (**Wolburg et al., 2011; Sofroniew and Vinters, 2010**). ACs are capable of inducing the expression of TJs molecules and releasing factors regulating BBB permeability via angiogenesis downregulation. Reciprocally ECs may contribute to the differentiation and development of ACs (**Abbott et al., 2006**).

1.5.4. Microglia

Microglial cells are found throughout the CNS parenchyma along white matter (WM) and grey matter. They present a ramified phenotype in normal physiological conditions, but can change their morphology upon activation induced by an insult to the parenchyma, to become round cells, what facilitates their migration. Microglial cells are down regulated in the CNS parenchyma and hardly express MHC molecules in healthy CNS (**Kierdorf and Prinz, 2013; Hanisch and Kettenmann, 2007**). In addition, they can regulate the activation of inflammatory conditions by expressing inhibitor receptors like CD200R whose ligand is expressed by neurons. Once the interaction ligand-receptor is giving the microglial cells are kept in the resting ramified phenotype of the health conditions (**Ransohoff and Perry, 2009; Linnartz and Neumann, 2013**).

Microglia express cytokine receptors, scavenger receptors, chemokine receptors (CX3CR1), which enable them to survive and communicate with other glial cells and neurons (**Tang et al., 2014**). Upon pathogen insult to the CNS parenchyma, they become activated and release molecular effectors that recruit immune cells and control the infection. Consequently, they become able to phagocytose pathogens and present antigens to immune cells (**Saijo and Glass, 2011**). In contrast microglia control the tissue damage through the production of anti-inflammatory molecules and assisting tissue regeneration after insult (**Neumann et al., 2008**).

1.6. Luminal side on BBB and brain Immune surveillance

As has been commonly accepted, the BBB normally restricts the passage of immune cells into the brain parenchyma, which rests in an isolated immunological state, given that it lacks afferent lymphatic vessels, which is a prerequisite for establishing a channel of communication with the immune system (**Becher et al., 2006**).

However a low number of immune cells ($CD4^+$, $CD8^+$) can cross the BBB into the perivascular space to allow the immunosurveillance of the CNS in normal physiological conditions (**Konsman et al., 2007**).

Thus lymphocytes can breach the BBB to survey into the brain and to eliminate any intruders. Otherwise, if are not activated by antigen recognition they can leave the brain parenchyma without any repercussion to the brain (**Engelhardt and Coisne, 2011**).

For still unknown mechanisms, T cells can turn their attack against cells that normally inhabit within the CNS, which allows the invasion of immune cells to sustain a chronic inflammatory response, as is the case in certain neuroinflammatory diseases such as multiple sclerosis. The mechanisms used by the immune cells to cross the BBB differ between healthy and disease conditions (**Kleine and Benes, 2006**).

The recruitment of immune cells through the BBB is mediated by lymphocyte adhesion on the ECs surface (**Ley et al, 2007; Steiner et al., 2010**). Thus P and E selectins are necessary for the recruitment of lymphocytes in the first step by inducing their rolling along the ECs surface. However, in healthy conditions, these selectins do not appear at the ECs membrane of the BBB, but instead the immune reactive JAMs are found able to capture lymphocytes T, B and NK cells (**Kleine and Benes, 2006**).

The lymphocyte-endothelium interaction is established and reinforced by intercellular adhesion molecules (ICAM) depending on activated BBB ECs. In consequence the ICAM-2 expression is increased more than that ICAM-1 expression, which appears in resting BBB ECs at low level. However ICAM-1 is also upregulated during inflammation in response to cytokines, hormones, virus or cellular stress (**Greenwood et al., 2011**). Furthermore vascular cell adhesion molecule-1 (VCAM-1), and PECAM-1 appears also to recruit lymphocytes on BBB activated ECs (**Kleine and Benes, 2006**).

Finally, when T cells are activated by recognizing their antigen, they release effector signals (mediated by cytokines) to induce the BBB activation, which allows opening of the TJs and the transmigration of more immune cells. In addition, the interaction of T cells with BBB ECs induces their proliferation, which triggers a proinflammatory state (**Loeffler et al., 2011**).

2. BBB in neuroinflammation

During inflammatory conditions the transmigration of immune cells across the activated BBB is mediated by CAMs, and chemokines on the EC surface, which bind to their specific receptors on the immune cells. CAMs allow firm attachment of the leukocytes on EC mediated by lymphocyte function-associated antigen 1 (LFA-1) and very late antigen (VLA-4) resulting in the formation of a high-affinity binding to ICAM-1 and VCAM-1, respectively (**Enzmann et al., 2013**). Once the T-cells are arrested to the BBB endothelium they may follow the chemokine gradient induced on the capillary walls. The expression of chemokines by BBB EC is induced during inflammation, which mediates the recruitment of inflammatory cells into CNS. For example chemokines CCL19 and CCL21 are expressed by BBB EC maintaining the neuroinflammation status during chronic autoimmune disease (**Greenwood et al., 2011; Alt et al., 2002**) **(Fig. 4**).

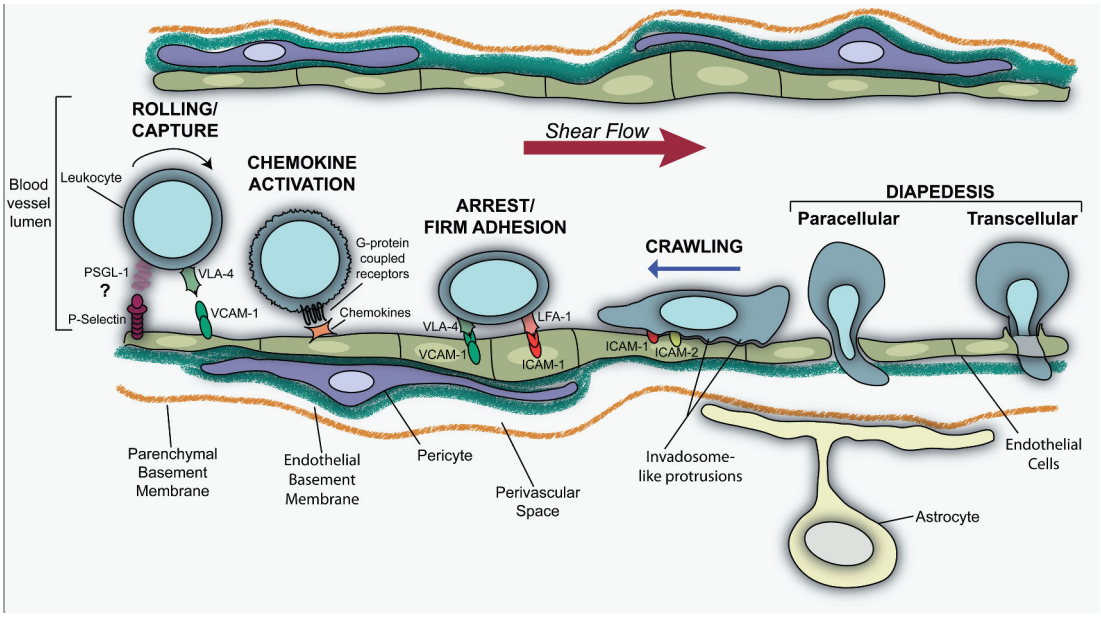

Fig. 4. Leukocyte infiltration into the brain: The leukocyte infiltration through brain endothelium is mediated adhesion molecules like ICAM, which are constitutively expressed in ECs. During Inflammatory episodes the release of immunomodulators cytokines triggers the up regulation of ICAM-I and ICAM-2 resulting in activation of brain endothelium to facilitate the infiltration of leukocytes. **Based on Greenwood et al., 2011**.

Furthermore the extravasation of mononuclear immune cells can be promoted by monocyte chemo attractant protein-1 (MCP-1/CCL2), macrophage inflammatory protein-1 (MIP-1/CCL3/4), among others, which were shown to be expressed in BBB ECs during neuroinflammation diseases (**Harkness et al., 2003; Strecker et**

al., 2013).

The lymphocytes activated by chemokines on the EC become polarized and then secrete proinflammatory cytokines such as TNF-α, IL-1β, IFN-γ and IL-6, leading to the up-regulation of selectins and adhesion molecules (ICAM-1 and VCAM-1) in the BBB. This increases furthermore the calcium influx and cytoskeletal rearrangement in ECs, which facilitate the extravasation of T-cells (**Fasler et al., 2010; Engelhardt and Coisne, 2011**). T cells that cross the BBB will further need to break the barrier formed by the basement membrane components and the perivascular cells. It has been proposed that mononuclear cells in the perivascular space can produce metalloproteinases (MT1-MMP, MMP-2, MMP-9), thus it facilitate that T cells reach the CNS parenchyma, where they start their attack on the CNS parenchymal cells (**Engelhardt and Coisne, 2011; Wu et al., 2009; Agrawal et al., 2006**).

However, due to the absence of professional APCs within the brain parenchyma, infiltrating T cells can not start or maintain an immune response. Nevertheless, pre-activated T cells in the immune organs may cross the BBB, inducing the endothelial MHCII expression which enables the BBB ECs and glial cells to serve as APCs. The inflammatory response is furthermore triggered by pro-inflammatory cytokines produced by Th1-cell activation (IL-2, IFN-γ, TNF-α, and GM-CSF), which are up-regulating effectors of the MHC expression in BBB endothelium and glial cells (**Romo-González et al., 2012**).

In addition, activated BBB ECs may also express granulocyte monocyte-colony stimulating factor (GM-CSF), which induces either the attraction of circulating dendritic cells (DC) or the differentiation of microglial cells into dendritic cells acting as important APC (**Clarkson et al., 2012**). Thereby activated BBB ECs expresses TGF-β and GM-CSF may also transform blood monocytes into DCs after transmigration, inducing stronger effector T-cell responses followed by sustained neuroinflammation (**Ifergan et al., 2008**). The activation of T cells with specific CNS antigen can be mediated by accumulating DCs into the brain parenchyma or by DCs trafficking outside the CNS. However, due to lack of an afferent lymphoid drainage system into the CNS, the DCs would migrate out of the CNS through other alternative drainage paths. It is suggested that fluids drain from brain across

arachnoid space into venous sinuses to enter the blood stream (**Karman et al., 2006; Zozulya et al., 2010**).

Additionally, some reports have shown that injection of myelin basic protein (MBP) or ovalbumin (OVA) into the brain activates an immune humoral response and cellular immune response mediated by antibody production and activation of specific CD8+ T-cells. They were found in the cervical lymph nodes and other organs of the immune system. These data indicate that antigens may drain or traffic from the brain to the cervical lymph nodes establishing a direct communication between the CNS and the immune system.

2.1. Multiple sclerosis

Multiple sclerosis (MS) is a progressive autoimmune neurodegenerative disease, characterized by focal leukocyte infiltrations into the brain parenchyma, triggering a chronic inflammatory response, which causes demyelination and axonal damage. It has to be noticed that myelin sheets formed by oligodendrocytes cells, wrap the axons and function as insulating membrane that facilitates and enhancing the electrical transmission along the axon (**Inglese, 2006**). Most commonly, focal lesions are located in the WM causing inflammatory demyelinating lesions. Nevertheless, other reports have provided evidence for development of grey matter lesions in the CNS, in particular in both the cerebral and cerebellar cortex and the hippocampus (**Kutzelnigg et al., 2005; Kutzelnigg et al., 2007; Geurts et al., 2007**).

The clinical symptoms of MS mainly represent sensory or motor impairment, ataxia, spasticity, fatigue and cognitive impairment. They often correlate with inflammatory plaques within the brain and spinal cord (**Pierson et al., 2012**). Most of MS patients manifest initially a relapsing–remitting form (RRMS) persisting for several years, during which episodes of remyelination contribute to total or partial clinical remission. However a vast majority of patients may worsen developing a secondary progressive MS (SPMS) characterized by irreversible neurodegeneration (mainly axonal and neuronal loss) in which the extent of recovery after each episode diminishes and fails to be reparative. Only a minority of patients (some 15 %) develops a primary progressive MS (PPMS), represented by a continuous disease

progression from onset without relapse or remission (**Jadidi-Niaragh and Mirshafiey, 2011**). The populations with higher prevalence of MS varies between 60–200 ⁄ 100,000 in Northern Europe and North America, and 6–20 ⁄ 100,000 in low-risk areas such as Japan (**Jadidi-Niaragh and Mirshafiey, 2011**) (**Fig. 5**).

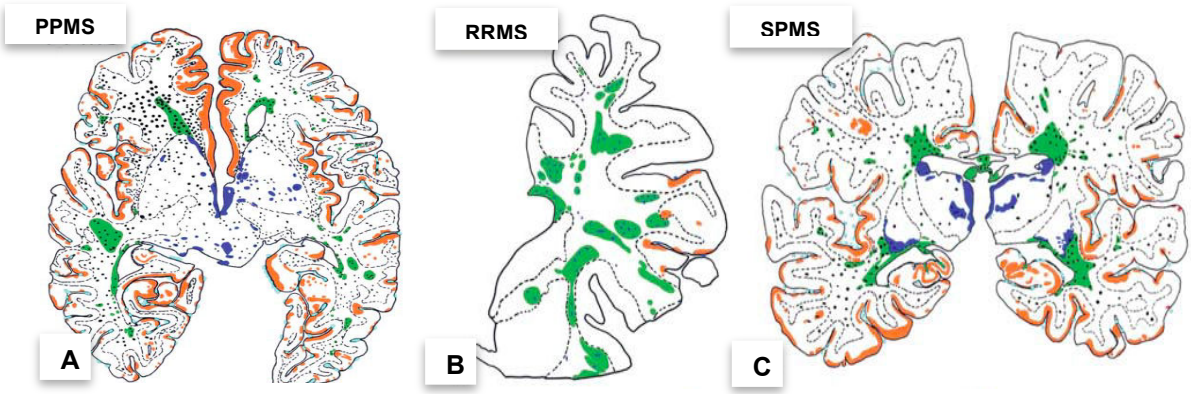

Fig. 5. Focal inflammatory demyelinated lesions in multiple sclerosis: The lesions are mainly focalized to the white matter in relapsing multiple sclerosis (RRMS), while cortical demyelination is characteristic of PPMS and SPMS.

The lesion maps of multiple sclerosis brains are represented as follows, green: focal demyelinated lesions in the white matter, red: cortical demyelination, blue: demyelinated lesions in the grey matter. **a**: PPMS: female, 55 years, 5 years disease duration; **b**: RRMS: female, aged 57 years, 13 years disease duration; **C**: SPMS: male, 43 years, 16 years disease duration. **Based on Kutzelnigg et al., 2005**.

2.2. Development of neuroinflammation in MS

The etiology of MS includes environmental and genetic factors leading to a selective demyelinating disease, mediated by entry of auto-reactive myelin-specific immune cells into the CNS, which in turn maintains the neuro-inflammatory response and subsequent neurodegeneration. Actually the nature of auto-antigens or auto-reactive immune cells responsible of the MS is not known, nor the action that triggers the immune response.

However inflammatory demyelinating lesions in MS, disseminated throughout the CNS, are associated with deregulated BBB permeability and massive CNS infiltration of auto-reactive leukocytes and inflammatory mediators of the immune system (**Zlokovic, 2008**).

Four different mechanisms of demyelination have been identified in MS lesions: Type I mediated by macrophage infiltration or macrophage toxins. Type II T cell and antibody mediated which is the most commonly observed in MS lesions. Type III is related to degenerative changes generating oligodendropathy, followed by oligodendrocyte apoptosis. Type IV results in primary oligodendrocyte damage followed by secondary demyelination (**Inglese, 2006**). Thereby focal lesion formation in MS has been more frequently associated with dysfunction of the BBB for which it is not well understood whether it precedes or follows to the leukocyte infiltration (**Floris et al., 2004**).

However Th17 cells releasing IL-17 and Th1 cells releasing interferon (IFN-γ) have been reported to be predominant in the sites of inflammation (**El-Behi et al., 2010; Brucklacher-Waldert et al., 2009**). IL-17 can lead to BBB breakdown by up-regulating the production of reactive oxygen species (ROS) in the ECs following the activation of contractile cytoskeleton machinery. Then the TJs are opening and adhesion molecules are also up-regulated increasing the transmigration of leukocytes across the BBB (**Jadidi-Niaragh and Mirshafiey, 2011; Stockinger et al., 2007; Kebir et al., 2007; Zlokovic, 2008**).

In addition to the course of T cell extravasation other inflammatory mediators such as chemokines (C-X-C motif) ligand (CXCL1, CXCL6), interleukins (IL-1β, IL-6, IL-8), tumor necrosis factor alpha (TNF-α), GM-CSF, macrophage inflammatory protein-2 (MIP-2), MCP-1 and Granulocyte colony-stimulating factor (G-CSF) are secreted (**Jadidi-Niaragh and Mirshafiey, 2011**). Derived populations of Th1 cells synthesize inflammatory cytokines (TNF-α, TNF-β, IFN-γ and IL-2), activating other immune cells such as monocytes /macrophages which in turn release cytotoxic cytokines and start a direct phagocytic attack of the myelin sheath.

The inflammatory environment can also activate the differentiation of microglia cells into macrophages. Thus the locally activated macrophages release cytokines like IL-1β, TNF-α, chemokines and reactive ROS, which influence the augmentation of adhesion molecule expression by the brain endothelium, and subsequently enhance the infiltration of leukocytes.

Also ACs can become activated to produce inflammatory molecules to attract immune cells into the CNS (**Sofroniew and Vinters, 2010**) and eventually anti-

inflammatory molecules. Thus ACs can form a scar as neuroprotective barrier around inflammatory cells, a process which is mediated by astrogliosis. In this case, the ACs have suppressive effects, being enabled to engulf immune cells along of focal lesion and restricting inflammatory cell spreading into the adjacent healthy CNS parenchyma (**Faulkner et al., 2004; Myer et al., 2006**). Once the microglia, ACs and brain ECs are activated they are an important source of pro-inflammatory (IFN-ϒ, TNFα, IL-1β, IL-6, and IL-12) and anti-inflammatory cytokines such as transforming growth factor (TGFβ), IL-10, and IFNβ within the CNS. In addition IL-4, IL-5, IL-10, and IL-13 cytokines produced by Th2-cell can induce B cell differentiation (**Salmaggi et al., 2002**).

On the other hand, the development of MS caused by the myelin sheath destruction might be the consequence of an aberrant apoptosis of the oligodendrocytes, which in turn induce an inflammatory response by the presentation of auto-antigens to lymphocytes and macrophages typically in surveillance around small blood vessels besides their traffic into the CNS parenchyma. This may ultimately lead to augmentation of demyelination and loss of oligodendrocytes (OLGs). It has been suggested that OLGs and neurons can present the auto-antigens on MHC class I molecules to activate $CD8^+$-T cells crossing the BBB. Furthermore MHC class II molecules expressed on activated microglia and ACs can also present the auto- antigens to CD4+ T cells crossing the BBB (**Inglese, 2006**).

2.3. Experimental autoimmune encephalomyelitis

Experimental Autoimmune Encephalomyelitis (EAE) is an experimentally induced demyelinating disease of the CNS used to investigate the pathogenesis of MS. Generally, progressive manifestations of motor deficits, are the predominant clinical signs in EAE in susceptible animal strains, starting with loss of tail tone followed by paralysis of the hind limbs, progressing later to the front limbs and occasionally even to the death of the animal. The clinical signs are associated with inflammatory cell infiltration into the spinal cord, followed by the rapid development of lesions in the brainstem, cerebellum and other brain regions. Although the animal and the human diseases are certainly not clinically identical, the neuropathological description of animal and human CNS lesions are so closely related that EAE is

considered to be the best animal model of MS (**Inglis et al., 2012; Pierson et al., 2012**) (**Fig. 6**).

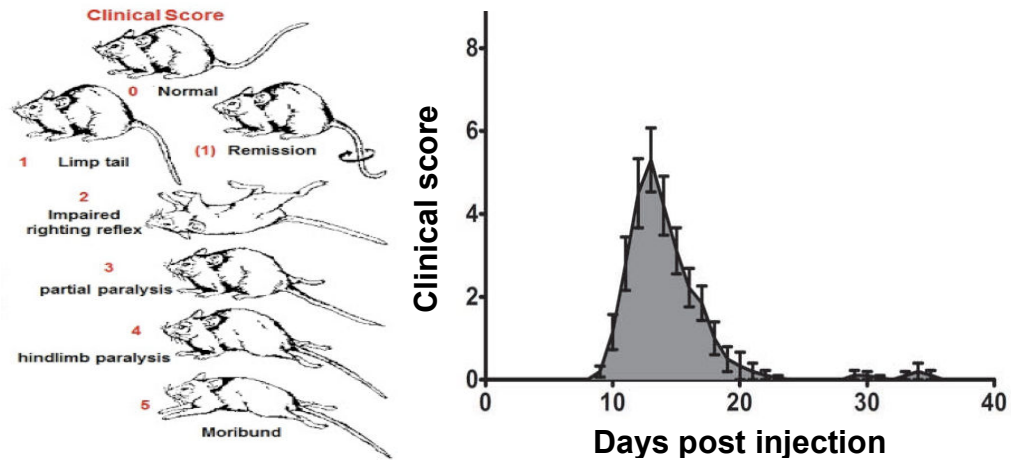

Fig. 6. Clinical development of EAE: Clinal score course of EAE in female Lewis rats injected with Guinea Pig MBP. The peak is generally reached between 11 and 14 days post injection, and recovery between 7-10 days after the peak. Relapses can occur in a few animals between 28 and 40 days post injection. **Based on Inglis et al., 2012**.

EAE can be actively induced by immunization with myelin antigens in susceptible rodents. These antigens include total spinal cord or brain homogenate or proteins/ fragments of myelin i.e. MBP, proteolipid protein (PLP), myelin oligodendrocyte glycoprotein (MOG), myelin-associated glycoprotein (MAG), calcium-binding protein S100 (**Sriram et al., 2005**). In addition, EAE can be induced by transfer of T lymphocytes that bear a T-cell receptor which recognizes a defined myelin peptide / epitope **(Kurkowska-Jastrzębska et al., 2013).**

The EAE model has been commonly studied in Lewis rats, which are syngeneic and develop an immune response mediated by CD4+ T cells and MHC class II. Thus Lewis rats have been useful for the investigation of reproducible immunologic and genetic aspects on EAE (**Stepaniak et al., 1995**).

Lewis rats are susceptible to EAE induction by injection of MBP peptides in emulsion of complete Freund's adjuvant (CFA), which increases BBB permeability and induces the disease development in about 10 days (**Stosic-Grujicic et al., 2004**). In addition MBP-EAE induction has been widely used to define the gene expression profile of the disease (**Inglis et al., 2012**).

Thus, it has been shown that 68-86, 73-86 and 87-99 guinea pig MBP residues are active encephalitogenic epitopes for EAE induction. MS patients respond also to this MBP87-99 region, which is apparently a mammalian highly conserved encephalitogenic antigen (**Stepaniak et al., 1995**).

In comparison dark agouti (DA) rats are also susceptible to EAE induction with MBP68-86 antigen with Tcell and MHC response, but resistant to immunization with MBP73-86 and MBP87-99 (**Stepaniak et al., 1995**).

After immunization Lewis rats develop neuropathological focal lesions mainly in the spinal cord and brain stem, but rarely in the cerebrum. Lesions are commonly characterized by edema, mononuclear cell infiltration (CD4+ T cells, macrophages, B cells and natural killer cells) and gliosis, but rarely demyelination. Therefore, they can get the maximum clinical score and then totally recover from paralysis and became resistant to re-induction of EAE (**Shin et al., 2012**). It can be compared with patients who develop a clinically isolated syndrome CIS, which also manifests an episode of neuroinflammation and demyelination and in some cases does not present a second demyelinating event in the future. In this case the patients may or not go on to develop multiple sclerosis (**Bomprezzi et al., 2011; Croxford et al., 2011**).

In consequence to EAE induction, activated $CD4^+$ T cells in the periphery are recruited in the CNS by adhesion molecules expressed by ECs such as P-selectin, E selectin, VCAM-1 and ICAM-1 which bind to their respective ligands PSGL-1 (P- and E-selectin), VLA-4, LFA-1 expressed on T-cells surface to facilitate the transmigration. However, reports have demonstrated that only combined blockage of adhesion molecules and ligands have a significant inhibitory impact on the recruitment of immune cells and therefore the development of EAE (**Engelhardt and Coisne, 2011; Pierson et al., 2012**).

In addition several studies have shown ICAM-1 and VCAM-1 upregulation on BBB ECs and on choroid plexus epithelium during EAE and MS. Thus some studies have demonstrated the successful therapeutic effect in EAE and MS of monoclonal antibodies against VLA-4 (natalizumab), LFA-1 integrins, used to block the immune cells binding to the BBB and subsequently to treat relapsing-remitting MS **(Deloire et al., 2004).**

Following the recruitment of lymphocytes in the capillary walls, their extravasation is mediated by chemokines CCL19 and CCL21 expressed on activated BBB during the development of the immune response (**Pierson et al., 2012**, **Greter et al., 2005; Sathe et al., 2011**).

On the other hand, a paracellular transmigration of leukocytes across the BBB as an alternative transcellular route has also been suggested. Lymphocytes can cross the ECs via diapedesis mediated by the formation of vesicular-vacuolar organelles or caveolae. Data of transmission electron microscopy on brain sections derived from mice with EAE, have reported neutrophil extravasation through ECs leaving the TJs morphologically intact. Indeed, in neuroinflammatory conditions the BBB ECs can form membrane protrusions on the luminal side, to which the leukocytes adhere to, be transported in pores–like structures to the abluminal side (**Carman and Springer, 2008; Engelhardt and Wolburg, 2004; Engelhardt and Sorokin, 2009; Lossinsky and Shivers, 2004**).

Upon the T cell entry into the CNS, IFN-γ can also activate the expression of MHC class II on cells of the CNS, including resident microglia, perivascular microglia, BBB ECs and probably DCs and macrophages. Once this happens the repertoire of APCs is determined to reactivate the infiltrating T cells. Then the BBB permeability is increased and attracts T cells that accumulate within the CNS. The chronic inflammation is finally spreading by the generation of new repertoires of APCs to myelin-specific T-cells (**Miller et al., 2007; Kivisäkk et al., 2009**). It has also been demonstrated in EAE, that the differentiation of microglia into APCs is mediated by GM-CSF released from activated BBB ECs (**Pierson et al., 2012)**.

2.4. Magnetic resonance imaging

Magnetic resonance imaging (MRI) has allowed developing non-invasive and repetitive molecular imaging *in vivo*. In MRI scanner a magnetic field is used to align atomic nuclei in the body, and an additional field is applied to systematically alter this alignment. Thus the rotating magnetic field of the nuclei is detected by the scanner, according with nuclei locations and rotation speeds, (**Hildebrandt et al., 2007**). The MRI relies on detection of abundant water protons in the tissues by analysis of proton density (Spin density), MR relaxation times (T_1, T_2), diffusion,

perfusion and flow.

Thereby it is possible to study the evolution of CNS injury by MRI in experimental animal models and humans, which may contribute to the diagnosis and to therapeutic strategies. Thus, for example, it was observed in rats with a cortical impact injury that the water dependent T_2 signal increases when intercellular or vasogenic edema develops. This enables MRI analysis to determine the extent, changes and location of CNS lesions (**Dijkhuizen et al., 2011**).

The MRI technology has contributed to improve the early diagnosis of MS, giving information about the mechanisms of neurological dysfunction, such as axonal damage and involvement of BBB disruption as an early event in lesion development. The use of MRI to monitor BBB integrity in relation to disease development of MS is based on detection of leakage of intravenously administered paramagnetic contrast agent from blood flow into the brain parenchyma (**Dijkhuizen et al., 2011**).

Focal inflammatory lesions in EAE and MS can be visualized and measured by MRI scans, after the intravenous injection of contrast agents, such as gadolinium-DTPA chelate (Gd-DTPA) or ultra small super paramagnetic nanoparticles of iron oxide (USPIO) (**Charil and Filippi, 2007; Petry et al., 2007**).

2.4.1. Gadolinium diethylene-triamine-penta-acetic-acid (Gd-DTPA)

Gd-DTPA MRI scanner enhanced BBB permeability imaging in which T_1-weighted MRI is executed 10-30 min after contrast agent injection, allows to assess over time the changes of contrast agent concentration in tissues and vasculature. This provides qualitative information on the integrity of BBB, but does not provide enough information about the extent of inflammation. However the use of increased doses of Gd-DTPA and delaying the image acquisition has improved the detection sensitivity of active MS lesions (**Zlokovic, 2008; Siccotte et al., 2011**).

2.4.2. Iron oxide contrast agents

Considering that Gd-DTPA-MRI presents limitations to provide information about the immune cells trafficking across the damaged BBB, technical breakthroughs were needed to realize molecular imaging of specific cellular targets. This was a possible measure of the evolution of the inflammatory demyelination and their impact in related neurodegeneration (**Stoll and Bendszus, 2009**).

Thus, it was proposed to use ligands directed against target cells conjugated to Iron oxide agents, which have more sensitivity to MRI analysis than Gd in order to induce signal intensity different from the non-targeted surrounding tissues (**Zlokovic, 2008**).

Unlike Gd-DTPA, iron is biodegradable, biocompatible and can be recycled by cells. Besides its dextran coat allows easy chemical linkage of the ligands and easy detection by light and electron microscopy (**Zaharchuk et al., 2007**).

Iron oxide agents are in the range of nano-sized such as 20-50 nm to ultrasmall superparamagnetic particles of iron oxide (USPIO) and 60-250 nm to superparamagnetic particles of iron oxide (SPIO) or micro-sized of 0.9-4.5 μm to particles of iron oxide (MPIO) (**McAteer and Choudhury, 2013**).

USPIO nanoparticles presents some limitations for application in MRI cell tracking. Thus, for example, millions of nanoparticles USPIO are needed to single cell detection, in comparison small number of MPIOs have sufficient iron oxide to labeling single cells with higher contrast effect and sensitivity *in vivo* and *in vitro* **(Shapiro et al., 2006; Heyn et al., 2006).**

However USPIOs and larger particles such as small particles of iron oxide (SPIOs) have been capable to be internalized by professional phagocytes (macrophages and activated resident microglia) on *in vivo* and *in vitro* specific cell labeling (**Modo et al, 2005; Stoll and Bendszus, 2010**) (**Fig. 7**).

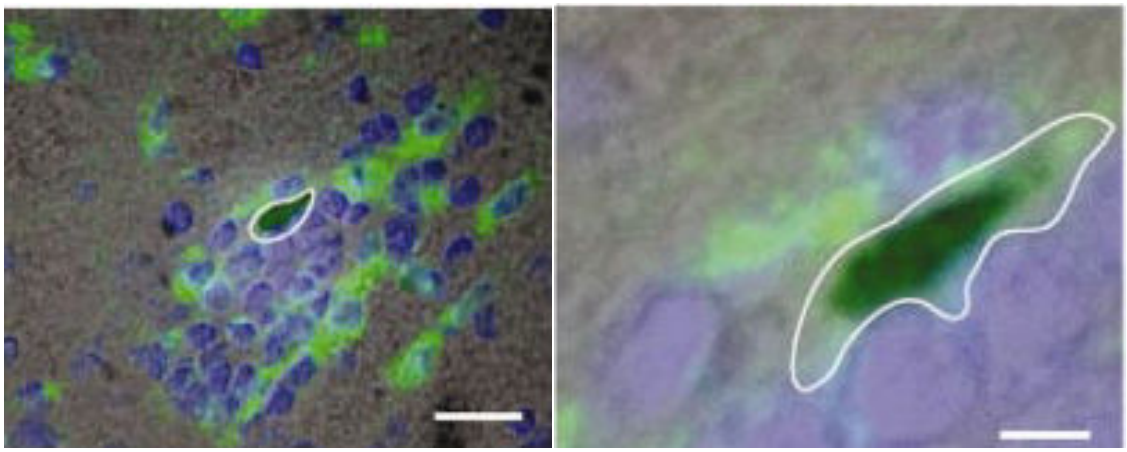

Fig. 7. Localization of USPIOs in infiltrating monocytes: Brain sections of an EAE animal (day 14), USPIOs were detected by Prussian blue staining (black spot within delineated cell) and co-localized with ED1 positive cellular infiltration. At right higher magnification. **Based on Floris et al., 2004**.

The other hand dextran-coated nanoparticles are biodegradable and after several weeks the iron can be recycled by the cell causing toxicity (**Shapiro et al., 2006; Heyn et al., 2006**). Besides nanoparticles have a long clearance time until 48h after administration, which increases the risk of toxicity and molecular non-specificity in comparison to microparticles which have short blood half-life of less than two minutes **(McAteer et al., 2011; Yang et al., 2010; Ye et al., 2008**).

Therefore MPIOs are potential contrast agents in experimental animal models. However are not biodegradable due to their polyurethane coat, allowing long-term analysis, which has to be also changed to reduce their toxicological profile and adopt them in human applications for clinical diagnosis and therapy in Multiple sclerosis (**McAteer and Choudhury, 2013**).

Consequently, lipid structures have been proposed which can carry high amounts of contrast agents, transforming these nanoparticles in efficient clinical agents for cellular and molecular imaging studies and therapeutic drug delivery in patients (**Hossann et al., 2013**).

In addition MPIOs conjugated to monoclonal anti-VCAM-1 antibodies (VCAM-MPIO) were applied for *in vivo* detection by MRI of mice brain endothelium activation. Thus, after focal inflammation induced by injection of IL-1β into the left cerebral hemisphere, the mice were administrated VCAM-MPIO intravenously. The results showed a potent contrast effect of VCAM-MPIO in the inflamed hemisphere,

binding to vasculature with high specificity. VCAM-MPIO has been also reported successfully in MRI analysis of multiple sclerosis murine model, for detection of VCAM-1 upregulation (**Serres et al., 2011; McAteer and Choudhury, 2013**).

2.4.3. MS studies by MRI

MRI is considered as a highly sensitive image detection tool, for the diagnosis of inflammatory MS lesions. The MRI analysis in MS patients and animal models by using the MRI contrast agent Gd-DTPA has allowed to visualize BBB leakage, but not activated microglia or macrophage infiltration (**Dousset et al., 2006**).

Thus ultra-small superparamagnetic particles of iron oxide (USPIO) were proposed to visualize cellular infiltration and to complement the analysis from Gd-DTPA in MS. USPIO-enhancement of MS lesions is partially different from Gd-enhancement in space and in time demonstrating that BBB leakage and cellular infiltration are two separate mechanisms (**Vellinga et al., 2008**). Thus, this remains as a question whether the Gd-enhancement is characterized by immunological episodes of microglia activation before infiltration from circulating immune cells without BBB rupture. This will be represented by no USPIO-enhancement and not cell infiltration (**Petry et al., 2007**) (**Fig. 8**).

Besides, it has been suggested by MRI analysis that BBB disruption in MS may precede myelin damage and leukocyte infiltration in MS patients. Thus a profound leakage of the serum protein fibrinogen into the brain parenchyma was shown, which is associated with abnormalities of the expression and structural composition of the brain endothelial TJ proteins zona-occludens-1 and occludin in active demyelinating lesions (**McAteer et al., 2007**).

MS is not only caused by inflammatory demyelinating lesions in CNS white matter: MRI studies have demonstrated also grey matter damages with neuroaxonal loss, which induces a neurodegenerative stage (**Charil and Filippi, 2007**). Thus MS has been defined in two stages, inflammatory demyelination in early stages and neurodegeneration in late stages of the disease.

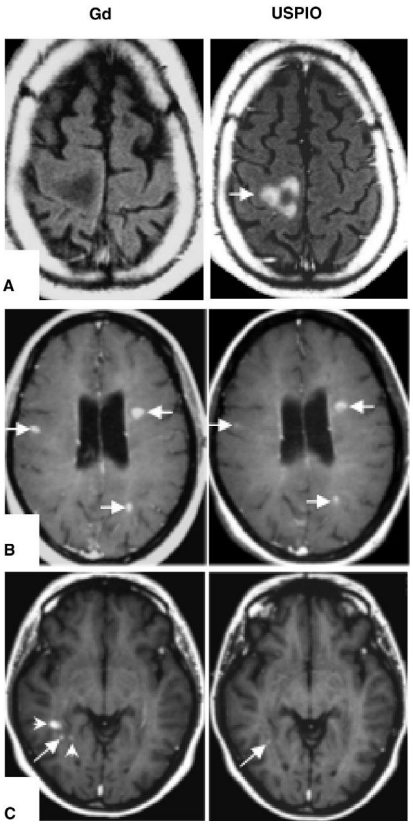

Fig. 8. Magnetic resonance imaging: Right panels, detection of macrophage brain infiltration with ultrasmall superparamagnetic iron oxide particles (USPIO). Left panels, BBB leakage visualized with gadolinium- chelate (Gd) in acute multiple sclerosis. A. Large lesion indicating no BBB leakage, but massive macrophage infiltration detected with USPIO high-signal intensity. B. Lesion formation with both BBB leakage (Gd) and macrophage infiltration (USPIO). C. Three lesions show BBB leakage (Gd) and only one macrophage infiltration (USPIO). **Based on Petry et al., 2007**.

3. Biomarkers of neuroinflammation

The brain is highly protected by the vascular barriers BBB and BCSFB, which present a high impermeability mediated by a specialized system regulating the blood flow into the brain parenchyma. Therefore, a large number of drugs and particles of high molecular weight can not cross the BBB, forming here the main challenge in drug therapy or even diagnosis of several CNS pathologies.

The development of nanotechnology of molecular nano-ligands derived from *in vivo* and *in vitro* screening could help in the understanding of human disease. Several types of molecular targeting screenings have been designed such as yeast two-hybrid screening, bacterial display screening and phage display screening.

The phage display screening offers rapid distribution into the organs across biological barriers, economical experimental reproduction and a wide diversity of selected clones, which could be used as targeting agents for, contrast imaging.

These advantages in recombinant phage display technology have facilitated the identification of peptide ligands, antibodies and antibody fragments which can be coupled to nanoparticles to target the brain vascular endothelial receptors (**Van Rooy et al., 2010**). In addition the development of nanoparticles has been used to deliver drugs into the brain, which is provided by their stability at room temperature, lack of immunogenicity of the small peptides and high affinity interaction with the target receptors (**Koffie et al., 2011**).

For example peptides binding to VCAM-1 generated by phage display screening were reported, and conjugated to iron oxide nanoparticles for *in vivo* MRI analysis. Thus VHSPNKK peptide with homology to VLA4 is able to block leukocyte– endothelial interactions by binding to VCAM-1, highly expressed by endothelial cells in inflammatory regions (**Kelly et al., 2005**).

In vitro cellular BBB models have allowed investigating the nanoparticle uptake mechanisms across the BBB. The nanoparticles are usually labeled with a fluorescent dye or quantum dots and then monitored by confocal microscopy or in some other cases when the nanoparticles contain heavy metals, phase contrast microscopy and transmission electron microscopy can be used.

The biodistribution and targeting of the nanoparticles *in vivo* can be also monitored using techniques for diagnostic medical imaging including MRI, positron emission tomography (PET), single-photon emission computed tomography (SPECT), computed X-ray tomography (CT), and optical imaging techniques (e.g. multiphoton microscopy) among others (**Barber, 2013**).

Labeled nanoparticles with Gd-DTPA or U/SPIO allow the application of strong energy and deep penetration, which facilitate a powerful analysis of *in vivo* monitoring by MRI. These nanotechnologies have allowed a more accurate diagnosis of neurodegenerative disorders compromising the BBB integrity and brain function, such as brain ischemia, Alzheimer's disease (AD), Parkinson's disease (PD) and multiple sclerosis.

The use of nanoparticles coated with targeting peptides may increase the cell penetration and selectivity therefore facilitating the diagnosis of BBB disorders. Some peptides commonly used in therapy of CNS diseases such as the HIV tat peptide (trans activator of transcription) can induce receptor-mediated endocytosis and facilitate crossing of the BBB for CNS drug delivery (**Wong et al., 2012**).

Recently, the use of peptide based carriers known as Angiopeps was reported for brain drug delivery. Angiopeps were shown to induce high transcytosis and parenchymal accumulation, which is a potent, purpose of therapy (**Wong et al., 2012**).

However, for diagnosis of diseases other approaches include fluorescent or radioactive labeling of either phage particles or synthetically manufactured peptide sequences. These strategies enable direct *in vivo* visualization of a peptide tissue distribution (**Wong et al., 2012**).

3.1. Phage display selection

The use of phage display has allowed to perform a massive selection technique either *in vivo* or *in vitro*, for specific ligands which are expressed as recombinant proteins on the phage surface, while maintaining physiological functions and viability of the phage (see below). Thus the same vector contains the foreign peptide molecules and the encoding DNA, which is an advantage with respect to other expression vectors (**Arap, 2005**).

3.1.1. Phage display library

A phage display library can be built to express random peptides or proteins fused to minor-pIII or major-pVIII coat phage proteins. The use of pVIII was limited because it presents 2700 copies forming the majority of the phage capsid, thus resulting in a higher number of displaying particles which increase the number of target binding and thereby decreasing the specificity of selection. In contrast pIII is mostly preferred because the phages present only 3 to 5 copies facilitating the specificity of the selection (**Arap et al., 2005**).

The recombinant peptide can be either linear construction PhD 7-mers, Ph.D.-12-mers or heptapeptides flanked by two cysteines (C7C), which form disulphide cross-link conferring the cyclic peptide. Ph.D. C7C library was supposed to allow enhanced interaction with the target molecules. As an example, page containing peptide flanked by two systems have been shown to improve tumour uptake or during evaluation of a brain homing peptide. However, libraries with linear peptides are widely used as well **(Zhou et al., 2013).**

The number of inserting random amino acids usually varies between 6 to 15, since the specific interaction is capable to occur within 3-amino acid motifs. Despite this, the search for homology to protein ligands mimicked by short peptides can encounter risks. Thus the identified sequence may share homologies with proteins not relevant to the target or may reside outside of the functional part of protein ligands. Despite of the search the homologies to one determinate ligand protein by using bioinformatics databases, the results should be experimentally confirmed.

The most commonly used phagemid vector derived to built Phage display libraries is the filamentous phage M13, containing circular single stranded (ss) DNA of 6500 nucleotides, which infects *Escherichia coli* bacteria via specific bacterial structures called F-pili. This infection / amplification in bacteria is necessary since the selection of phage repertoires expressing specific ligands requires to be amplified in bacteria to obtain a stock of the selection repertoire for the next selection round (**Karlsson, 2004**). Three to five selection rounds are indeed necessary to concentrate the repertoire in ligands with high affinity and specificity.

Therefore the Ff phage particles do not kill their hosts, establishing a relationship in which new virons are continually released. For that it is possible to grow high-titre cultures of the virus. The growth curve of Ff phage shows a rapid increase of virus after a short latency period. Thus the first progeny of phage particles is released about 15 minutes after infection, and the rate of production is exponential for the first 60 minutes, the result is then 1000 phages per bacteria produced within the first hour. After that the infected cells continue to grow and divide indefinitely, but with a significantly lower rate (**Karlsson, 2004**).

3.1.2. Phage peptide panning

Phage peptide selection allows identifying structural epitopes, ligands mimicked of phage peptide displaying for different target molecules (antibodies, enzymes or cell surface receptors). Basically, the phage screening called “panning” is carried out by incubation of immobilized targets (*in vivo or in vitro*) with at least 10^{12} phage peptides/ml to ensure the highest amount of different particles per round. The unbound phages are washed away while the bound phages are eluted and separated from the targets. The recovered phage repertoires are amplified in bacteria and the diversity of phage repertoire is evaluated by sequencing. Following this procedure, the diversity of the library is still quite high, the reason why screenings have to be repeated during several rounds of selection, following the same protocol or increasing the selection stringency, to raise the amount of specifically binding phage peptide clones. Finally the phage peptide collected in the last round of selection is sequenced to identify the peptide ligands that were selected (**Kitagawa et al., 2005; Tipps et al., 2010**).

The phage repertoire collected in the last round of selection is then amplified into the bacteria E.coli for subsequent panning of specific clones. However, it should be mentioned that during the synthesis of M13 particles in E. coli, individual clones could be lost from the library due to an incompatibility between the peptide insert and the host synthesis/assembly machinery (**Steiner et al., 2006**).

3.1.2.1. *In vitro* selection

Initially the phage display screening was developed by *in vitro* panning of specific targets (proteins, enzymes, antibodies, etc.…) (**Scott and Smith, 1990**). Also cell lines with over-expressed target receptors are useful tools for identification of cellular receptors and their ligands. However, this molecular targeting approach does not consider the complexity and heterogeneity of the living organism.

Peptide library has been used to select ligands mimicking the epitope to which an antibody binds, based to three or four conserved residues. This has allowed determining the region of recognition in a ligand protein, which is represented by the peptide displayed on the page surface. Indeed, uncovered mimotopes to the human

hepatitis B virus envelope protein (HBsAg), which were successful to induce a humoral response in immunized population, suggesting that peptide ligands mimicking a determinate antigen are a potent tool for diagnosis and even therapy (**Arap et al., 2005**). Other examples discovered by phage display technology include peptide ligands recognizing MHC molecules, peptide ligands mimicking integrin receptors binding to any ECM protein containing the RGD motifs, peptide ligands recognizing SH2 domain in several protein kinases (**Arap et al., 2005**).

In MS there is an elevation of IgG in the CSF, however, it's specific target and its role in pathogenesis of MS has not been determined. It has been suggested to use *in vitro* phage display selection to find the target antigen of CSF IgG in MS patients. Thus CSF of MS patients was incubated with Protein A-boards, to obtain a pool of IgGs, then the IgG-beed complexes were incubated with random PhD-12 peptide library during two rounds of selection and finally thirty clones were selected and sequenced. Common peptide motifs were searched by combining Multiple Expectation Maximum for Motif Elicitation (MEME) version 3.0 and BLAST.

The results identified molecules related to microbial agent of MS. Thus three peptide motifs were detected: SPxxMH, DPYQxP, and PYxxYQxP homologous for Epstein Barr Virus (EBV) (**Fujimori et al., 2011**).

Other studies have reported that CSF IgG antibody from American patients with MS recognizes the amino acid sequence motif RRPFF that is found on EBV nuclear antigen. However, it has also been exposed that the greatest difficulty to detect an epitope is that the MS CSF IgG may recognize a conformational epitope or nonprotein antigens (**Fujimori et al., 2011**).

The selection of peptide ligands in biological system was initially directed against molecules over-expressed on the cell surface in a system of *in vitro* cell culture. However, this raised the background generated by unspecific binding, which interfere with the results. The screening and selection of phage peptides bound to cell surface can be carried out by centrifugation of the phage-cell complex in the no miscible phase and separation of the unbound phages in the miscible phase. The phage–cell pellet is recovered and the phages are amplified by bacterial infection. With this method several phage peptide ligands were screened for binding to VEGF receptor on ECs (**Arap et al., 2005**).

3.1.2.2. *In vivo* selection

The use of cell culture to perform page peptide screening has given valuable information when the cells are exposed to different stimuli. However, this doesn't give real information about the legends from the cellular microenvironment surrounding the targeted tissues. Some phage display experiments were carried out *in vivo* directly in human patients by intravenous injection of phage library followed by tissue biopsies of several organs (prostate, liver, metastatic tumors, skin, adipose tissue and skeletal muscle), and the subsequent Bioinformatics analysis of millions of clones. This procedure was followed by three rounds of panning, identifying by this way peptide sequence consensus, such as CGRRAGGSC, which mimics the IL-11 in the prostate (**Pasqualini et al., 2002**). However the development of phage screening in humans has been limited because of ethical reasons.

In consequence the use of animal models was proposed for *in vivo* phage display screening. The phage particles are injected directly into vasculature of living animals, allowing the phages to distribute in the different organs after 15 mins of circulation in the blood stream; the washing of the unbound phages is carried out by perfusion via the left ventricle with saline buffers. The fate of the phage particles depends of the receptor binding and tissue extravasation (**Bábíčková et al., 2013; Van Rooy et al., 2010**).

Then the animals are sacrificed at a defined time point and the desired organs are extracted and homogenized. One fraction of the organ lysates, which contains bound phages, is then amplified in bacteria and the amplified phages are then reinjected into another animal; the fraction remaining is used for phage titration. This procedure is followed during three or four rounds of selection (**Pasqualini and Ruoslahti, 1996**). Then the phage repertoires are analyzed either by a classic procedure of cloning / sequencing or by a massive sequencing analysis. In all cases, the sequence determination is followed by a Bioinformatics analysis. Also immunostaining with anti-phage antibodies after phage circulation allows to determine the clone tissue distribution (**Fig. 9**).

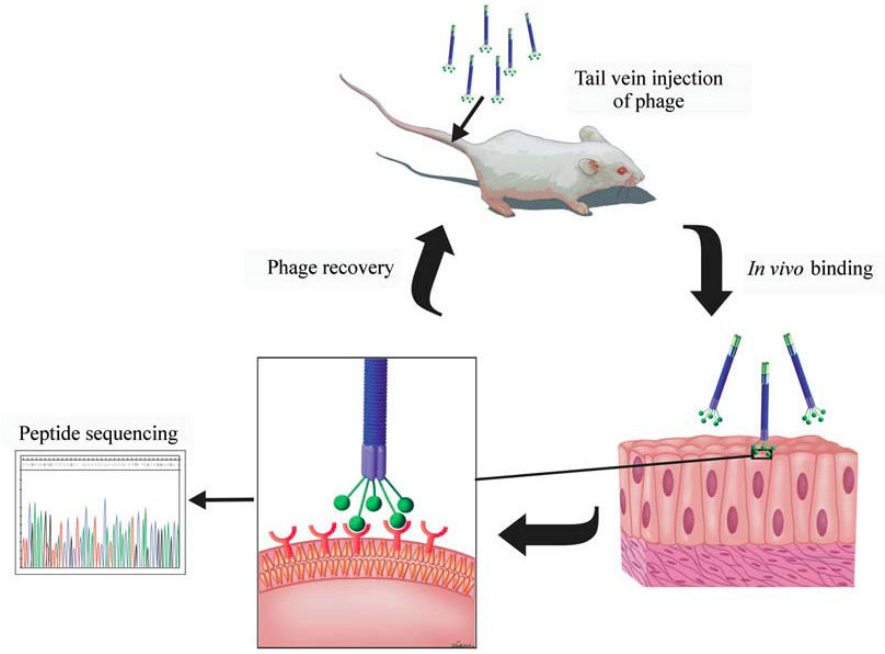

Fig. 9. *In vivo* phage selection: The phage library is injected into vasculature of animals. Then the phages are able to recognize specific receptors in the capillary ECs until they can infiltrate into the organs. Finally, diversity of the repertoire of phage peptide ligands is evaluated by peptide sequencing and Bioinformatics analysis. **Based on Arap et al., 2005**.

The first screening by phage display carried out in animals showed that peptide ligands with the sequence consensus SRL appear in high proportion in the brain with respect to other organs (**Pasqualini and Ruoslahti, 1996**). Several years later, another brain vasculature targeting peptide was discovered with the sequence CAGALCY, which was able to inhibit platelet adhesion**.** Additional experiments have shown GLAHSFSDFARDFV and GYRPVHNIRGHWAPG peptides homing into brain ECs and then were also found to bind to human brain ECs (hCMEC/D3), compared to human umbilical endothelial cells (HUVECs), suggesting their specificity of brain endothelial cell (**Van Rooy et al., 2010; Bábíčková et al., 2013**).

Phage peptide screening on brain vasculature and parenchyma were performed in Male Sprague-Dawley (SD) rats, then phage peptides with efficient binding to BBB were isolated, and then by using Bioinformatics analysis conserved motifs of brain-associated peptides were identified. Thus AC-SYTSSTM-CGGGS, most frequently found with selective tropism for the BBB was identified (**Smith et al., 2012**).

In vivo BBB integrity is regulated by the surrounding cellular microenvironment and by the blood components. For this reason the phage display procedure was

suggested to be performed *in vivo* to enrich the phage repertoire in a BBB microenvironment associated with disease conditions and in comparison, in healthy conditions.

Experiments of the phage peptide selection performed in EAE mice have proposed the use of PhD-7 peptide displayed. In this way four phage peptides mimic chemokines binding to CCR5 were selected and the peptides were synthesized to subsequent injection into EAE. Thereby the potent inhibitory effect of mimic peptides targeted to CCR5 was demonstrated, which is important as a tool in diagnosis or therapy of the different stages of the neuroinflammation (**Zheng HM al., 2011**).

4. OBJECTIVES OF THE THESIS

The multiple sclerosis (MS) is the most common autoimmune inflammatory demyelinating disease of the CNS, mainly characterized by leukocyte infiltration into the brain parenchyma and resident microglial activation. Those events involving the immune response have been extensively studied and associated with alterations on the blood-brain barrier (BBB) permeability.

However, still not well understood the mechanisms affecting BBB ECs and increasing the permeability of the BBB to infiltrating leukocytes. There is not even enough information that allows finding out which of these two processes starts first, leukocytes cell infiltration or BBB disruption. For these reasons several studies using animal models of neuroinflammation have been proposed to develop biomarkers to have a better understanding of the mechanisms. The biomarkers discoveries have been based on molecular alterations of the BBB.

To target such alterations we have advised the use of page displaying peptide ligands to screen in an EAE animal model of MS, allowing the selection of peptide ligands. Such peptide ligands have the potential to be applied as biomarkers in EAE and MS neuroinflammation.

Therefore in this project we have applied *in vivo* phage display screening into the CNS of EAE and Healthy rats during three rounds of selection. A subsequent DNA subtraction between the phage repertoires selected from EAE and from healthy controls allowed to select peptide ligands specific for inflammatory lesions.

The main goal of this project was to identify *in vivo* peptide ligands that bind to specifically or to highly expressed targets at the BBB during acute neuroinflammation in the EAE rat model.

To study the binding capacity of the candidate peptides we tested them by immunohistochemistry in CNS sections from EAE and control rats and on *in vitro* BBB model under neuroinflammation conditions. We further performed experiments to identify the target molecules of the identified peptides.

5. STRATEGY

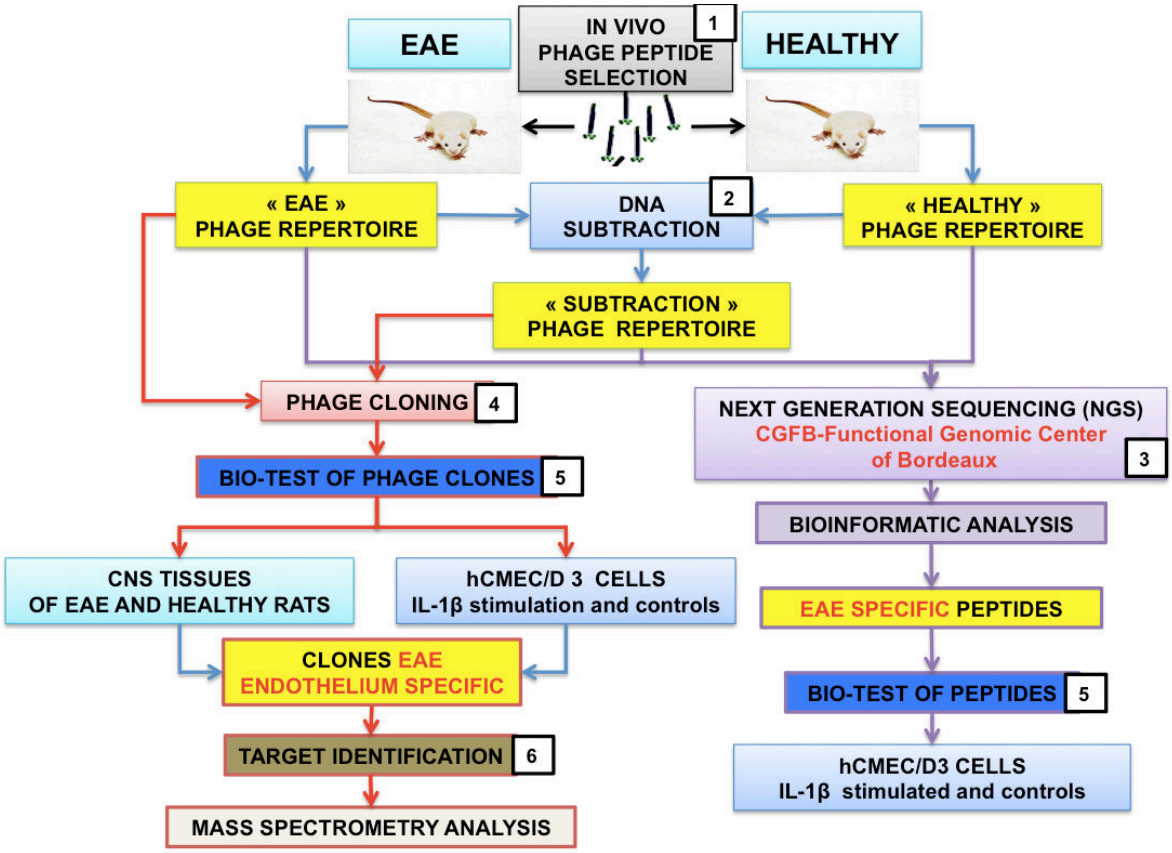

Fig. 10. Experimental strategy: **1)** Three rounds of *in vivo* phage peptide selection in EAE female Lewis rats ("EAE repertoire") *vs* controls ("HEALTHY repertoire"). **2)** DNA subtraction of the most common sequences between «HEALTHY» and «EAE» phage repertoires to obtain a third EAE specific «SUBTRACTION » phage repertoire. **3)** Massive sequencing of the three repertoires and bioinformatic analysis to identify the peptides sequences with high EAE specificity. **4)** Biological tests of potential EAE specific phage clones with CNS tissues from EAE and Healthy control rats. **5)** Biological tests of the EAE specific peptide and phage clones on the BBB *in vitro* model (hCMEC/D3 cells) under inflammatory conditions (IL-1β stimulation). **6)** Target separation and identification by cross-link between the selected phage clones and hMEC/D3 endothelial cells targets under IL-1β stimulation *vs* controls.

6. METHODOLOGY

6.1. Materials

6.1.1. Animals

Female Lewis rats (Janvier France) aged 6 to 7 weeks, weighing around 150 to 170 g were housed in cages (five animals per cage) with standard conditions of light and free access to water and food.

Animal handling and experimentation conformed to guidelines of the European Union (Permissions No. 6305 and 33/00055 of the local Animal Experimentation Commission).

6.1.2. Phage peptide library and Bacteria

Phage peptide library of 1 x 10^{10} transformants (**New England Biolabs**), with foreign random peptides of 12aa, displayed as a fusion to the coat protein pIII of M13 phage.

E. Coli ER2738 host strain (New England Biolabs), with F^+ pilus to allow the phage infection. The F-factor contains a mini-transposon, which confers tetracycline resistance.

6.1.3. Immunostaining

First antibodies:

Rabbit polyclonal antibody to M13 + Fd bacteriophage coat proteins (Abcam, ref ab6188). Working concentration 12 μg/mL.

Mouse monoclonal antibody RECA-1 (Abcam ab9774). Working concentration 2 μg/mL.

DAPI (Euromedex, ref S7113). Working concentration 10 ng/mL.

Secondary antibodies:

Goat anti-rabbit polyclonal IgG Cy3 (Abcam ab98416). Working concentration 3 μg/mL.

Goat Anti-Mouse IgG polyclonal Alexa Fluor® 488 (Invitrogen A11001). Working concentration of 6 μg/mL.

Goat Anti-Rabbit IgG (H + L) horseradish peroxidase (HRP) (Bio- Rad, ref 170-6515). Working dilution of 1:1000.

Other materials:

Streptavidin DyLight 488 (Invitrogen, ref S11223). Working concentration of 2.5 μg/mL.

Streptavidin, Rhodamine-Red™-X conjugate (Invitrogen, ref S32354).

6.1.4. Human brain endothelial cell line hCMEC/D3

The immortalized human brain endothelial cell line, hCMEC/D3, was obtained under license from INSERM, France (Dr P.O. Couraud). The procedure to generate the immortalized hCMEC/D3 cell line was carried out at Kings College Hospital, London. Thereby the original brain ECs were isolated from human brain tissue following surgical excision of an area from the temporal lobe of an adult female with epilepsy. Microvessel fragments and single cells like primary ACs were separated from other material and thereafter plated onto coated flasks with type I collagen in EGM-2 growth medium containing FBS and growth supplements, as indicated in the **annex 1** (**Weksler et al., 2005**). The ECs were purified from non ECs by adding puromycin, which result in more than 95% pure endothelial cultures, as assessed by morphological criteria and by expression of endothelial-specific markers. The immortalization of the primary culture of brain ECs was performed by induced sequential expression of the catalytic subunit of human telomerase hTERT in combination with an oncogene SV40-T antigen (this prevents telomere shortening and extends cellular lifespan), via lentiviral vector system.

Following the established protocol (**Weksler et al., 2005**), with minor changes, immortalized hCMEC/D3 cells were used between passages 26 and 35. The cells were seeded at a concentration of 27000 cells/cm^2 in flasks pre-coated with rat-tail collagen type I solution at a concentration of 150 µg/mL and grown in EBM-2 basal medium supplemented with 5 % decomplemented fetal calf serum, 10 mM HEPES, 1 ng/mL bFGF (Sigma), hydrocortisone (1.4 µM), ascorbic acid (5 µg/mL) and antibiotics (Penicillin- Streptomycin) 1 % (**annex 5**). Cells were cultured in an incubator at 37 °C with 5 % CO_2, 95 % fresh air and saturated humidity. Cell culture medium was changed twice a week. To perform the experiments the cells were cultured in petri dishes (diameter 100 mm) or labteck chambers for 15 days until they reach confluence and tight junction properties.

6.2. Methods

6.2.1. EAE Immunization

During the immunization process the rats were anesthetized with isoflurane. EAE was induced by subcutaneous inoculation of an emulsion containing 1 mg *Mycobacterium tuberculosis* H37Ra strain, 50 µL Complete Freund's adjuvant and 100 µg MBP (**Deloire et al., 2004**). Immunized rats and healthy controls were housed separately in cages; all animals were daily weighed and handicap was described according to the following scale: 0, no handicap; 1, flaccid tail; 2, flaccid tail and hind limb weakness; 3, complete paralysis of one hind limb; 4, paraplegia; 5, death. Clinical EAE onset was defined as the day a rat developed a flaccid tail (score 1).

6.2.2. *In vivo* Phage display selection from EAE *vs* Healthy rats

EAE rats presenting score 3 and healthy littermates were deeply anesthetized by intraperitoneal injection of Pentobarbital (6 mg/100 g weight). Absence of vibrissae or spontaneous body movement, absence of nociceptive reflex (no movement after hind limb pinching) and absence of behavioral reflex (no eye blinking) were ensured throughout the experiment.

At each selection round, 1 x10^{10} pfu phages of the library suspended in 400 µL NaCl, 0,9 % solution were injected into the circulation.

With the aim of collecting the phages, which are internalized, and also those which are bound just on the endothelial cell membranes. We have performed the phage injection in two steps as follows:

An intravenous phages injection and 10 minutes later, the thorax was opened for an intracardiac phage injection. Immediately after, cold PBS 1x was pumped through the left ventricle, to wash the unbound phages. Thereby the first injection allows for phage circulation into the organs while the second injection allows the phage just to be associated with the cell membrane.

To enrich the harvested phage repertoires with specific phages, the phage screening was performed during three rounds of *in vivo* selection by injection of 1 x 10^{10} pfu of the previously selected and amplified phages. On the other hand, as each round of bacterial phage amplification is susceptible to bias the repertoire by favoring some phage clones, therefore resulting of a misinterpretation of selection results, only three rounds of *in vivo* phage selection were performed.

6.2.3. Phage isolation from CNS tissues

After phage circulation followed by PBS washing the rats were dissected to extract brain and spinal cord. Tissues were homogenized in the presence of 1% NP40 (1 mL/g tissue) in 0.9% NaCl.

Thus the tissues and phage suspension was added to 10 mL of bacterial suspension grown at 0.5 $O.D_{600nm}$ to allow phages to infect the bacteria. Incubation was performed for 45 minuntes at 37 °C. An aliquot of 100 µL from the infected ER2738 bacteria was taken to make a titration of transducing-unit (T.U) harvested from the CNS tissues. The suspension containing infected bacteria was grown for 4 h at 37 °C in 40 mL LB broth, allowing phage amplification (**annex 1**).

The culture was cleared of bacteria by two successive centrifugations (8000 rpm, 10 minutes at 4 °C). Phages in the supernatant were precipitated overnight at 4 °C by adding 20 % PEG8000 in NaCl 2.5 M (**annex 1**).

The next day, phages were collected by centrifugation (9000 rpm, 10 minuntes at 4 °C) and recovered in 1 mL TBS (**annex 1**). Remaining bacteria were eliminated by a second centrifugation (8000 rpm, 10 minutes) at 4 °C and phage precipitation was repeated with PEG8000/NaCl (1 h at 4°C). After centrifugation (14000 rpm, 10 minutes at 4 °C, phage pellets were dissolved in TBS/ 0.02% NaN_3. Aliquots were stored at 4 °C until use.

All steps of phage collection and amplification to obtain the repertoire were controlled by titration of transducing-unit (T.U) as described in (**annex 1**).

After each selection round, amplification by PCR of phage DNA coding for the peptides was performed (**annex 2**). Then the purity of the PCR products was confirmed by agarose gel electrophoresis (**Fig. 16, results**). The PCR products were also sequenced to confirm the diversity of the phage repertoires.

6.2.4. Subtractive hybridization for enrichment of EAE specific clones

The protocol was designed to perform a physical DNA subtraction of peptide DNA sequences displayed on the pIII protein, which are common to EAE and Healthy repertoires. It was performed by adding compounds to a test tube without any withdrawal or purification steps. Single stranded circular genomes from the EAE phage repertoire were hybridized with single stranded linear DNA obtained by asymmetric PCR from the last round of the healthy repertoire. The subtractive hybridization is explained in the results, (**Fig. 17**).

6.2.4.1. DNA extraction of circular phage genome

Phages repertoires from the third round of the EAE selection were amplified in *E. coli* at 37 °C, with agitation (250 rpm) for 4 h. Bacteria were discarded after centrifugation at 8000 rpm by 10 minutes and the phages suspended in the supernatant were extracted and purified, using the standard PEG/NaCl protocol described above. Genomic DNA was obtained by phage lysis according to the New England BioLabs (NEB) protocol. Thus 1 $x10^{10}$ phages/µL were lysed in a solution of NaI 4 M in TE buffer for 5 minutes in dark at room temperature (RT). Then it was added ethanol 100% doubling the initial volumen and the solution was maintained in

the dark for 10 minutes at 4 °C and centrifuged at 14000 rpm for 30 minutes. The pellet corresponding to the phage DNA was precipitated again with ethanol 70% in the same conditions. Finally the DNA pellet was suspended in Tris-HCl-EDTA (TE) buffer and then stored at -20 °C until use. The DNA concentration was determined by spectrophotometry and the purity confirmed by PCR as described above.

6.2.4.2. Recombinant region amplification by PCR

The PCR amplification of recombinant region (fusion region of the coat protein pIII, coding for the sequence of peptide insert) was performed with the phage repertoire of the "Healthy" selection. For the production of the subtractor linear DNA strand, asymmetric PCR was performed using a tenfold excess of the -28 primer with respect to +18 primer, to favor the production of single stranded unpaired products of the negative strand (**annex 2**).

6.2.4.3. Subtractive hybridization

Single stranded circular genomic DNA extracted from the EAE repertoire (3.3×10^{-3} M) was mixed with PCR products of the Healthy repertoire (3.3×10^{-2} M), 1:10 molar ratio, in 100 µL of KpnI reaction buffer.

DNA species were melted by incubation at 95 °C for 10 minutes, then the temperature was slowly decreased (1 °C/min.) to reach 85 °C. Hybridization was carried out at this temperature for 2 h, after that the reaction mixture was rapidly cooled to 37 °C. 2 µL of KpnI (annex 3) was added and the mixture incubated at 37 °C, for 10 minutes. 10 µL of the subtraction solution were taken before and after digestion to verify the completion of KpnI digestion by agarose gel electrophoresis. The final products were used for bacteria transformation without purification.

6.2.4.4. Bacteria transformation and recovery of the subtracted repertoire

Chemo-competent bacteria were prepared utilizing the Rapid Transit Kit (annex 3) according to the kit's protocol. 10 ml of log growth phase bacteria (ER2738) was recovered by centrifugation (7000 RPM/10 min.), suspended in 100

μL of 1x Rapid Transit Transformation Buffer, and incubated for 10 minutes on ice, then 100 μL of the subtraction products was added and the mixture was further incubated for 10 minutes on ice. A heat shock was done at 42 °C for 30 Sec. Therefore 900 μL of LB Medium was added and the bacterial culture was incubated for 1 h at 37 °C under agitation (200 rpm) to allow the production of phages, then 1 mL log growth phase bacteria (ER2738) was added and the infection carried out for an additional hour at 37 °C under agitation (200 rpm). Finally the phages were amplified in 10mL of log growth phase bacteria (ER2738) during 4 h at 37 °C under agitation (200 rpm).

After phage amplification, bacteria were eliminated by centrifugation at 8000 rpm, 10 minutes, and the supernatant containing the viral particles was saved and purified according to the PEG/NaCl protocol described above. Transformation efficacy was determined by titration and the purity controlled by PCR electrophoresis.

6.2.5. High-throughput sequencing of phage repertoires

The phage repertoires recovered after the last round of selection from EAE pathology developing rats, healthy control and the phage repertoires produced by DNA subtraction, were used to perform PCR amplification. Thus the PCR products were submitted to High-throughput sequencing (next generation sequencing - NGS). NGS was performed in the plateforme de Génomique Fonctionnelle from Bordeaux University on an Illumina Genome Analyzer IIx.

The Illumina genome analyser technology performs massively sequencing of 100 of millions of DNA sequences as represented briefly in **figure 11**. Single molecules are isothermally amplified and uploaded up in the CBOT cluster amplification system. DNA library samples are bound to complementary adapter oligonucleotides grafted on the surface of the flow cell. The templates are copied from the hybridized primer by 3' extension using a high fidelity DNA polymerase. These copies are isothermally amplified to create clonal clusters of ~1,000 copies each, ready for high support sequencing. Each cluster of clonal sequences, when analyzed is defined as " a read".

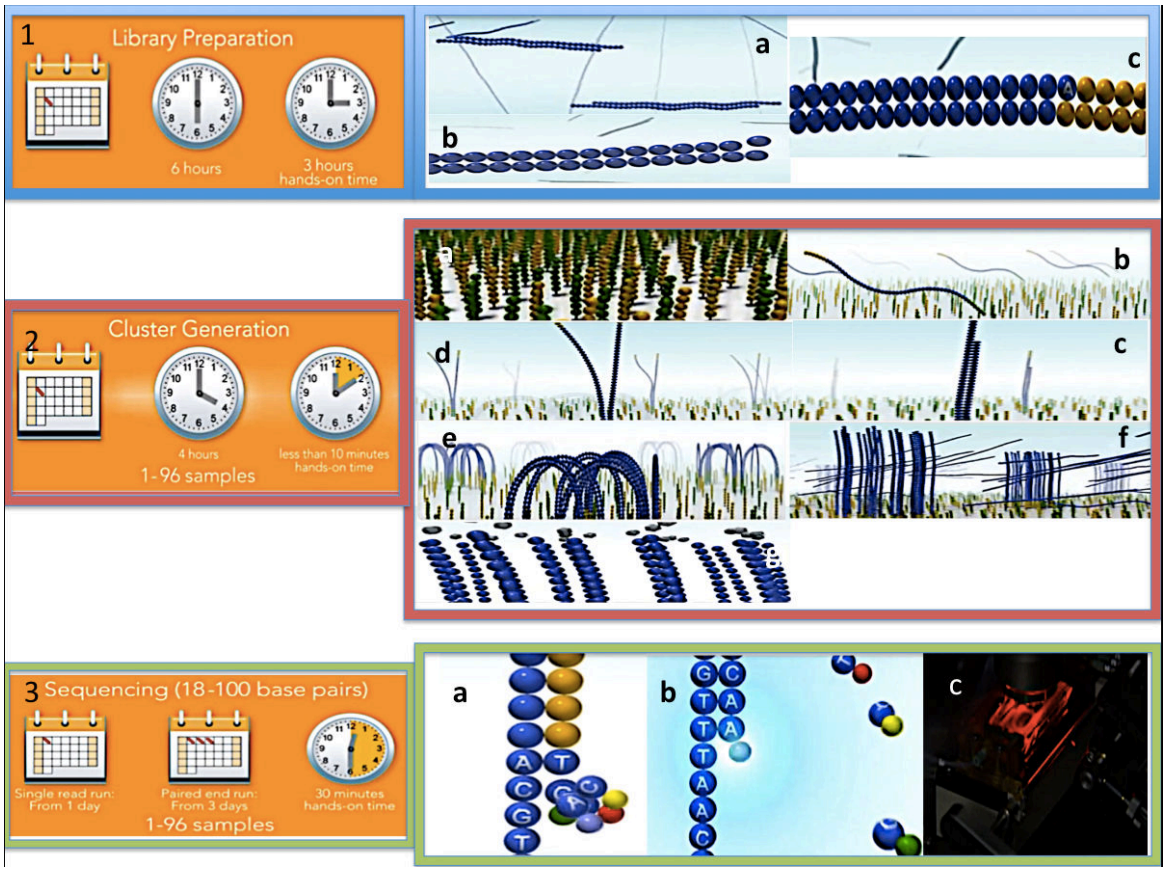

Fig. 11. NGS: 1) a. The PCR products are fragmented, **b.** Repaired and **c.** Adenylated. **2) a.** Oligonucleotide adapters are grafted on the surface of the genome analyzer. **b.** These oligonucleotide adapters bind to the adapters bound into the Single DNA molecules of the library fragments. **c.** Bound fragments are extended to create copies. **d.** These copies are covalently bound to upload surface. **e.** Each library fragment is clonally amplified resulting in 100 of millions of unique clusters. **f.** The reverse strands are cleaned and washed away, **g**. The sequencing primer is hybridized to the DNA templates. **3) a.** Using four fluorescently labeled reversibly terminated nucleotides, DNA template is sequenced base by base. All four bases compete with each other to bind to the template. **b.** The fluorescent label and blocking group are excited by a laser and then removed, allowing the addition of the next base. **c.** The excited group emits a color, which allows identifying the newly added base. **Based on http://www.illumina.com/technology/sequencing_technology.ilmn**.

6.2.5.1. Repertoire sequencing

Genomic DNA of the phages repertoires was extracted by the NaI method, as described above. The PCR of the recombinant region of the phage protein pIII was performed with the primers +18 and -28 to produce DNA fragments encoding for the displayed peptides and then used for sequencing. The complexity of the resulting products was first verified by pool sequencing (BigDye Terminator v3.1 Cycle

Sequencing Kit and ABI 3130 XL, Invitrogen) and then sequenced on an Illumina Genome Analyzer IIx. All sequencings were performed by the team of the university's sequencing facility (**Plateforme de Génomique Fonctionnelle de Bordeaux**). Sequences were retrieved as FASTA files, demultiplexed per sample and further processed using a home made workflow on the Galaxy platform. **Based on http://www.cgfb.ubordeaux2.fr/fr/content/galaxyunworkflowpourl%E2%80%99analyse-bioinformatique**.

Processing included elimination of sequences with peptide read scores lower than 30, reorientation of the reads to represent the positive strand of the phage, extraction of the sequences encoding for the displayed peptides, occurrence counting and frequency calculation. The DNA sequences were translated to their equivalent of peptides using the genetic code of the ER2837 strain. Finally the peptide sequences were clustered to subsequent analysis of its homolog proteins mimicked by SPack application, a homemade bioinformatic analysis tool. **Based on http://services.cbib.u-bordeaux2.fr/spack/index.php**.

6.2.6. Characterization of individual phage peptide clones

6.2.6.1. Phage clone selection

Samples of the phage repertoires from EAE selection and the "Subtraction" of EAE minus Healthy were grown on plates with log growth phase bacteria (ER2738) /LB-AGAR /IPTG:Xgal. From each repertoire about 100 clones were randomly picked and amplified in E. coli ER2738 bacteria, according to the NEB protocol. Phage DNA from each clone was amplified by PCR using the +18/-96 couples of primers and the products were sequenced. Clones expressing different individual peptide sequences were chosen for further binding studies.

6.2.6.2. Phage clone binding on CNS tissue

6.2.6.2.1. Tissue sections of EAE and Healthy rats

EAE rats developing clinical scores 3 or 4 and healthy rats were deeply anesthetized with an intraperitoneal injection of pentobarbital sodium (6 mg /100 g of rat weight). Animals were perfused into the left heart ventricle with 50 mL PBS followed by 200 mL formaldehyde (FA) 4 % in PBS 1x. Brains and spinal cords were removed and post-fixed by maintaining in FA 4% PBS 1x for 4 days. The tissues were cut in slices of 30 μm by vibratome (LEICA VT1000S) and kept in PBS 1x /sodium azide 0.02 % at 4 °C to preserve the tissues from contamination until use.

6.2.6.2.2. Immunohistochemistry on tissue sections

Three slices of the brain and spinal cord from EAE (clinical scores 3 or 4) and Healthy rats for each tested phage clone and wild type phage controls were placed in plates of 24 wells and then washed three times with PBS1x before use. Then the tissues were permeabilized with TritonX100 0.3 % and saturated with goat serum 3 % in PBS1x (**annex 4**) for 1 h at RT. Tissues were then incubated with selected phage clones from EAE selection and wild type (WT) phage clone (negative control) at 10^{10} transducing-unit (T.U.) overnight at RT under shaking.

The experiments were also controlled by following the immunostaining protocol on tissues without phage incubation. Then to remove unbound phages the tissues were washed three times for 10 minutes with PBS 1x at RT. After washing the tissues were incubated for double labeling with the first antibodies, anti-M13 and anti-RECA-1 for 2 h at RT and as negative control tissues without first antibody incubation. Tissues were washed three times with PBS 1x for 10 minutes, and incubated them with the secondary antibodies for 1 h in the dark at RT.

After washing 3 times for 10 minutes in PBS 1x, the tissues were incubated with DAPI in Tris-HCl (**annex 4**), for 5 minutes and washed twice more for 10 minutes with Tris-HCl. The sections were mounted on glass slides and covered with VECTASHIELD Mounting Medium and coverglass. Tissues were observed and

photographed using an epifluorescence (Nikon 90i) or a confocal fluorescence microscope LEICA SP8 WLL2 (Mannheim, Germany).

6.2.6.3. Phage clone binding on hCMEC/D3 cells

6.2.6.3.1. hCMEC/D3 Cells

Immortalized human brain ECs hCMEC/D3 (**Weksler et al., 2005**) were grown for 15 days on rat tail collagen coated to lab-teck chamber slides. Upon Confluency they develop tight junctions. Cells were simulated or not with 20ng/mL rhIL-1β for 2 h (**annex 5**). Then the medium was changed for the subsequent incubation step with the phage clones and WT control.

6.2.6.3.2. Immunohistochemistry on hCMEC/D3 Cells

Single phage clones selected and wild type phages (negative control) at 10^{10} pfu were incubated with cells (previously IL-1β stimulated or not) for 5 h at RT in the medium. Unbound phages were eliminated with 3 washings for 15 minutes with PBS1x. The cells were fixed with FA 1 % in PBS 1X, for 20 minutes and washed three times for 15 minutes with PBS 1x/ 0.3 % Triton X100. The cells were then saturated with goat serum 3 % in PBS 1x for 1 h at RT. The experiments were also controlled by following the immunostaining protocol on cells without phages incubation. The cells were incubated with the anti-M13 first antibody for 1 h at RT and as negative control cells without first antibody incubation. The cells were then washed three times for 15 minutes with PBS 1x and incubated with the secondary antibody for 1 h in the dark at RT.

After washing 3 times for 15 min, the cells were incubated with DAPI in Tris-HCl for 10 minutes and washed 2 times for 10 minutes with Tris-HCl. Finally, after removal of the lab-tek chamber, cells were covered with VECTASHIELD® Mounting Medium and coverglass. The cells were observed and photographed using an epifluorescence (Nikon 90i) microscope.

6.2.6.4. Dot blot: Phage clone binding on hCMEC/D3 protein extracts

ECs hCMEC/D3 were lysed by scraping in 1 mL non-denaturing lysis buffer, (**annex 6**) to extract the proteins on ice in the presence of protease inhibitors. After lysis the protein suspension was centrifuged for 1 minutes at 14000 rpm to eliminate remaining cellular debris and then the protein content was quantified according to the BCA protein assay (**annex 6**). 900 ug/mL of protein extract of hCMEC/D3 cells either stimulated or not with IL-1β were homogeneously absorbed on nitrocellulose membranes Hybound C, (**annex 6**) for 30 minutes under shaking. Then the membranes were shortly rinsed with TBS and allowed to dry.

Non-specific sites on nitrocellulose membranes were blocked by soaking in 1% BSA/ TBS (30 minutes at RT). Membranes were mounted in a Dot blot apparatus (**annex 6**) allowing rapid and parallel testing of individual phage clones (10^{10} pfu) expressing various peptides and the control wild type phage (2 h, RT). After intensive washing (5 times 5 minutes, PBS) the membranes were incubated with antibody anti-M13 for 2 h; after 5 washings with PBS1x incubated with the secondary antibody anti-rabbit horseradish peroxydase (HRP) for 30 minutes at RT. The membranes were revealed with 4-chloro-1-naphtol in Methanol-TBS at 0.3 mg/mL in the presence of H_2O_2 0.3% (**annex 6**). The reaction was stopped by washing with tap water.

6.2.7. Characterization of EAE specific phage peptides

6.2.7.1. Synthesis of EAE specific phage peptides

Four peptide sequences of 8aa present with occurrence in EAE repertoire and also present in the Subtraction repertoire were chosen, and then synthesized as follows: Nter-GGXXXXXXXXXGGGKGK-Cter, where XXXXXXXXX (peptide), Nter-GG, N terminal with two glycines as a spacer, GGGKGK-Cter, three glycines as spacers for the KGK tripeptide, presenting two lateral chain primary amines for attachment to NHS-label biotin (Genecust). Thus the final constructions were: Biotin-LC-Gly-Gly- xxxxxxxx-Gly-Gly-Gly-Gly-Lys-OH.

6.2.7.2. Phage peptide binding on brain ECs hCMEC/D3

hCMEC/D3 cells were grown in plates of 96 wells to $5x10^4$ cells/cm^2 during 15 days. Then the cells were stimulated overnight with IL-1β (20 ng/mL) or VEGF (50 ng/mL) *vs* controls at 37 °C with 5 % CO_2, 95 % fresh air and saturated humidity in an incubator. The biotinylated peptides were complexed with Streptavidin Rhodamine-Red at ratio about 4-1 for 30 minutes at RT.

The cells were incubated with the peptide-streptavidin complex in culture conditions at a ratio of 1 x 10^6 complexes/cell, in a total volume of 200 µL/well during 5 h at RT.

After three times wash with PBS 1X by 15 minutes, RT, the cells were fixed with formaldehyde (1 % in PBS 1x, by 20 minutes at RT). Then three times washing with PBS 1X (15 minutes, at RT), and finally incubation with DAPI in PBS 1X during 10 minutes at RT. The cells were observed and photographed using an epifluorescence (Nikon 90i) microscope.

6.2.8. Characterization of target proteins labeled by phage peptide ligands

The separation of target proteins was performed by crosslinking between phage peptide ligands and target proteins on human brain ECs hCMEC/D3, using Sulfo-SBED crosslinker reagent (**annex 7**) (**Reynolds et al., 2011; Wang et al., 2010**). After that the target identification was carried out by mass spectrometry analysis. **Based on http://www.cgfb.u-bordeaux2.fr/fr/proteome**.

Individual phage clones were labeled with Sulfo-SBED which is a trifunctional crosslinking reagent containing thereby three arms, 1) a sulfonated N-hydroxysuccinimide (Sulfo-NHS) active ester with a disulfide bond, 2) a photoreactive aryl azide 3) an S-S disulfide bond and 4) a biotin (**Fig. 12**).

The strategy was followed in 4 steps:

1) The Sulfo-NHS ester reacts with primary amines at pH 7-9 to form covalent amine bonds. This molecular arm can therefore bind to the peptide insert on the phage surface, but also in the great majority to the coat protein pVIII.

2) Upon UV photoactivation the aryl azide reacts with amine groups, which are able to crosslink, the cell surface proteins in the vicinity of the phage. The arm containing the active ester has a cleable disulfide bond, allowing separating the phage particles once the crosslinking is established.

3) The disulfide bond is cleaved by reduction with TCEP (Tris 2-carboxyethyl phosphine hydrochloride) and the glycine solution at pH 2.5 cleaves the protein-protein interaction between phage peptide and protein target on the cell surface.

4) Finally, on the cell surface the aryl azid remaining bound with an extension of biotin allows to separate or to detect the proteins recognized by the phage peptides by using biotin-streptavidin interaction.

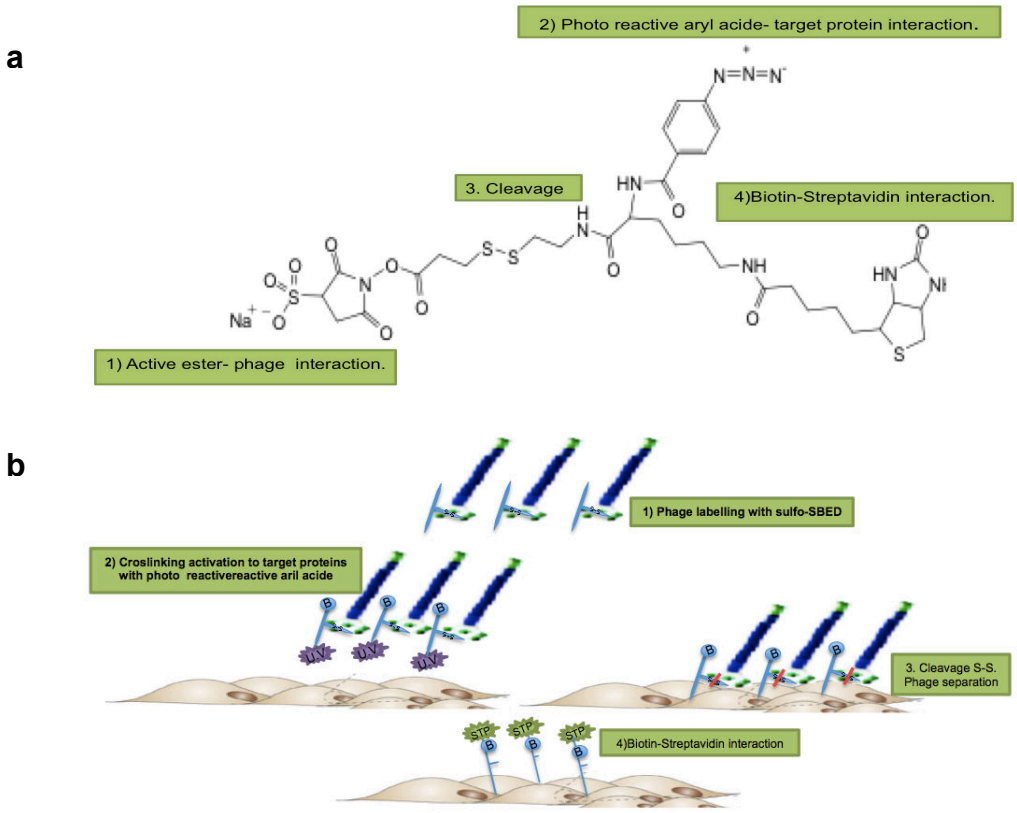

Fig. 12. Target identification: a) Molecular structure of sulfo-SBED, **b)** Crosslinking Phage peptide ligand - hCMEC/D3 Targets.

6.2.8.1. Immunohistochemistry to detect the cross linking on human brain ECs hCMEC/D3

Individual phage peptide clones and wild type phage at several concentrations (10^{10}, 10^{11} and 10^{12} transducing-unit (T.U)) in 1mL of PBS 1x, were labeled with 50 µL of Sulfo-SBED 70 mM, by 1 h at 4 °C in the dark (**Reynolds et al., 2011; Wang et al., 2010**). The labeled phages were purified to discard unbound Sulfo-SBED by precipitation in PEG/NaCl according to the protocol described above and resuspended in PBS1x.

Human brain ECs hCMEC/D3 were grown for 15 days in lab-tek and stimulated or not with 20 ng/mL of rhIL-1β for 4 h. After 3 times washing with PBS 1x, the cells were incubated with 100 µL by well of individual phage clones and wild type phage (negative control) pre-labeled with Sulfo-SBED for 1 h at 4 °C in the dark. Then the cells were fixed with FA 4 % for 30 minutes and washed 2 times with PBS 1X. After fixation the cells were saturated with goat serum 3 % in PBS 1X by 1 h. The unbound phages were removed by washing 3 times for 5 minutes with PBS 1X, Tween 0.1% (**annex 7**).

The lab-tek chambers were placed on ice and the cross linking between phages and the target proteins was induced by UV exposure with a lamp 8 watt 365 nm for 15 minutes.

The phages bound to their specific target proteins were eluted by cleaving the cross linking with 100 µL TCEP in the glycerin solution (**annex 7**) during the 10 minutes. The cells were washed 2 times for 5 minutes with glycine solution, then washed once with PBS 1X 5 minutes. Cells were incubated with streptavidin-dylight 488 for 1 h in the dark at RT, then washed 3 times for 5 minutes with PBS 1x.

Cells were incubated with DAPI for 5 minutes and washed 2 times for 10 minutes with Tris-HCl. Finally, after removal of the lab-tek chamber, the cells were covered with VECTASHIELD® Mounting Medium and cover glass. Then the cells were observed and photographed using an epifluorescence microscope (Nikon 90i).

6.2.8.2. Separation of target proteins by crosslinking

Human brain ECs hCMEC/D3 grown for 15 days in petri dishes 100 mm and stimulated or not with 20 ng/mL IL-1β for 2 h and then the cells were placed on ice for 30 minutes to metabolic inactivation.

After washing 3 times for 5 minutes with cold PBS 1x, 1 mL of each phage peptide clone and wild type phage (negative control) at 1 x 10^{13} transducing-unit (T.U) pre-labeled with Sulfo-SBED (according to the protocol described above) were incubated with hCMEC/D3 cells for 1 h at 4 °C in the dark. The unbound phage were removed by washing 3 times 5 minutes with PBS 1x, 0.1 % Tween 20.

The cross-linking between phages and protein targets was induced by U.V exposure with a lamp (8 watts at 365 nm) on ice for 15 minutes. The bound phages to the target proteins were eluted with TCEP reducer agent and glycine solution. Then the cells were washed once with glycine solution and once more with PBS 1x.

The cells were lysed in 1mL of non-denaturing lysis buffer and then transferred to button-tubes. The cell lysate was incubated for 20 minutes with 40 µL Dynal M-280 streptavidin beads. The proteins were retained by placing the tube to DYNAL MPC-1 magnet during 5 minutes and then the cell debris suspended in the supernatant were discarded and washed with triton x100 1% in PBS 1X by three times (**annex 7**).

The proteins-magnetic beads were suspended in 200 µL of denaturation buffer and boiled in water bath for 5 minutes to cleave the biotin-streptavidin interaction. The proteins were spin at 14000 rpm to discard the magnetic beads pellet and the proteins suspended in the supernatant were transferred into new tube. The concentration of proteins was determined according to the BCA protein assay. Finally the proteins isolated by this procedure were submitted for identification to mass spectroscopy analysis.

6.2.8.3. Identification of target proteins by LC/Mass spectrometry analysis

The protein samples obtained from crosslink-target identification were prepared to perform LC/Mass spectrometry analysis (**http://www.cgfb.u-bordeaux2.fr/fr/proteome**). The general followed protocol is described below.

SDS-PAGE, electrophoresis was run in poly-acrylamide gel under denaturing conditions to purify the proteins from the samples. Then the gel was stained with coomassie blue, and destained with acetonitrile (which reduces the hydrophobic interactions between proteins and coomassie blue).

After electrophoresis, the gel was processed to separation of the bands and then, gel fragments were processed to facilitate an efficient tryptic digestion following a treatment of reduction with a solution of DTT/ammonium bicarbonate (promega/sigma) (to reduce the disulfide bonds and resolve the tertiary structure of the proteins) and irreversible alkylation of the SH groups with iodoacetamide/ ammonium bicarbonate (sigma). Several steps of wash with ammonium bicarbonate to reach the pH 7.5-8.5, needed for a subsequent tryptic digestion).

The trypsin digestion and the sample preparation for LC/MS/MS was performed according to iTRAQ™ Reagents protocol. LC/MS/MS was carried out according to following parameters:

Chromatography

- A	95/05/0.1 H_2O/ACN/HCOOH v/v/v
- B	20/80/0.1 H_2O/ACN/HCOOH v/v/v
- Gradient	5-40 % B in 35 minutes
- Injected volume	10 µL
- Precolumn	300-µm ID x 5-mm C18 PepMapTM (THERMO SCIENTIFIC)
- Precolumn flow rate	20 µL/minute
- Column	75-µm ID x 15-cm C18 PepMapTM (THERMO SCIENTIFIC)
- Column flow rate	200 nL/minute

Mass spectrometry

- Needle voltage	1.8 V
- Capillary voltage	40 V
- µScan MS	1
- µScan MS²	1
- MS range m/z	300-1700
- M/MS strategy	MS + 6 CID MS/MS
- Min. signal required	500
- Ion isolation window	3 m/z units
-Normalized collision energy	35%
- Default charge state	3
- Activation Q	0.25
- Activation time	30
- Dynamic exclusion	Repeat count 1,repeat duration 30s,Exclusion duration 30s
-Charge state rejection	+1, +4

The data obtained were analyzed by Progenesis LC-MS 4.0 on a Homo sapiens database.

7. RESULTS

7.1. *In vivo* Phage display selection from EAE and Healthy rats

7.1.1. Strategy of phage selection

To obtain the major profiles of phage binding during different stages of the neuroinflammatory conditions during EAE development, we have performed a double strategy. First, selection on EAE rats during the first acute neuroinflammation presenting clinical scores 3 or 4 and on EAE rats during the recovery phase (score 1 after maximum clinical score of 3 or 4) and second, selection in healthy rats. Clinical score development and strategy are presented in the **figures 11 and 12**. Comparison between the different clinical stages has been proposed to get new information of the profile of gene expression after an episode of acute neuroinflammation, which could be associated with MS patients that manifest a relapsing–remitting (RRMS) form with partial episodes of remyelination that contribute to partial clinical recovery.

During three rounds of selection, 1 x 10^{10} pfu of M13 phages which present a linear peptide insert of 12aa displayed on the coat protein pIII, were injected into EAE rats and healthy ones in two times, first via intravenous injection and 10 minutes later directly in the heart.

We considered that after ten minutes of phage circulation, they could bind to targets that could eventually be internalized by the cells and then the rapid phage injection in the heart allowed to select the phages that could remain bound to the cell surface (**Bábíčková et al., 2013; Vanrroy et al., 2011**). These phages were collected from the CNS organs (brain, cerebellum and spinal cord) and could be amplified in order to obtain 1 x 10^{12} pfu /µL. Then 1 x 10^{10} pfu were injected in the next selection round.

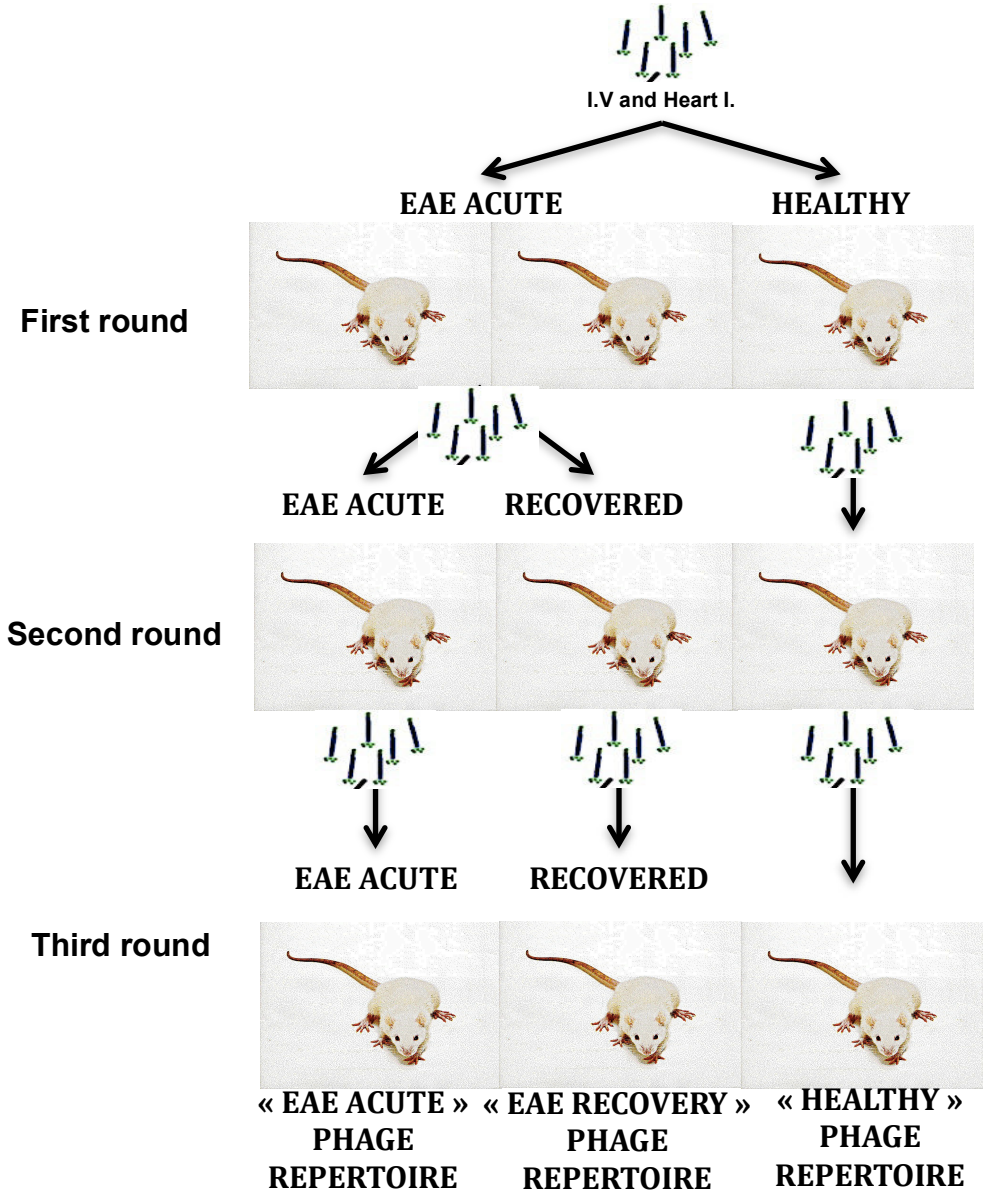

Fig. 13. Three rounds of phage selection on EAE rats and Healthy controls: In the first round, the phage library was administered by intravenous injection (I.V) and direct injection at the heart in two EAE rats with acute neuroinflammation (clinical score 3-4) and one healthy control rat. The phage collected from the first round were injected in the second round to two rats one with acute neuroinflammation and one after recovery (clinical score 1) *vs* one healthy control. Finally the third selection round was performed under the same conditions than during the second selection round.

7.1.2. Phage selection at different stages of the clinical EAE development

In the first selection round two EAE rats which reached a maximum clinical score 3 or 4 (acute EAE) at 13 days post immunization and one healthy rat, were injected with the original M13 phage library at 10^{10} pfu/µL displaying randomly 200 copies of each peptide ligands (**Fig. 9**). The animals were sacrificed and the phages

bound to the CNS (brain, cerebellum and spinal cord) tissues were collected (First phage EAE repertoire). After phage amplification the first repertoire was reinjected into EAE rats for the second round of selection.

In the second selection round also two EAE rats were used. One of them had reached handicap score 3 (acute EAE) at 14 days and the second one had reached handicap score 4 in 15 days (acute EAE) and then the recovery was set to score 1 at 18 days. The two rats were injected with the EAE acute phage repertoire obtained in the first selection round when the EAE acute and recovery was set respectively. In addition, another healthy rat was used for the second round of the "healthy selection". After phage circulation the three rats were sacrificed and the phages bound to CNS tissues were collected to get three phage repertoires (acute, recovery and healthy control).

Finally the third selection round was performed in the same conditions than the second round. Thus, one rat had reached handicap score 4 in 11 days and the second one at 14 days and recovery at 15 days. Then the rats were injected with the phage repertoires obtained in the second round “acute” and “recovery” respectively. Also the third round of the healthy control selection was performed (**Fig. 14**).

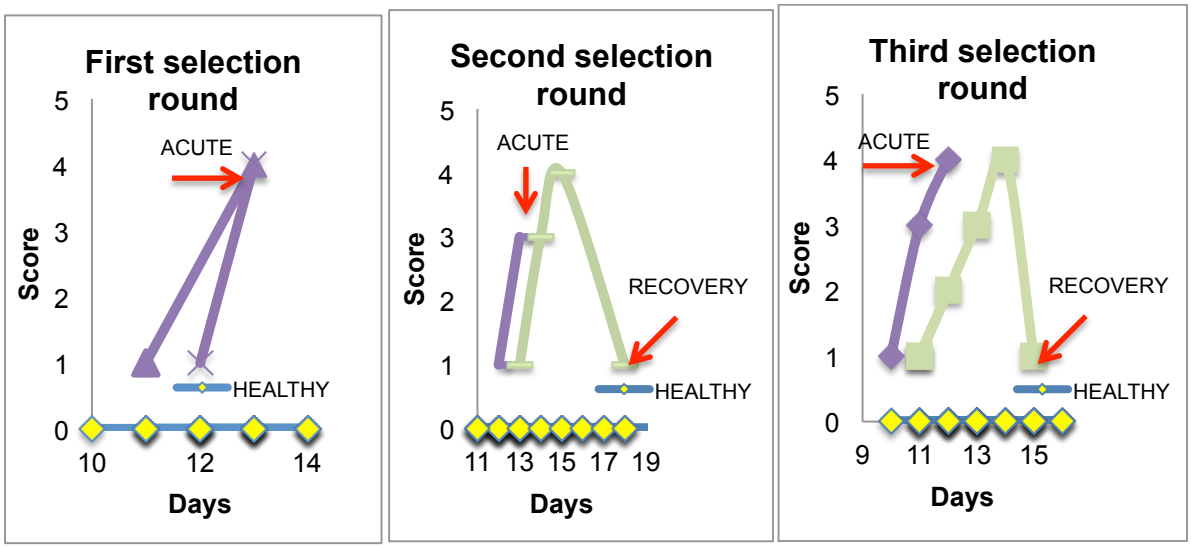

Fig. 14. EAE score development during three rounds of phage selection: Each graph represents the clinical scores reached after immunization for two EAE rats in each selection round (acute (purple) and recovery (green)) and healthy controls (yellow). The red arrows represent the day point when the rats reached acute or recover stated.

7.1.3. Phage selection efficiency during the selection process

As shown in the **figure 15**, the number of phages collected in each selection round was increased by x100 and x1000 between the first and the third selection rounds, indicating that the repertoires after the third selection rounds might be enriched in ligands binding to specific targets.

After the three selection rounds we obtained 3 phage repertoires: from acute neuroinflammation (CNS), from recovery phase of neuroinflammation (CNS) and Healthy Controls (CNS).

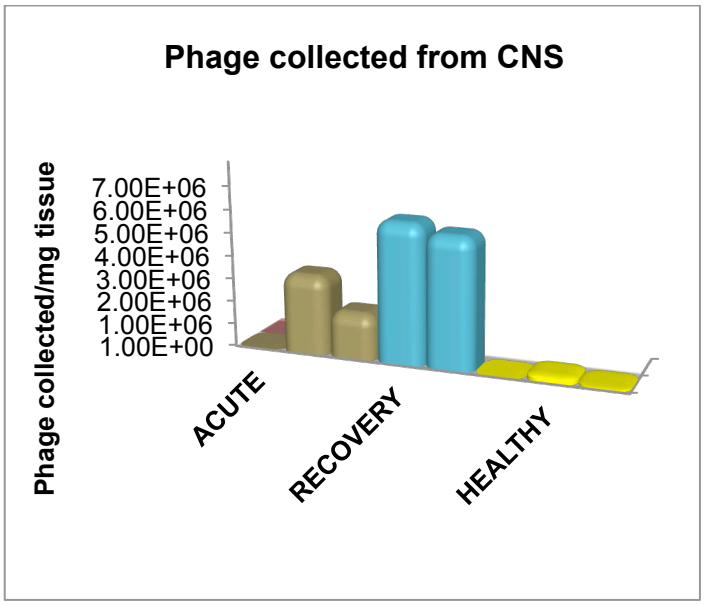

Fig. 15. Number of phages collected during three rounds of selection: The graphs represent the phages collected by milligram of tissue (CNS), in each treatment (acute EAE, Recovery and Healthy). The brown bars represent the “acute EAE” phage repertoires collected during three selection rounds, the green bars represented the “Recovery” phage repertoires collected in the second and third rounds and the yellow bars correspond to the “Healthy” phage repertoires collected during the three selection rounds.

7.1.4. Control of phage purity

As contamination of phages by wild type (WT) phages is a recurrent problem during phage display selection, in each selection round the purity of the phage repertoire collected was controlled by PCR and subsequently by agarose gel electrophoresis (**Fig. 16**).

The fragments of phage DNA from the selected repertoires present a recombinant insert fused to the pIII gene, encoding peptide ligands of twelve amino acids. As the WT phages do not present recombinant insert, phage repertoire contamination with WT phages can be detected on agarose gel electrophoresis of the PCR products where WT phages appear as a shorter fragment than the phage DNA fragments of the phage display selection.

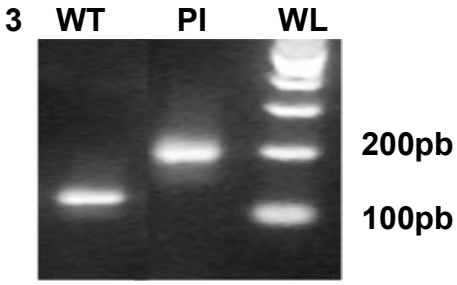

Fig. 16. Purity analysis of the harvested phage repertoire: Electrophoresis of the PCR products from the phage with a peptide insert (PI) (190pb) *vs* WT (160pb), run on agarose gel 1.6% with a weight ladder (WL) of 1000-100pb.

7.2. Subtraction EAE *vs* Healthy phage repertoires

We have obtained phage repertoires of EAE and healthy CNS. We can expect that many clones present in both repertoires might be identical due to the fact that compared to the healthy CNS; most of the CNS in the EAE is not affected by pathological development. In order to enrich the phage repertoire for peptides specific of EAE CNS tissues we applied a strategy recently developed in the laboratory (Patent FR 2952071-A1, Boiziau, Vekris, Petry) that consist of a physical DNA subtraction between the phage DNA of the EAE repertoire and as subtractor the amplified DNA of the healthy repertoire.

The technique is based on the hybridization between a single stranded circular DNA $^{(+)}$ from the phage repertoire (EAE selection) and a single stranded linear DNA $^{(-)}$ from the phage repertoire (Healthy selection) (**Fig. 17**). The hybridization was performed in conditions favoring the stability of the hybrids with homologous peptide encoding sequences. Thus the hybridized common sequences between EAE phage repertoire and healthy phage repertoire were processed by Kpn1 digestion proximal to the 5' position of the recombinant DNA. In contrast not common sequences, as they failed to form stable hybridization, remained as single stranded

DNA, which were not suitable substrates for the restriction nuclease Kpn1. The remaining circular DNA sequences that were only present in the EAE repertoire could not be hybridized and were able to be separated by their ability to transform and replicate in *Escherichia coli.*

E. coli bacteria are indeed able to process circular DNA transformants to produce the (replicative form) RFII necessary for phage propagation, while linear DNA molecules are rapidly degraded by bacterial exonucleases. In this way only phage peptides specific of EAE CNS (a circular DNA+ single strand) were amplified in *E. coli*.

Thus, after DNA subtraction were enriched EAE specific phage DNA in a SUBTRACTION repertoire, which was sent to Massive sequencing.

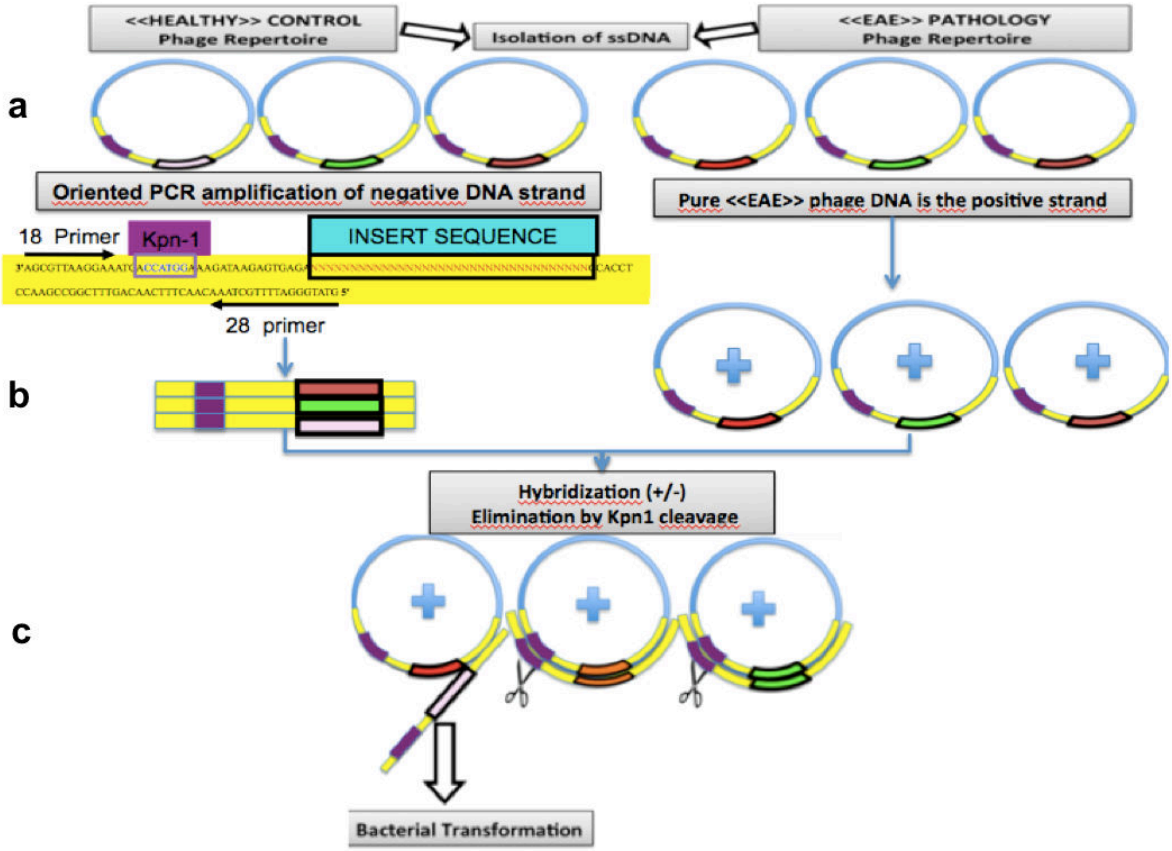

Fig. 17. DNA Subtraction: a) Phage DNA isolation from "EAE" and "Healthy" repertoires, **b)** Common sequences between the single strand circular DNA $^{(+)}$ strand (EAE repertoire) and single stranded linear DNA $^{(-)}$ strand (Healthy repertoire) were hybridized and **c)** the hybridized sequences present as a local double strand were eliminated by Kpn-1 digestion. In contrast the single strand DNA $^{(+)}$ (EAE specific) remained circular and then was able to transform bacteria and be amplified.

7.3. Phage peptide Sequencing

7.3.1. Massive sequencing: First quantitative data

For reasons of time only the repertoires collected from CNS of EAE rats with acute neuroinflammation, healthy rats and the "EAE-Healthy" SUBTRACTION repertoires were submitted to massive sequencing analysis (NGS, next generation sequencing).

Massive sequencing NGS was performed on the plateforme de Génomique Fonctionnelle from Bordeaux University on an Illumina Genome Analyzer IIx.

The encoding variable peptide repertoires allowed defines a total of about 3.1 million reads (**Fig. 18**).

The peptide encoding parts of each read was extracted using a Galaxy workflow and translated into peptide sequences. **Based on http://www.cgfb.u-bordeaux2.fr/fr/content/galaxy-un-workflow-pour-l%E2%80%99analyse-bioinformatique**.

The numbers of individual peptides in each repertoire (13308, 44278 and 38681 for EAE acute, Healthy and Subtraction respectively, are far lower than the numbers of reads, because of redundancy: in the EAE repertoire, 23 peptides encoding sequences were found more than 1000 times (from 1032 to 269855). In the Healthy repertoire, it was the case for 238 peptides (from 1003 to 20251) (**Fig. 19**).

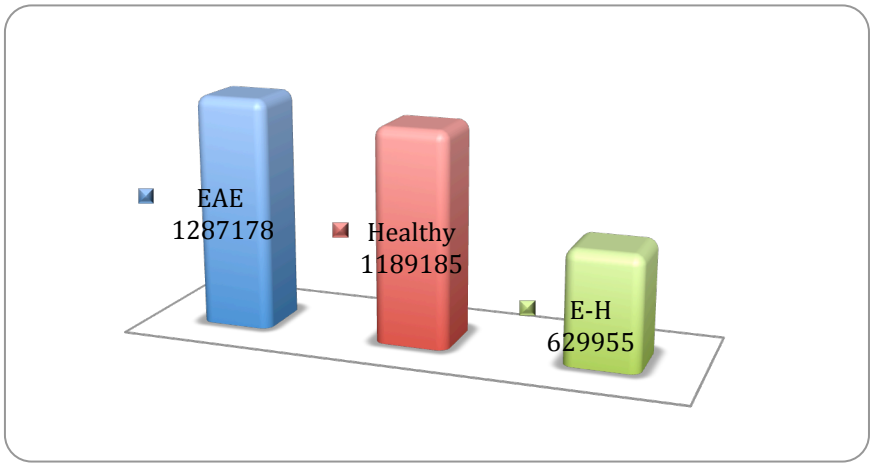

Fig. 18. Massive sequencing reads: Peptide DNA sequences selected from a phage display selection in the CNS of EAE «acute », "Healthy" controls and "subtraction" between EAE and Healthy phage repertoires.

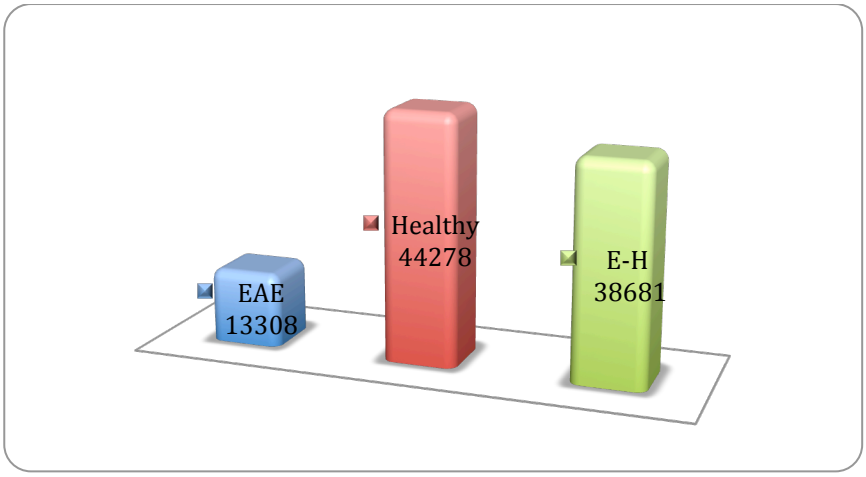

Fig. 19. Individual peptide sequences: Peptides sequences selected from EAE, Healthy and Subtraction repertoires.

7.3.2. EAE specific peptide sequences

The EAE repertoire had 4098 sequences in common with the subtraction repertoire. Peptides common to EAE and the Healthy repertoire were subtracted with a high efficiency of 97%.

3% (n = 422) peptides of Healthy repertoire remained in the subtraction repertoire. From those 234 sequences presented a low concentration in the subtracting DNA of the Healthy repertoire, which probably failed to hybridize to their counterpart DNA during the 2 h hybridization.

For the remaining 188 peptides representing about 1% of the total Subtraction repertoire, their presence was possibly aberrant, as these sequences were not read in the EAE repertoire (**Fig. 20**).

In addition 12 sequences were abundantly present in the EAE repertoire and poorly in the Healthy one.

From the 4098 common peptides between the EAE and the Subtraction repertoires 3914 are enriched in the Subtraction repertoire, while the remaining 184 seemed to be residues of incomplete subtraction. It might be difficult to avoid this source of background by increasing the hybridization time without compromising the integrity of clones of interest, which might be severely degraded at the temperature of hybridization (85 °C).

The peptide diversity in the Subtraction repertoire was higher than in the EAE repertoire that was used to create it (38681 *vs* 13308 different peptides). Although there is no proof, this fact could be explained by the elimination of highly frequent sequences common to both the EAE and Healthy repertoires. Such elimination would allow the sequencing of relatively minor clones of the EAE repertoire persisting in the Subtraction repertoire. In the following steps, however, only those sequences from the Subtraction repertoire that were also identified in the EAE original repertoire were considered for Bioinformatics analysis.

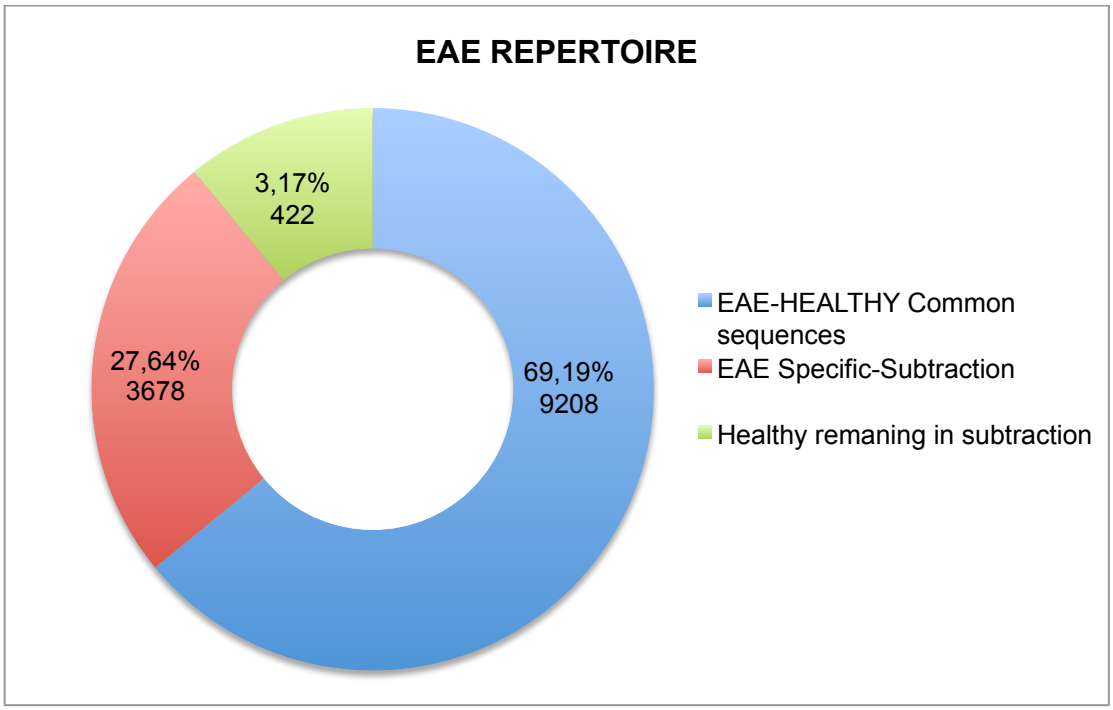

Fig. 20. Peptide sequences EAE specific: From the 13308 peptide sequences present in the EAE repertoire, 4098 sequences are enriched in the Subtraction repertoire. 422 sequences are also present in the Healthy repertoire with low concentration. The 3678 remaining peptides are considered as EAE specific.

7.4. Bioinformatics analysis: characterization of phage peptide sequences highly present in EAE and Healthy repertoires

7.4.1. Analysis of the peptide occurrence in the repertoires

Peptide sequences were classified according to their occurrence in the repertoires, the **table 1** shows a list of clones that were recovered with high occurrence in the EAE repertoire (202 to 269.855 times) and low occurrence in the Healthy repertoire (≤ 52 times). The **table 2** is the other side of high occurrences in the Healthy repertoire (331 to 1900 times) and low in the EAE one (≤ 3).

The high occurrence values to EAE and healthy peptide sequences can be directly related with a high specificity to each repertoire and could be considered as potential molecules to target the neuroinflammatory CNS lesions, as their association with the healthy CNS tissue was very low. However, it was necessary to verify that the high occurrence values do not appear as artifacts of the bioformatics analysis or amplification in bacteria, Nevertheless, this analysis allows to select

potential peptides that are EAE specific to be experimentally tested in priority. In opposite, “Healthy specific” peptides could be still alike peptides of great interest, but were not further studied (**Table 3**).

In addition the 24 peptide sequences selected for their high occurrence in EAE repertoire were also found in the Subtraction repertoire, which highlights their EAE specificity.

The peptide sequences were selected by the *in vivo* phage display strategy and were protected by patents after confirmation of their potential industrial interest. Thereby the sequences were designed with the name: "NGS" related to their identification by Massive Sequencing-Next generation sequencing, "EAE" and "H" related to the repertoire origen (EAE / Healthy) and the numeration of each peptide.

Table 1. Peptides with high occurrence in EAE: 24 peptides with the highest occurrence in EAE were selected and their ratio of E/H occurrence was calculated.

	PEPTIDE 12aa	OCC EAE	OCC HEALTHY	RATIO E/H
High occurrences in the EAE repertoire	NGS-EAE-01	269855	2	134928
	NGS-EAE-02	167644	2	83822
	NGS-EAE-03	135211	3	45070
	NGS-EAE-04	135211	52	2600
	NGS-EAE-05	96588	35	2760
	NGS-EAE-06	93764	40	2344
	NGS-EAE-07	68702	4	17176
	NGS-EAE-08	52306	4	13077
	NGS-EAE-09	45505	28	1625
	NGS-EAE-10	43049	22	1957
	NGS-EAE-11	28820	13	2217
	NGS-EAE-12	20389	9	2265
	NGS-EAE-13	19918	9	2213
	NGS-EAE-14	11324	5	2265
	NGS-EAE-15	9641	2	4821
	NGS-EAE-16	9610	5	1922
	NGS-EAE-17	6583	3	2194
	NGS-EAE-18	4235	3	1412
	NGS-EAE-19	1210	1	1210
	NGS-EAE-20	887	2	444
	NGS-EAE-21	656	1	656
	NGS-EAE-22	645	1	645
	NGS-EAE-23	375	1	375
	NGS-EAE-24	202	1	202

Table 2. Peptides with high occurrence in Healthy: 25 peptides with the highest occurrence in Healthy were selected and their ratio of H/E occurrence was calculated.

	PEPTIDE 12aa	OCC HEALTHY	OCC EAE	RATIO H/E
High occurrences in the Healthy repertoire	NGS-H-01	1399	2	699,5
	NGS-H-02	1360	1	1360
	NGS-H-03	1082	1	1082
	NGS-H-04	1061	2	530,5
	NGS-H-05	924	1	924
	NGS-H-06	914	1	914
	NGS-H-07	812	1	812
	NGS-H-08	799	1	799
	NGS-H-09	597	0	597
	NGS-H-10	549	0	549
	NGS-H-11	519	0	519
	NGS-H-12	511	0	511
	NGS-H-13	493	0	493
	NGS-H-14	473	0	473
	NGS-H-15	452	0	452
	NGS-H-16	427	0	427
	NGS-H-17	408	0	408
	NGS-H-18	406	0	406
	NGS-H-19	405	0	405
	NGS-H-20	394	0	394
	NGS-H-21	362	0	362
	NGS-H-22	354	0	354
	NGS-H-23	337	0	337
	NGS-H-24	331	0	331
	NGS-H-25	331	0	331

7.4.2. BLAST analysis of some peptide selected sequences

The peptide sequences with a higher occurrence in EAE repertoire, which are also present in the Subtraction repertoire (NGS-EAE-01 to NGS-EAE-24) and Healthy repertoire (NGS-H-01 NGS-H-08) were aligned by blast against Rattus norvegicus, Homo sapiens and mammals. Then the proteins with the highest homology to each peptide are presented below (**Tables 3 and 4**).

The blast analysis allows giving a first approximation of the proteins whose high homology designs them as potentially mimicked by the phage peptide selected from each repertoire EAE, Healthy.

Acording to the goal of this project, here we present in the **table 4** some peptides showing a homology with proteins that can be ligands of expressed targets on the brain endothelial cell surface and that could be related with the BBB alterations in neuroinflammatory conditions, having an important implication in the development of neuroinflammatory diseases such as multiple sclerosis.

Several proteins could be identified by various peptides potentially mimicking different regions of the same protein, such as:

- Mucin-16 (*Homo sapiens*): NGS-EAE-02, NGS-EAE-05, NGS-EAE-08, NGS-EAE-22), (underlined in red).

- Laminin 5 (*Homo sapiens*, *Rattus norvegicus* and *Mus musculus*): NGS-EAE-01 and NGS-EAE-15 have homology at the same region conserved in *Homo sapiens*, *Rattus norvegicus* and *Mus musculus* (underlined in yellow).

On the other hand, peptides, which have homology with some proteins in different mammals, are also presented. This allows considering them as a conserved motif in mammals. In contrast, there are some peptides, which have not presented homology with any protein related to BBB cell surface.

Table 3. EAE Peptide BLAST Alignments: Proteins expressed in rats, human and mammals, which present a high homology to the peptides selected with a high occurrence in the EAE repertoire, are present here as follows.

PEPTIDE 12aa	Alignments (Rattus norvegicus)	Alignments (Homo sapiens)	Alignments (mammals)
NGS-EAE-01	-**Laminin 5** -Immunoglobulin superfamily member 1	- **Laminin 5** -Leucine-rich repeat transmembrane protein flrt3 -Immunoglobulin superfamily member 1 isoform 4	- **Laminin 5**
NGS-EAE-02	-Toll-like receptor 7 -Serine-rich and transmembrane domain-containing protein 1	-**Mucin 16** -Toll-like receptor 7 -Solute carrier family 22 member 17	-**Mucin 16** -Igsf member 10 - Pcdh beta 13
NGS-EAE-03			
NGS-EAE-04			
NGS-EAE-05	-Disabled homolog 2-interacting protein	-**Mucin-16** -Collagen alpha-1 -Mucin-5b	- **Mucin 16** - Disintegrin & metalloproteinase isoform
NGS-EAE-06		-Mucin-17	- Tenascin-R
NGS-EAE-07	-Netrin receptor UNC5D -P-selectin glycoprotein ligand 1	-P-selectin glycoprotein ligand 1	-Thrombospondin-1 -Putative EGF-like - Mucin 6
NGS-EAE-08	-Proline-rich protein 11	-Afadin isoform 1 and 2	- **Mucin 16**
NGS-EAE-09			
NGS-EAE-10		-Toll-like receptor 9 precursor	- Pred: ADAMTS-like
NGS-EAE-11	-B-cell CLL/lymphoma 9 protein		
NGS-EAE-12	-Kinesin-like protein KIF13B Membrane protein. -IL-10 receptor subunit beta-like		
NGS-EAE-13	-Solute carrier family 22 member 3	Solute carrier family 22 member 3	- Pro-, glu-, leu-rich protein 1
NGS-EAE-14			-
NGS-EAE-15	**-Laminin -5**	**-Laminin 5**	**-Laminin 5**

NGS-EAE-16	**-Laminin subunit beta-1**	-Solute carrier family 13 member 2 isoform b	
NGS-EAE-17	-Tumor necrosis factor ligand superfamily member 13 -Immunoglobulin superfamily member 21-like		
NGS-EAE-18	-Lymphocyte antigen 6 complex locus protein g5b -A disintegrin and metalloproteinase with thrombospondin motifs 2		
NGS-EAE-19	-Toll-like receptor 7 -Integrin beta-1	- Ig sf member 10	
NGS-EAE-20	-Matrix metalloproteinase-17		
NGS-EAE-21	-Epidermal growth factor receptor substrate 15		
NGS-EAE-22	-Kremen protein 1	**-Mucin-16**	
NGS-EAE-23	-Toll-like receptor 4		
NGS-EAE-24	-Precursor IL-1 -Receptor accessory protein-like 1		-ECM protein 2 precursor -IL-1 receptor accessory protein-like 1

In the **table 4** are presented some peptides with high occurrence in Healthy repertoire which present homology with some proteins expressed on the BBB surface. According to these results, it is important to note that some of these proteins are constitutive of the BBB, such as tight junction protein ZO-1. Therefore any change in the expression of this protein may be indicative of BBB disruption, thus the peptide that mimics this protein can be used as a potential biomarker of normal BBB conditions.

Table 4. Healthy Peptides BLAST Alignments: Proteins expressed in rats, human and mammals, which present a high homology to the peptides selected with a high occurrence in the Healthy repertoire, are present here as follows.

NGS-H-01	-Inducible T-cell costimulator		
NGS-H-02	-Multidrug resistance protein 1		- Metal transporter - Protein fam71f1
NGS-H-03			
NGS-H-04	-Tight junction protein ZO-1		- ZO-1
NGS-H-05		Catenin alpha-1	
NGS-H-06	-Transmembrane glycoprotein NMB precursor -Integrin alpha-11		
NGS-H-07	Laminin subunit alpha-2		
NGS-H-08	Antithrombin-III		

7.4.3. Spack analysis

To further analyze the thousands of sequences identified after massive sequencing, peptide sequences with high scores selected from every phage peptide repertoires (EAE, Healthy and Subtraction selections) were processed by peptide clustering. Each cluster contains homologous peptide sequences, which present variations in some amino acids and are represented by one peptide sequence for which the frequency is the highest one.

The packs of clusters for each phage repertoire were compared between them to identify the peptide sequences highly present in the EAE repertoire in the way that a bioinformatics subtraction was performed and then compared with the DNA SUBTRACTION repertoire. Thus the sequences with highly occurrence in the EAE repertoire are enriched in the SUBTRACTION repertoire and set as EAE specific.

The sequences were also organized in both directions of reading (5'-3' or 3'-5`), to include the homologous proteins according to the two possible conformational orientations of the peptides.

Given that some reports have shown that some amino acids located at the ends of any peptide displayed by the phage peptide library can be used by the assembly machinery of phage particles in bacteria during amplification, it is possible that these amino acids cause distortions of the repertoires during phage amplifications. To avoid artificial assignment of importance of these flanking amino acids in the phage peptide ligand to recognize the target we considered the central 8 amino acids for further analysis (**Steiner et al, 2006**).

According to that the peptide cluster sequences of the EAE and SUBTRACTION repertoires, respectively, were reduced from 12aa displayed in the phages to 8aa by removal of the first two amino acids and the last two ones.

These clusters were submitted to "Spak application" to identify putative protein mimics of the phage displayed peptide sequences on Mus musculus data base. Spack was built on Mus musculus data base, to have a major approximation of the proteins expressed in rats and humans by genetic similitude.

Spack application, which was built in collaboration of INSERM U1049, Bordeaux (**Dr. Antoine VEKRIS**) and CBiB, Plateforme de Génomique Fonctionnelle de Bordeaux (**Dr. Macha Nikolski**) is accessible (**http://services.cbib.u-bordeaux2.fr/spack/**).

The Spack application creates "packs" of peptides matching by homology with some parts of a single protein, then builds "super packs" of several proteins sharing homology with a set of peptides and finally scoring its findings according to the size of the packs and the similarities to the identified proteins.

Functional informations about the extracted proteins were gathered by feeding the results to "StRAnGER and String", which enriches the Spack analysis with protein functions and participation in signal transduction or metabolic pathways.

In this way some of the EAE specific peptide sequences and their homologous protein, putative mimics obtained by SPACK analysis are presented in the **table 6**. The proteins presented have been chosen according to their expression or interaction on the BBB extracellular surface, which can be potentially mimicked by the phage peptide ligands.

The peptide sequences are named as NGS-EAE (#) a or b corresponding to sequences in both directions.

Peptides sharing homology with the same protein in different regions were identified, such as: Mucin-1: NGS-EAE-19, NGS-EAE-02a, Aquaporin-3: NGS-EAE-23, NGS-EAE-06a, Adherents junction-associated protein 1: NGS-EAE-18: NGS-EAE-01b, NGS-EAE-02a.

Besides some peptides share homology with proteins of the same Mucin family, such as: NGS-EAE-02b (Mucin-4), NGS-EAE-08 (Mucin-15).

In comparison with the results obtained by blast analysis, it should be noted that in blast analysis the peptide NGS-EAE-03 and 04 do not present homology with any protein expressed in rats or human, that could be considered ligand of BBB ECs, however in spack analysis those appear with homology to one protein expressed in mus musculus.

By contrast in SPACK analysis NGS-EAE-09-10, 12-14, 20-22 and 24 expressed in mus musculus do not present homology with any protein related as a ligand of BBB ECs, however, by blast analysis those appear with homology to some possible ligands proteins expressed in rats and humans.

Table 5. Spack analysis: Proteins homologous to the peptide sequences with EAE specific peptides.

PEPTIDE 12aa	**Alignments (mus musculus) spack**
NGS-EAE-01a	-Metalloprotease TIKI2
NGS-EAE-01b	-Adherents junction-associated protein 1
NGS-EAE-02a	- Adherents junction-associated protein 1 -**Mucin-1**
NGS-EAE-02b	-Leucine-rich repeat-containing protein 19 -**Mucin-4**
NGS-EAE-03a	-Inducible T-cell costimulator
NGS-EAE-03b	-Inducible T-cell costimulator
NGS-EAE-04	-Inducible T-cell costimulator
NGS-EAE-05a	-CMRF35-like molecule 9 isoform 1 and 3 -Transmembrane channel-like protein 6 isoform 2 -Urocortin-2

NGS-EAE-05b	-Angiomotin -Autoimmune regulator isoform 1 -Tumor necrosis factor receptor superfamily member 19L
NGS-EAE-06a	-Aquaporin-3 -Synaptogyrin-4
NGS-EAE-06b	-C-C motif chemokine 2 p -Cortexin-3 -Transmembrane protein 42 isoform 1
NGS-EAE-07	Transmembrane protein 215
NGS-EAE-08	**-Mucin-15**
NGS-EAE-09	
NGS-EAE-10	
NGS-EAE-11a	-Phosphatidylinositol 4,5-bisphosphate 5-phosphatase A 126
NGS-EAE-11b	
NGS-EAE-12	
NGS-EAE-13a	-Phosphatidylinositol 4,5-bisphosphate 5-phosphatase A 126 -Fibronectin type III domain-containing protein 1 -Protein enabled homolog isoform 1 -Vasodilator-stimulated phosphoprotein isoform 1 -Voltage-dependent L-type calcium channel subunit beta-1 isoform C
NGS-EAE-13b	-Fibronectin type III domain-containing protein 1 -Proline-rich transmembrane protein 4 -Spastin isoform 1
NGS-EAE-14	
NGS-EAE-15a	-Metalloprotease TIKI2
NGS-EAE-15b	-Adherents junction-associated protein 1
NGS-EAE-16	-Proline-rich transmembrane protein 4
NGS-EAE-17	-voltage-dependent L-type calcium channel subunit beta-1 isoform C
NGS-EAE-18	-Proline-rich transmembrane protein 1 -Phosphatidylinositol-binding clathrin assembly protein isoform 1
NGS-EAE-19	-Adherents junction-associated protein 1 **-Mucin-1**
NGS-EAE-20	
NGS-EAE-21	
NGS-EAE-22	
NGS-EAE-23	-C-C motif chemokine 2 precursor -Aquaporin-3
NGS-EAE-24	

7.5. Phage Cloning

In parallel with the Bioinformatics analysis of the NGS results, we have made a physical selection of 100 phage clones from EAE and SUBTRACTION repertoires to obtain sequences of EAE specific peptide ligands. The phage clones were randomly picked to be characterized by sequencing. 30 clones showed individual sequences, while the others were duplicates of them.

Individual phage clones which present different sequences were compared with the sequences obtained from NGS of EAE and Subtraction repertoires.

The clones, which were present with high occurrence in EAE and SUBTRACTION repertoires, were selected to be characterized by immunohistochemistry and immunobloting.

7.5.1. Characterization of phage clones by immunohistochemistry

From the clones randomly selected and compared with sequence repertoires (NGS), only the clone 88, whose sequence is denominated NGS-EAE-22, was found with high occurrence in the EAE repertoire against healthy repertoire (645-1 E: H) and is also part of the Subtraction repertoire.

However, another clone (clone 45) was found with lower occurrence, being 4 times more present in EAE than in Healthy and also present in the Subtraction repertoire. The sequences of the clones remaining are not present in either EAE or SUBTRACTION NGS repertoire.

Therefore the clone 88 was selected to be tested for binding characterization on CNS tissue of EAE and Healthy rats in parallel with a binding test on hCMEC/D3 cells under different conditions of stimulation.

7.5.1.1. Phage clone binding on CNS tissues

Brain and spinal cord extracted from EAE rats suffering maximum clinical score and Healthy control were studied for binding of phage clone 88.

The phage binding is detected with M13 + Fd bacteriophage coat proteins and the respective polyclonal IgG antibody Cy3 (Red), in co-labeling of RECA-1 on the ECs, which is detected by polyclonal IgG antibody Alexa Fluor® 488 (green) (**Fig. 21**).

EAE spinal cord presents high leukocyte infiltration around blood vessels into the parenchyma, which is characteristic in the neuroinflammatory lesions. Phage clone 88 presents binding to the vascular structure, potentially the ECs in EAE but no binding in Healthy control.

EAE

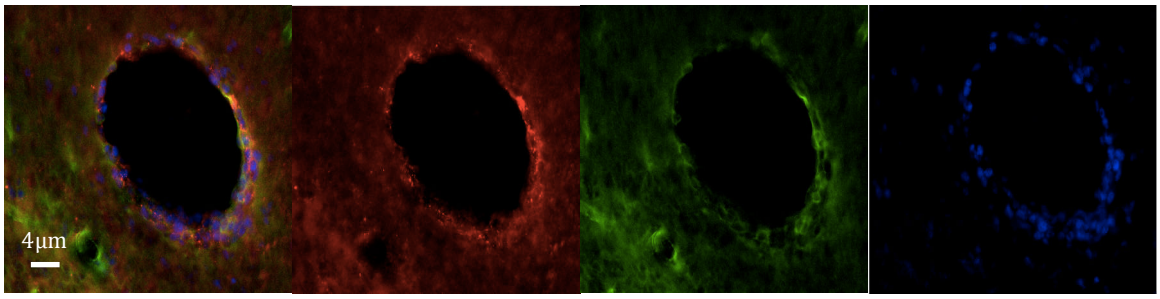

HEALTHY

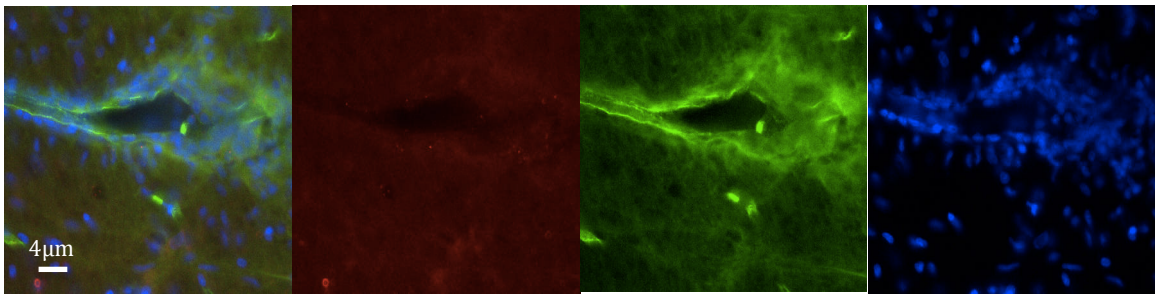

Fig. 21. Phage clone 88 binding to the spinal cord: The clone 88 incubated on spinal cord slices (30µm thick) from EAE rats and Healthy controls is detected by Cy3 (Red) labeling, ECs labeling by Alexa Fluor® 488 (green) and the cellular nucleus with DAPI (blue).

7.5.1.2. Phage clone binding to brain ECs hMEMC/D3 under IL1β stimulation *vs* controls

The hCMEC/D3 cell line is a long-lasting source of human brain ECs, which express specific BBB properties such as cell surface adhesion molecules and tight junction markers, (PECAM-1, ICAM-1, ICAM-2, VE-cadherin, and catenins, ZO-1, JAM-A, and claudin-5) (**Cucullo et al., 2008**). Moreover the expression of chemokine receptors was detected which makes them responsive towards stimulation by proinflammatory cytokines (**Weksler et al., 2013**). Proinflammatory

cytokines have been shown to be involved in the regulation of BBB permeability, (**Cucullo et al., 2008**). In multiple sclerosis it has been reported the action of IL-1β in brain injury by BBB breakdown occurring after 2 h of IL-1 stimulation and subsequent leukocyte extravasation. In addition, increased paracellular permeability of hCMEC/D3 cells grown as a differentiated monolayer and then stimulated for 2 h with IL-1β was reported (**Blamire et al., 2000; Fasler et al., 2010**).

According to these reports we have used hCMEC/D3 cells grown in monolayer during 15 days to get the differentiated tight junction formation and then stimulated or not with the recombinant human cytokine IL-1β (20 ng/ml rhIL-1β for 2 h). The IL-1β stimulation allows to simulate neuro-inflammatory conditions and to induce the expression of profile proteins that could be related to the BBB breakdown and paracellular permeability.

Given that the clone 88 presents high affinity for the BBB ECs on infiltrating blood vessels in CNS tissues, we have tested the direct binding of this clone on hCMEC/D3 cells (stimulated or not with L-1β).

The phage clone 88 was incubated during 5 h on the cells and the detection was carried out by labeling with rabbit polyclonal antibody to M13 + Fd bacteriophage coat proteins and the respective Cy3 conjugated secondary antibody Goat anti-rabbit polyclonal IgG (Red).

As shown in the **figure 20** the clone 88 presents strong binding to hCMEC/D3 cells under IL- 1β stimulation, but no significant binding in resting conditions.

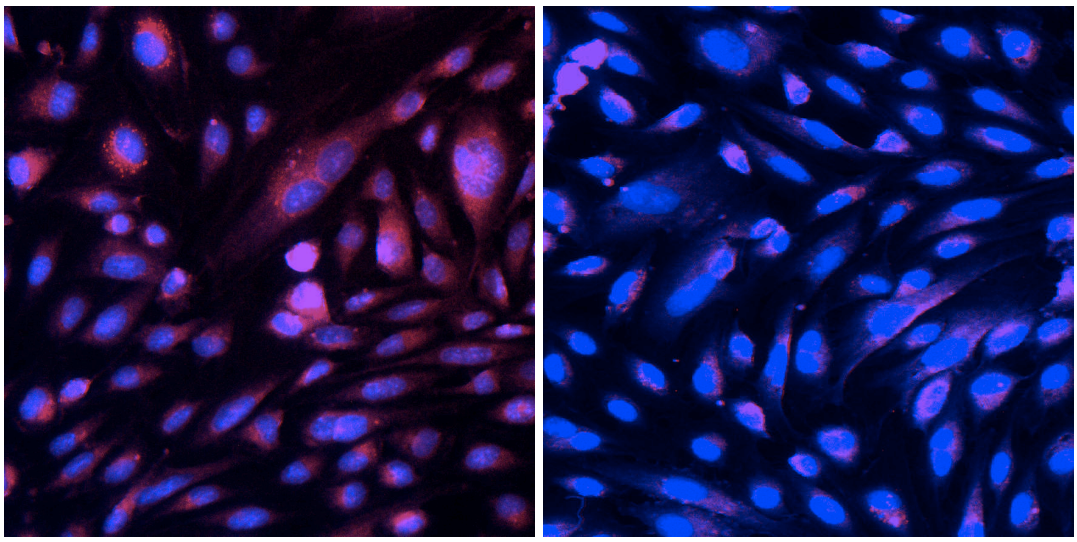

+IL-1β **-IL-1β**

Fig. 22. Phage clone 88 binding to hCMEC/D3 cells: The clone 88 incubated on hCMEC/D3cells +IL-1β stimulation or not is detected by Cy3 (Red) labeling and the cellular nucleus with DAPI (blue).

7.5.2. Characterization of phages, clones by binding to protein extracts from hCMEC/D3

We have tested the binding of several phage clones randomly selected on nitrocellulose membranes soaked with protein extract of hCMEC/D3 cells stimulated or not with IL-1β (the experiment was repeated three times).

The phage binding was revealed as dots on the membrane after incubation with an anti-M13 antibody (rabbit polyclonal antibody to M13 + Fd bacteriophage coat proteins) followed by anti-rabbit HRP.

The experiment was controlled with the WT phages (negative control) and phage clone 48 (EAE specific positive control), selected in a previous work in (INSERM U1049).

Phages showing major differences between IL-1β stimulation or not, are presented in the **fig. 23**.

It is important to highlight that the clone 88 is efficiently bound on protein extract of hCMEC/D3 cells during IL-1β stimulation and shows much less affinity

without IL-1β stimulation. The positive control clone 48 has the same behavior. In comparison, the clone WT (wild type) does not present any binding in either of these two conditions. This reinforces the results obtained in CNS tissues and hCMEC/D3 cell culture which allows to consider the clone 88 as a potential binder to neuroinflammatory lesions.

Among the 29 phage, clones that were tested, some other clones showed also to be better binders when cells were IL-1β activated than with not activated. These indicate that the expression of the potential targets increases with the stimulation. Although most of the tested clones showed reproducible results in the 3 replicates of the Dot blot assay, a few clones did not present conclusive results.

Given that, not all the sequences of these phage clones were found to be present in the group of EAE specific peptide sequences obtained after bioinformatics analysis (NGS results), the fact that some of these clones are strongly bound during IL-1β stimulation can be explained because the extracted proteins have changed their structural conformation from the native form presented in the cells, thus they can show all their recognition domains and then the affinity of phage binding can be increased.

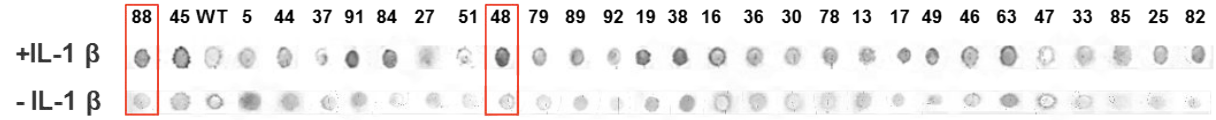

Fig. 23. Dot-blot Phage binding on protein extracts (900 µg/mL) of hCMEC/D3 BBB model: N° represent individual phages clones, +IL-1β = stimulation, -IL-1β= control without stimulation. The test was repeated for three times under the same conditions with phage clones at 10^{10}/µL.

7.6. Synthesis and characterization of EAE specific peptides

After the two parallel analyses of the peptide sequences given by the massive sequencing (Blast and Spack), we determined peptide sequences that could be chemically synthesized for further characterization.

Four peptides sequences with high occurrence in the EAE repertoire and also present in the Subtraction repertoire, were chosen to be synthesized following this schema: Nter-GGXXXXXXXXXGGGKGK-Cter, where XXXXXXXXX corresponds to the 8 amino acids peptide, Nter-GG, N terminal extension by two glycines as spacer

for the N-terminal amine, GGGKGK-Cter, three glycines as spacer for the KGK tripeptide, presenting two lateral chain primary amines for attachment to NHS-label biotin (see below).

Thus the final constructions were:

Biotin-LC-Gly-Gly- NGS-EAE-06 -Gly-Gly-Gly-Lys-Gly-Lys-OH
Biotin-LC-Gly-Gly- NGS-EAE-05 -Gly-Gly-Gly-Lys-Gly-Lys-OH
Biotin-LC-Gly-Gly- NGS-EAE-24-Gly-Gly-Gly-Lys-Gly-Lys-OH
Biotin-LC-Gly-Gly- NGS-EAE-23 -Gly-Gly-Gly-Lys-Gly-Lys-OH.

7.6.1. Peptide binding on brain ECs hCMEC/D3 under IL-1β and VEGF stimulation *vs* controls

Unlike IL-1β which directly induces BBB permeability through activation of chemokine receptors which in turn induces the break of molecular tight junctions interaction, VEGF increases BBB rupture and permeability through VEGF-VEGF-R interaction which activates phospholipase C (PLC) downstream signaling pathway, having effect on intracellular calcium ions concentration, which in turn activates also the nitric oxide synthase and subsequent transvascular vesicular pathways or vacuolar channel activation. In this way IL-1β and VEGF are proposed here as ~~a~~ model of BBB permeability and rupture stimulators which are also up-regulated in neuroinflammation (**Cucullo et al., 2008; Bates et al., 2002; Nowacka and Obuchowicz, 2012**).

According to that, hCMEC/D3 cells were grown during 15 days and stimulated with IL-1β (20 ng/mL) or VEGF (50 ng/mL) *vs* controls overnight at incubator at 37 °C with 5 % CO_2. After that the cells were incubated with streptavidin-biotin-peptide complex during 5 h at RT.

The labeled peptides are named as they appear in the NGS list of peptide sequences with high occurrence in EAE and subtraction repertoire.

As shown in the **figure 24** the four peptides are higher binders to IL-1β and VEGF stimulated hCMEC/D3 cell culture than without stimulation. This reinforces the results obtained from NGS Bioinformatic analysis, by which the four peptides

represent potential binders to neuroinflammatory lesions.

A) NGS-EAE-05

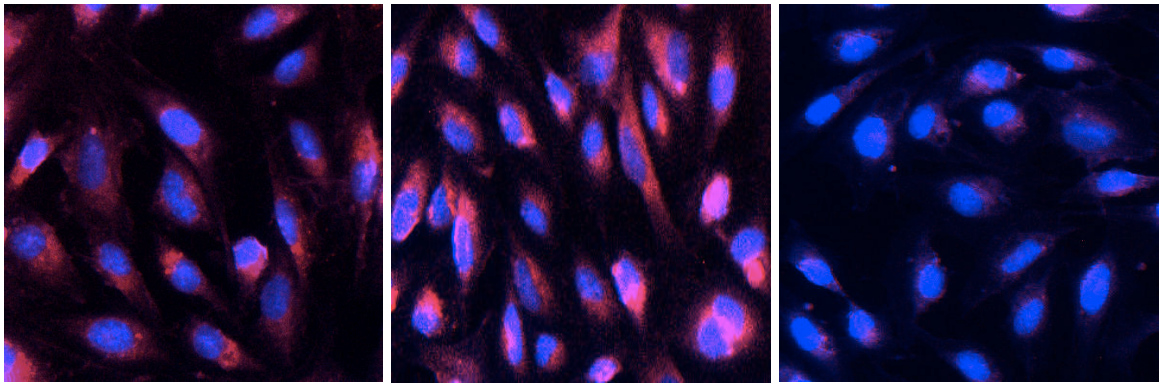

IL-1β **VEGF** **hCMEC/D3**

B) NGS-EAE-06

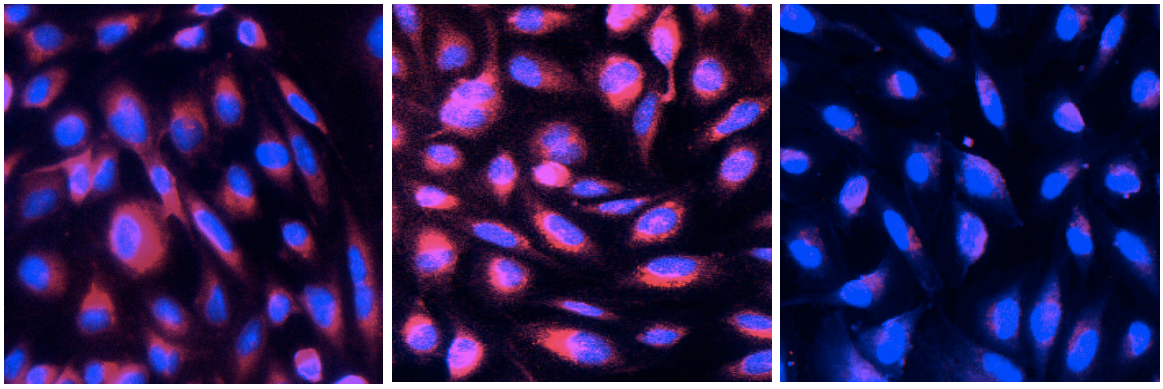

IL-1β **VEGF** **hCMEC/D3**

C) NGS-EAE-23

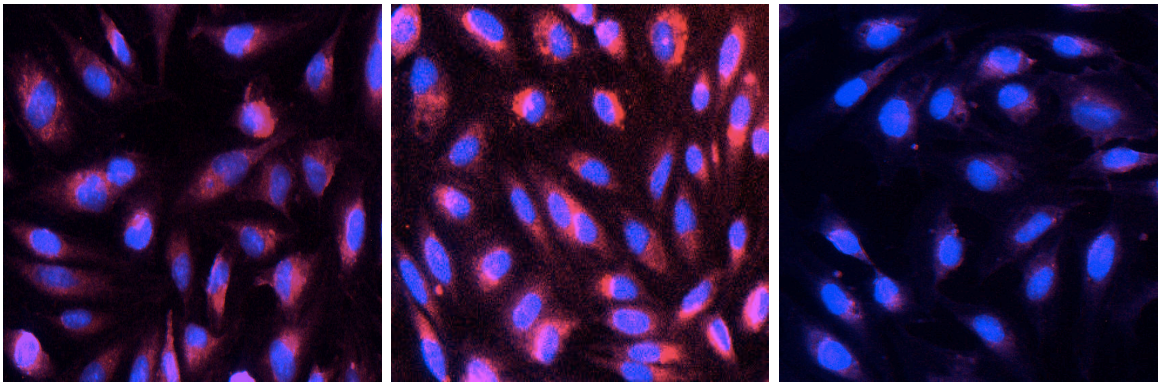

IL-1β **VEGF** **hCMEC/D3**

D) NGS-EAE-24

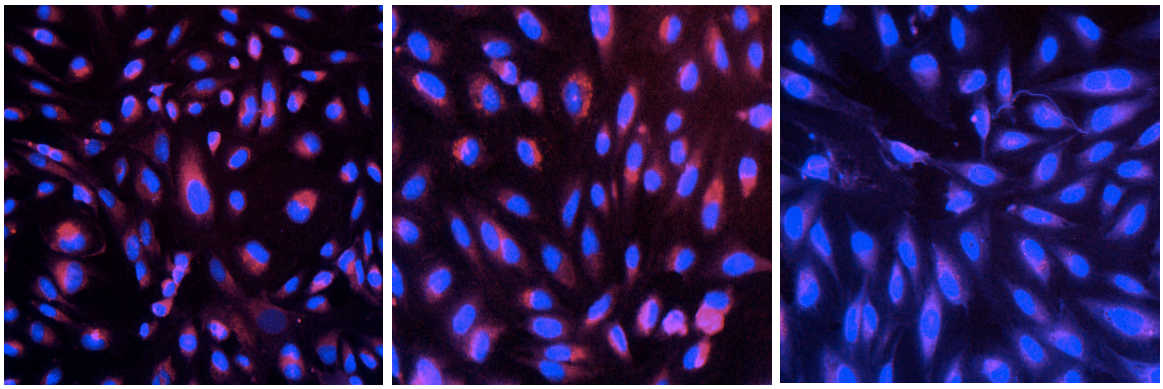

IL-1β **VEGF** **hCMEC/D3**

Fig. 24. Peptide binding on brain ECs hCMEC/D3: Four peptides biotin-streptavidin labeled: **a)** NGS-EAE-05, **b)** NGS-EAE-06, **c)** NGS-EAE-23, **d)** NGS-EAE-24, were incubated on the hCMEC/D3 cells stimulated with IL-1β and VEGF vs controls hCMEC/D3 without stimulations as is represented bellow of the pictures. The peptide labeling is detected by streptavidin dye-flourochrome (red).

7.7. Characterization of target proteins to phage peptide ligands

Two phage clones that were identified as specific for EAE tissue: Ph88 (see above) and Ph48, were further studied to identify the respective target molecules expressed at the surface of hCMEC/D3 cells IL-1β stimulated and controls. We followed the procedure described by (**Reynolds et al., 2011**).

7.7.1. Immunohistochemistry to detect the crosslinking on human brain ECs hCMEC/D3

The clones 88 and 48 EAE specific and the wild type phage (WT) (negative control) were labeled with Sulfo-SBED and the crosslinking reaction were perfomed on human brain ECs hCMEC/D3 stimulated or not with IL-1β (20 ng/mL rhIL-1β for 2 h).

The labeled phage clones were incubated to three different quantities (10^{10}, 10^{11} and 10^{12} pfu). Then the phages were separated and eluted from the cell culture, thus the Sulfo-SBED arm remaining bound to the phage targets was

detectable with streptavidin dye-flourochrome (green) as shown in the pictures below (**Fig. 25**).

This confirmed that the phage clones 88 and 48 present higher affinity for the hCMEC/D3 stimulated with IL-1β than without stimulation. However the affinity of the clone 48 is higher that the clone 88.

Given that the phage-target affinity was decreased in function of the phage concentration as shown below, we have chosen to work with a higher phage quantity (10^{13} pfu) to search and characterize the targets as is shown in the next experiment.

A) Phage clones at 10^{12} (pfu)

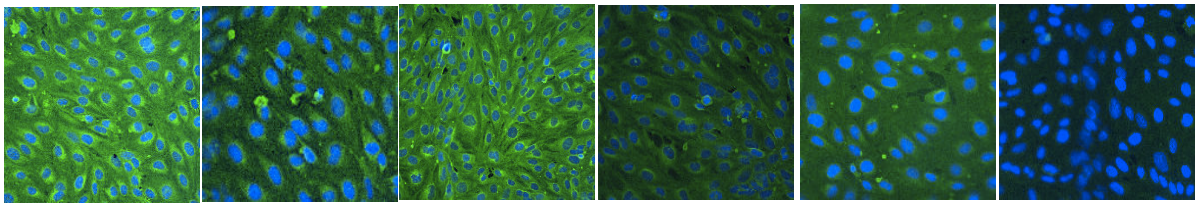

Clone 88 +IL-1β **Clone 88 - IL-1β** **Clone 48 +IL-1β** **Clone 48 - IL-1β** **WT phage +IL-1β** **WT phage -IL-1β**

B) Phage clone at 10^{11} (pfu)

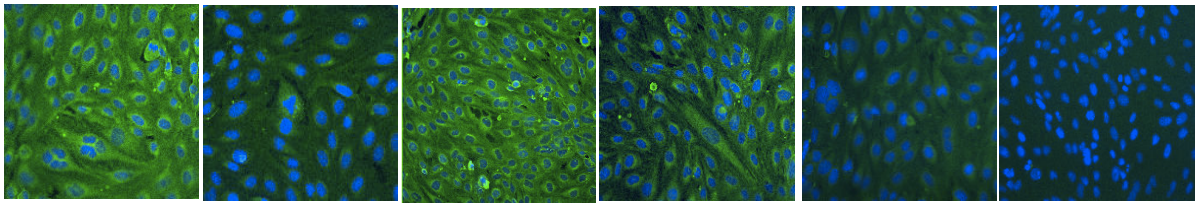

Clone 88 +IL-1β **Clone 88 - IL-1β** **Clone 48 +IL-1β** **Clone 48 - IL-1β** **WT phage +IL-1β** **WT phage -IL-1β**

C) Phage clone at 10^{10} (pfu)

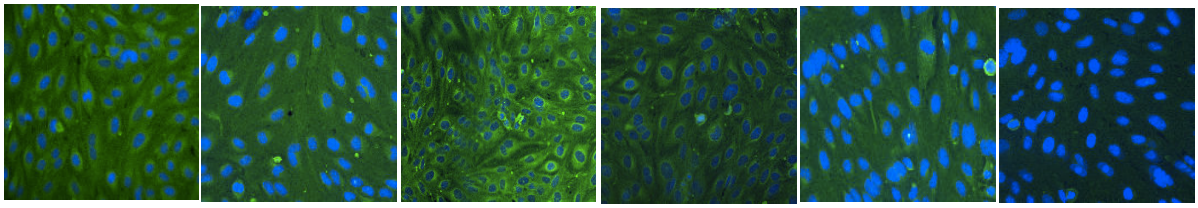

Clone 88 +IL-1β **Clone 88 - IL-1β** **Clone 48 +IL-1β** **Clone 48 - IL-1β** **WT phage +IL-1β** **WT phage -IL-1β**

Fig. 25. Crosslink of phage clone and hCMEC/D3 cells: Sulfo-SBED labeled phage clones (88, 48 and WT) to three different quantities (**10^{12} pfu, 10^{11} pfu, 10^{10} pfu)** were crosslinked with protein targets on the hCMEC/D3 cells stimulated or not with IL-1β. The crosslink is detected by labeling of Sulfo-SBED with streptavidin dye-flourochrome (green).

7.7.2. Target separation by Phage peptide and protein targets cross-linking on human brain ECs hCMEC/D3

Clone 88, 48 and the wild type phage (WT) (negative control) at 10^{13} pfu/mL were labeled with Sulfo-SBED and the crosslinking reaction was performed on hCMEC/D3, stimulated or not with IL-1β. Given that the WT phage does not present any peptide insert, it is supposed to evaluate the background.

The separation of the crosslinked proteins was carried out after cell lysis in non-denaturating conditions and then by incubation with streptavidin magnetic beads. Proteins bound to the magnetic beads were separated by incubation in denaturating buffer (Tris-HCl/ SDS) at 100°C. Then the protein concentration was determined.

The experiment was repeated two times recovering 6 samples from each one:

1. Clone 88 + IL-1β,
2. Clone 88- IL-1β,
3. Clone 48 + IL-1β,
4. Clone 48- IL-1β,
5. WT + IL-1β,
6. WT- IL-1β.

Finally the samples were submitted to Liquid Chromatography/Mass Spectrometry (LC/MS).

7.7.3. Liquid Chromatography / Mass spectrometry analysis (LC/MS)

The protein samples separated from hCMEC/D3, IL-1β stimulated or not, after sulfo-SBED cross-link with phage clones (48, 88 and WT) suppose to be the proteins targets from these clones (the experiment crosslink experiment was repeated two times). Then the six samples from each experimental replicate were run on a SDS-PAGE (PolyAcrylamide Gel Electrophoresis). The protein bands were cut from the gels and then the proteins were prepared for tryptic digestion and LC/MS liquid choromatography-mass spectrometry. **Based on http://www.cgfb.u-bordeaux2.fr/fr/proteome**.

Using the Proteome Discoverer application (Progenesis LC/MS) it was possible to identify proteins recovered in each sample from the mass spectra of digested peptide fragments. This application allows to compare the raw data from mass spectrometry (peaks mass spectra representing the peptide fragments for a given mass and charge) to the information of selected database (Homo sapiens as hCMEC/D3 are human cells).

The intensity of the proteins identified after Bioinformatics analysis was calculated by summing the intensity of the digested peptide fragments, which were detected by LC/MS. The relative normalization was done by dividing the data of each identified protein by the total intensity of all proteins in each sample.
A second normalization was done by calculating separately the ratio of each clone (48 and 88) against the WT phage in the two different conditions:

- 88 + IL-1β/ WT + IL-1β
- 88- IL-1β/ WT- IL-1β
- 48 + IL-1β/ WT + IL-1β
- 48- IL-1β WT- IL-1β).

In the **table 6**, we present the proteins sharing sequence homology with more than three digested peptide fragments, which were detected from each sample after (LC/MS).

The results have shown reproducible significative differences between hCMEC IL-1β stimulated or not during the two experimental replicates, thus the intensity of the proteins recognized by the clones is higher during IL-1β stimulation, which is in agreement with the previous results showing high affinity in inflammatory conditions.

There are also significant differences between the intensity of the proteins appearing to the clone 48 and 88 in the two experimental replicates. As this is noted, these proteins suppose to be higher recognized for the clone 48 than for the clone 88. Therefore, there was not found proteins appearing with differential high intensity for the clone 88. This result is consistent with the fact that the two clones should have different protein targets, however, we have not found a presumable protein target to the clone 88. In addition, in both experiments appear reproducibly

two proteins highly recognized to the clone 48 during hCMEC/D3 IL-1β stimulation which are Fascin and galectin-1.

Table 6. Candidate proteins identified after LC/MS analysis: The table shows some of the proteins identified with Proteome Discoverer application (Progenesis LC/MS) in Homo sapiens data base, which share homology with the peptide fragments detected from LC/MS as possible proteins recognized by the phage clones on hCMEC/D3 cells (IL-1β or not stimulated).
The data were normalized by each sample 1) Dividing the intensity of each protein in the total intensity of all proteins recognized. 2) Dividing the data obtained for each clone by the data obtained for the WT in correspondence with the same hCMEC/D3 stimulation (+ IL1β or -IL1β).

Proteins identified in homo sapiens data base Exp 1	**# Peptide fragments detected**	**Clone 88 + IL1b**	**Clone 48 + IL1b**	**Clone 88 - IL1b**	**Clone 48 - IL1b**
AP-2 complex subunit alpha-2	6	0,93	7,07	1,05	1,13
AP-1 complex subunit mu-1	7	0,76	4,52	0,91	1,30
Huntingtin-interacting protein 1	5	1,10	2,55	0,89	1,12
Fascin	7	0,83	2,56	0,99	0,94
Coronin-1	6	0,89	1,52	0,84	1,11
Dynamin-1-like protein	6	0,93	2,49	1,12	0,75
Inositol 1,4,5-trisphosphate receptor type 3	3	1,81	7,33	1,14	1,92
Coronin-7	4	0,85	2,20	0,84	1,23
Galectin-1	5	0,67	3,61	0,28	0,58
T-complex protein 1		1,03	3,00	0,95	0,86
Kinesin-like protein KIF23	4	0,52	3,14	0,48	1,02
Septin-10	3	0,49	3,91	0,43	0,76
Septin-2	14	1,10	3,49	0,83	1,08
Fermitin family homolog 2	16	0,90	4,65	0,90	1,14
Collagen alpha-1(XII) chain	4	1,53	3,13	0,95	1,15

Proteins identified in homo sapiens data base Exp 2	#Peptide Fragmentes detected	Clone 88 + IL1b	Clone 48 + IL1b	Clone 88 - IL1b	Clone 88 - IL1b
Annexin A5	10	1,73	13,09	0,89	1,13
Fascin	7	2,09	5,25	0,62	1,41
Vinculin	7	5,56	17,31	0,73	1,29
Annexin A6	7	3,97	9,58	0,50	1,14
Actin-related protein 2/3 complex subunit 2	3	2,81	5,03	0,72	1,23
Caldesmon	4	1,64	5,66	0,65	0,70
Protein NDRG1	3	4,59	8,43	0,76	0,71
Profilin-1	3	7,83	13,07	1,05	1,20
Galectin-1	4	0,78	2,11	1,21	1,28

8. DISCUSSION

The search for sensitive techniques to identify molecular changes occurring at the cellular level during the development of any disease has found limitations due to the molecular post-transcriptional and post-translational modifications, which in addition can be influenced by any environmental occurring event. This makes it difficult to determine the targets that are relevant in different stages of a human disease (**Reynolds et al., 2011**).

To overcome these problems phage display peptide ligands have been useful tools to screen for specific ligand-target interaction on an *in vitro* system or even on cellular cultures previously stimulated to induce environmental changes occurring during diseases, in comparison with healthy conditions (**Wang et al., 2010; Kitagawa et al., 2005**). However the results obtained from an *in vitro* screening on a cell culture can be affected by conditions of culture manipulation inducing the loss of protein expression, which are representative to obtain a good approximation about what is occurring in an *in vivo* system (**Smith et al., 2012**).

The development of *in vivo* phage display screening has allowed to improve the identification of phage peptide biomarkers for pathological conditions in a natural cellular system influenced by expression level and molecular behavior occurring in a tissue *in vivo* (**Pasqualini et al., 2002; Smith et al., 2012**).

Here we concentrated the work in the search of potential phage peptide biomarkers to BBB in EAE, an autoimmune and neuroinflammatory model of Multiple sclerosis.

8.1. *In vivo* phage display selection in EAE rats and HEALTHY rats

BBB is constituted by blood vessels and neighboring cells and is reinforced by the constitutive formation of TJs between the brain ECs that maintain the normal state of paracellular impermeability in the brain microvessels (**Abbott, 2005**). This barrier is highly restrictive to the passive transport of hydrophilic molecules and

infiltrating cells, which allow protecting the brain parenchyma from an autoimmune attack.

Therefore it has been important to screen by phage display selection, the molecular expression changes occurring in the brain ECs that can affect the stability of this barrier during EAE neuroinflammatory conditions.

The *in vivo* screening of phage displayed peptide ligands on the endothelial cell surface depends of their binding affinity to mimic the potential interaction of proteins with specific targets. The phage peptide affinity (kd) is determined for the displayed motif consensus, by which the phage peptides can recognize with high affinity a specific target in a nM range (**Fleming et al., 2005; Smith et al., 2012**).

In addition the concentration of phage peptides and targets are important to maintain a constant equilibrium of association. Indeed, the number of harvested phages decreases in the function of the competition with the mimicked ligand. In this case the phage concentration should be sufficiently high to obtain an efficient harvest (**Brockmann, 2010**).

Here we have show that the number of harvested phage peptides by mg of tissues, normally tends to increase with the repeated selection rounds which suggests enrichment of sequences with high target affinity (**Fig. 8**).

After phage harvest from tissues, the phage population diversity can be altered by bacterial phage amplification in which case some clones can be amplified with major predominance, favored by phage assembly into the bacterial machinery (**Steiner et al., 2006**).

Finally an altered inefficient or artificial over amplification can be mirrored in the presentation of some phage peptide clones hypothetically highly selected. In such circumstances we recognize the importance to test each individual phage peptide ligands selected with high occurrence by an *in vitro* and *in vivo* system.

8.2. Massive sequencing analysis of the EAE and HEALTHY phage repertoires

After massive sequencing analysis of each phage repertoire from the last selection round were obtained $1.29x10^6$ reads (EAE) and $1.29x10^6$ reads (HEALTHY). However, the number of different peptide sequences given for each repertoire (EAE: 13308 and Healthy: 44278) is lower than the sequence reads because there are 23 peptide sequences appearing redundantly between 1032 to 269855 times in the EAE selection and 238 peptide sequences appearing 1003 to 20251 in the Healthy one.

It is necessary to consider that a high occurrence of one peptide, for example, in order of 269855 times in EAE or other one 20251 times in Healthy may be the product of high target affinity and specificity of this peptide sequence, but it may also simply be artifacts.

For this reason to eliminate these problems after *in vivo* phage peptide selection from EAE and Healthy rats we have concentrated the work to enrich for EAE specific binders within the selected EAE phage peptide repertoire. We have developed a physical DNA subtraction of the most common sequences present in both EAE and Healthy page repertoires resulting in the Subtraction repertoire EAE minus Healthy.

8.3. DNA Subtraction analysis

NGS and bioinformatic analysis of the three repertoires revealed that the Subtraction repertoire is constituted of 4098 sequences in common with the EAE repertoire and that only 3 % of sequences that are present both in the EAE and healthy repertoires (422 sequences) remained in the subtraction repertoire. This indicates that the efficiency of subtraction was of 97 % to eliminate common peptides in the EAE and Healthy repertoires.

The 3 % corresponding to the peptide sequences from healthy selection that still remain after DNA subtraction is probably due to their relatively low concentration which influences their inability to hybridize with the common EAE

sequences and consequently they cannot be eliminated by Kpn-1 restriction enzyme hydrolysis.

On the other hand, peptides, which mimic proteins that are upregulated in EAE rats might also be eliminated from the final subtraction repertoire because they are also, expressed in the HEALTHY CNS, for example tight junctions proteins. Thereby after DNA subtraction the remaining phage repertoire corresponds to peptide ligands differentially specific or highly enriched in EAE repertoire.

8.4. EAE specific peptides selection.

From the given EAE peptide sequences we have chosen the 24 ones which are present with high occurrence in the EAE repertoire and also present in the Subtraction repertoire and 28 which are highly present in the Healthy repertoire, to be analyzed by their homology with a database of possible proteins mimicked in mouse, human, rats and mammals.

In parallel the complete given EAE and SUBTRACTION peptide repertoire sequences were also analyzed by SPACK analysis on the NCBI database of Mus musculus proteins. Thus the complete EAE and Healthy peptide sequences given were clustered by their sequence homology and then analyzed with SPACK bioinformatic tool on the NCBI database of Muss musculus proteins. **Based on http://services.cbib.u-bordeaux2.fr/spack/index.php**.

Thus, with SPACK analysis, it is possible to build group packs of peptides presenting significant homologies with some parts of a single protein. Then to obtain a superSPacks, consisting of homologous proteins (at least 2) with significant alignment with a set of said peptides. Finally to Score its findings according to the size of the Packs and the similarities to the identified proteins.

The advantage of SPACK analysis is to highlight the proteins which match with big packs of peptide mimics with high homology in the same region for a single protein and to score the homologous proteins that align with these packs of peptides by a specific region, which shows them as high potential biomarkers for specific conserved region maybe in the same family or sharing similar biological functions.

Moreover the SPACK analysis was performed with the peptide sequences in both senses (5'-3' and 3'-5'), which are represented as peptide (a-sense) or (b-antisense). The two orientations allow approximating the possible target-peptide ligand interaction, which is determined by the correct orientation of the molecules to allow the proximity necessary to set the hydrogen bonds or hydrophobic interactions.

Thus, from the list of peptides with high occurrence in EAE, SPACK showed homology with some members of the Mucin family, such as Mucin 1 (NGS-EAE-02a) (NGS-EAE-19), Mucin 4 (NGS-EAE-02b), and Mucin 15 (NGS-EAE-08).

Additionally adherent junction-associated protein 1 (NGS-EAE-02a, NGS-EAE-01b, NGS-EAE-19) and aquaporin 3 (NGS-EAE-06a, NGS-EAE-23a) were found with high occurrence in EAE.

However the proteins which present homology with a small pack of peptides in determined region, were discarded from the SPACK analysis even if the peptide presented a high homology. This is the case of Laminin subunit beta-1 (NGS-EAE-16), laminin alpha 5 isoform (NGS-EAE-01), solute carrier family 13 member 2 isoform b (NGS-EAE-02), Integrin beta-1 (NGS-EAE-19), mucin-6 NGS-EAE-07, mucin 17 (NGS-EAE-06), mucin 5b (NGS-EAE-05).

In addition, the fact that the SPACK analysis was made only on Mus musculus database due to its major similarity with human and rats has reduced also a great number of proteins which are found on the human and the rats date base for which groups of peptide present also homology. For example, Mucin 16: NGS-EAE-02, NGS-EAE-05, NGS-EAE-08, NGS-EAE-22 present high homology in Homo sapiens. Toll-like receptor 7: NGS-EAE-02 and NGS-EAE-19 have homology in rats.

These results showed a high occurrence of phage peptide ligands EAE specific sharing homology with some members of the Mucin family (1, 4, 5, 16, 17) and laminin α5 as possible mimicked proteins.

Mucins (MUCs) are members of a family of about 20 glycoproteins, which are classified as secreted (MUC2, MUC5AC, MUC5B, MUC6-8 and MUC19) or

membrane-bound (MUC1, MUC3, MUC4, MUC12-17 and MUC20) (**Senapati et al., 2009**). The post-translational modifications such as glycosylation, sialylation and sulfation facilitate their interaction with the extracellular and membrane bound proteins (**Godula and Bertozzi, 2012**).

Some members of mucin family have been shown to suppress inflammatory responses in EAE. For example $Muc1^{-/-}$ mice developed strong EAE severity with increased numbers of Th1 and Th17 cells infiltrating into the CNS and greater amounts of proinflammatory cytokines IL-1β, IL-6, and IL-12. This is attributable to Muc-1 deficiency in DC; in that case DC became more efficient to activate T cell proliferation and Th1/Th17 differentiation (**Yen et al., 2013**). Thus we can suggest that mucins upregulation by DCs during neuroinflammatory events could present a compensatory neuroprotective behavior.

In addition, it has been proposed that mucins can bind to TLR toll-like receptor (TLR) and mask the TLRs and also sequester the ligands, thus inhibiting the activation of downstream signalling pathways. However mucins can also interact with TLRs and ErbB2 leading the overexpression of proinflammatory cytokines **(Tarang et al., 2012).**

Several studies have shown TLR2, TLR3 and TLR4 may be expressed and active in the brain endothelial cells, being involved in pathological modulation. Despite brain endothelial cells have an important role to protect the CNS from immune cellular insult, thus it can be also involved in innate immune mechanisms of antigen activation.

In that case we can also propose that overexpression of mucins can be mediated by perivascular immune cell activation. Then mucins could upregulate the proinflammatory cytokines secretion and BBB permeability by directly interacting with TLRs or ErbB2 receptor.

Additionally Muc-1 upregulated in activated T-cells, lead the transendothelial transmigration by ligating to ICAM-I responding to chemokine mediated inflammation (**Rahn et al., 2005**).

Furthermore, it has been reported that in ECs CD146 also known as Melanoma cell adhesion molecule (MCAM) or mucin 18 is concentrated at the intercellular junctions controlling the paracellular permeability, monocyte transmigration and angiogenesis (**Jouve et al., 2013**).

The soluble form of mucin 18 (sCD146) has been reported to be present in various inflammatory diseases and displays pro-inflammatory properties. It is significantly elevated in the cerebro-spinal fluid of patients with active MS compared with that of inactive MS or patients with non-demyelinating diseases. Importantly, the level of CSF sCD146 is correlated with levels of inflammatory factors, such as TNFα, IFNγ, IL-2, and IL-17A in the CSF. It was also found that CSF sCD146 might originate from membrane-bound CD146 on inflamed blood–brain barrier (BBB) ECs. In addition, sCD146 promotes leukocyte transmigration *in vitro*, at least in part by stimulating the expression of ICAM-1 and VCAM-1 on ECs. Thus sCD146 was shown as a potential marker for monitoring disease activity in MS patients (**Duan et al., 2013**).

Laminins are a family of ECM glycoproteins and the major constituent of basement membranes. They have been implicated in cell adhesion, differentiation, and migration and signaling. Laminins are present in 16 isoforms composed of 3 chains: laminin alpha, beta and gamma. Several laminins have been shown to be expressed in the rodent brain in neurons and ACs, including α1 to 5, β1 to β3 and γ1. Laminin alpha 3 and 5 can be produced by PCs supporting the maintenance of BBB integrity (**Kruegel and Miosge, 2010**).

Laminins α4β1γ1 and α5β1γ1 are constitutively expressed in endothelial basement membranes at the CNS, however α4β1γ1 is upregulated during inflammatory events by immunomodulators cytokines. The T cell transmigration across brain endothelial cells is facilitated by Laminin α4β1γ1 (isoform 8), while is restricted by α5β1γ1 (isoform 10) (**Sixt et al., 2001**). Then the rolling of T cells on the endothelial cell surface is mainly integrin α4β1 mediated as a receptor of Laminin α4β1γ. Furthermore, it has been shown that laminin α4β1γ deficient (Lama4–/–) mice reduce the development of EAE and present upregulation of α5β1γ1. This is due to α5β1γ1 selective inhibition of integrin α4β1-T cell infiltration through laminin α4β1γ (**Wu et al., 2009**).

During EAE development, leukocytes arrive and concentrate in the perivascular space between the endothelial and parenchymal basement membranes. Once the T cells cross the brain endothelial basement membrane, they find laminin 1 and 2 isoforms expressed on the parenchymal basement membrane. Those isoforms are not adhered to T cells and the transmigration has to be mediated by proteolysis involving matrix metalloproteinases (MMPs) (**Wu et al., 2009**).

Laminin α5 is a major component of the ECM in brain vessels which maintains the interaction with ACs through members of the integrin family of ECM receptors. Some reports have shown that during CNS injury the breakdown of the blood brain barrier is associated with down or up regulation of laminin-5 and their corresponding interaction with the ACs (**Ji and Tsirka, 2012**).

8.5. Selection of EAE specific phage clones

Our research group has developed *in vivo* phage display selection since previous works using a phage library displaying peptide ligands of 7aa flanked by cysteine residues (C7C) that allows to form cyclized peptides.

From that previous selection phage clone (clone 48) was identified, which presents high affinity to neuroinflammatory lesions in EAE rats and also in IL-1β stimulated hCMEC/D3 BBB cells but not to healthy controls or *in vitro* BBB in resting state.

In the present project a new phage selection was performed on EAE rats by using a phage library displaying peptide ligands with 12aa. We chose this library system to enlarge the potential spectrum of peptide binders.

None of the peptide sequences selected with phages displaying 12aa peptides revealed similarities to that corresponding to phage peptide clone 48. However several peptide sequences of 12aa presented three amino acids conserved to clone 48 sequences, which is most probably not enough to set the same high EAE specificity given to the complete peptide sequence of the clone 48.

Once compared the peptide sequences of EAE and Subtraction repertoire we have selected 100 phage clones picked out randomly from each one. Then the clones were sequenced and searched by occurrence in each repertoire.

Only one clone (clone 88) was found with high occurrence in the EAE repertoire (600 times more present in EAE than in healthy) and also present in the Subtraction repertoire.

If one phage peptide sequence is present thousand of times in a repertoire compared with the thousands present in solution, the probability to pick it randomly with high occurrence is 0.1. It is the reason why the selection of EAE specific clones can be a wasteful work, which requires too much time to test thousands of clones to obtain potential candidates. This highlights the importance of our proposal to obtain EAE specific phage peptide sequences by DNA Subtraction of common sequences from healthy controls, which can be synthesized after reducing the number of candidates to test with a certain major specificity.

The clone 88 is represented by the sequence NGS-EAE-22. After blast analysis it presents homology with the Mucin 16 in Homo sapiens as well as NGS-EAE-02, NGS-EAE-05, NGS-EAE-08, NGS-EAE-22. In contrast, by SPACK analysis its homology is shown with SEC16 homolog A (which is described as an endoplasmic reticulum membrane protein).

Some others phage clones with low occurrence in EAE and not appearing in Subtraction repertoire, for example, clone 17, 44, 37, 78, 34 present sequence consensus which were already reported (**Kitagaw et al., 2005**). They have shown the potential homology of this sequence consensus with CD154, which plays an important role in the control of both humoral and cellular immunity in various autoimmune disorders, including multiple sclerosis.

The clone 88 was chosen for their high occurrence in both repertoires to be tested by binding in CNS tissues (EAE *vs* Healthy) and hCMEC/D3 ECs. The clone 88 has shown a high affinity to blood brain ECs activated *in vitro* by proinflammatory cytokines as IL-1β or in neuro-inflammatory conditions triggered for leukocyte infiltration which increase the production of more proinflammatory effectors *in vivo.*

Although we have not concluded approximations of protein candidates to be mimicked by the clone 88, it is possible, proposes Mucin 16 according to their specific region homology with this clone. However, there is not reported publications that show its direct relation with BBB.

8.6. Biological tests of EAE specific peptides

Four peptides with high occurrence in EAE and Subtraction repertoires were chosen to be synthesized and tested on hCMEC/D3 cells (IL-1β and VEGF stimulated *vs* controls). These peptides are represented with their possible mimicked proteins obtained by Blast and SPACK analysis as follows: NGS-EAE-05 (Mucin-16, Mucin-1, Mucin-5b, Disintegrin and metalloproteinase isoform, CMRF35-like molecule 9 and Urocortin-2), NGS-EAE-06 (Mucin 17, aquaporin 3), NGS-EAE-23 (Aquaporin-3, Toll-like receptor 4) and NGS-EAE-24 (ECM protein 2 precursor, IL-1 receptor accessory protein-like 1).

The four peptides are shown also to be potential binders to hCMEC/D3 cells (IL-1β and VEGF stimulated *vs* controls).

Despite that, these peptides are certainly better binders to recognize targets in inflammatory conditions in comparison with the control; this is a qualitative but not quantitative analysis of binding affinity.

Here we present the implications in neuroinflammation for some of the proteins that present high homology with the four peptides selected as EAE specific.

CMRF (CD300): These are immune receptors expressed by myeloid and lymphoid cells. It has been shown that knockout mice for CD300 exhibit an increased neuropathology in EAE, presenting a possible neuroprotective role an acute brain injury (**Peluffo et al., 2011**).

UROCORTIN-2: UCN belongs to the corticotrophin releasing hormone (CRH) family of peptides. The CRH-R1 and CRH-R2 receptors are expressed in brain neurons and glial cells involved in stress responses. More importantly, UCN is considered a powerful anti-inflammatory agent; it alleviates inflammation and

neurotoxicity mediated by endotoxin-activated microglia. *In vivo* studies have shown that, intracerebroventricular (ICV) treatment with UCN post-intracerebral hemorrhage reduces brain injury, brain edema, and BBB permeability (**Liew et al., 2010**).

The CRH-R1 and CRH-R2 receptors can be also expressed in brain ECs and in stress conditions can be activated in direct response to UCN, it led to cyclic adenosine monophosphate (cAMP) elevations and subsequent increased BBB permeability. In addition cAMP may active the (MAP) kinase pathway that results in the activation of NF**k** B, leading to transcription of pro-inflammatory cytokines (**Esposito et al., 2002**).

ADAMs (A Disintegrin and Metalloproteinase) are transmembrane proteins that bind to integrins and are important in cell adhesion. ADAMs have a catalytic domain at the end of the extracellular extension composed by a disintegrin domain that binds to integrins, a cysteine-rich region that interacts with proteoglycans. The cytoplasmic tail attached to the epidermal growth factor domain through the membrane. The catalytic region of the ADAMs molecules releases bound proteins from the ECM and cell surface. ADAMs have been implicated in cellular proliferation, migration, differentiation and survival **(Rosenberg, 2009).**

Other reports have shown that ADAMTS- 1, -4 and -5 proteases (A Disintegrin and Metalloproteinase with Thrombospondin motifs) are able to cleave the aggregating chondroitin sulphate proteoglycans, aggrecan, phosphacan, neurocan and brevican on ECM during CNS inflammation in EAE (**Cross et al., 2006**).

These proteins candidates are only approximations of proteins hypothetically mimicked by the peptides selected with High occurrence in EAE and Subtraction repertoire.

These approximations show the wide range proteins that can affect directly the barrier formed by brain ECs. These proteins can form part direct of the BM (Mucins and laminins) or can affect directly the cell adhesion between ECs (ADAMS). Besides some other proteins are upregulated in activated myeloid cells as a neuroprotective response during brain injury (CMRF). Finally the stress induced

during brain neuroinflammation can induce the liberation of hormonal mediators (Urocortin-2) that can affect directly the stability of the BBB.

8.7. Target identification for EAE specific peptides

We have applied a proteomic method based on phage display screening and crosslinking step in attempts to identify the targets of the phage peptide clones 88 and 48 binding to ECs. Using the hCMEC/D3 *in vitro* model of the BBB under IL-1β stimulation or resting conditions.

The first test to verify that the crosslink was working was by immunohistochemistry: in that case the results showed that the high phage concentration and cell stimulation increased the phage binding.

Then a second experiment was performed to identify the targets. Thus hCMEC/D3 cells (IL-1β stimulated *vs* controls) were cross-linked with the phage peptide clones and then the targets were harshly separated after several steps of membrane lysis and purification.

The SDS-PAGE gel electrophoresis of the proteins recovered from bound phage peptide clones (88, 48 and WT) presented no specific bands for each clone. This was also highlighted in the mass spectrometry analysis where many peptide fragments collected from each sample appeared, sharing homology with nuclear and cytoplasmic proteins. However, most of the protein fragments appearing for each sample presented more intensity in hCMEC/D3 cells IL-1β stimulated than not stimulated, which is also in agreement with the results obtained by immunohistochemistry. This allowed highlighting that the mass spectrometry analysis reinforces the argument of those phage clones (48 and 88) as potential binders in inflammatory conditions.

It is remarkable that the macromolecular dimensions of the M13 phages are 10 nm x 1 μm and hundreds of Sulfo- SBED crosslinkers can bind randomly along their entire length. The specific displayed peptide is located on the pIII protein at one of the ends of phage. It has been hypothesized that the phage could be crosslinked with the targets by any group of surface proteins previously labeled

along of the entire phage length, independently of the binding specificity of the displayed monomeric penta peptides.

However, Reynolds and coworkers have proposed the alternative scenario in which the phage particles bind perpendiculary to the cell surface. In such circumstances phages can only crosslink targets within few nanometers. Therefore, it is possible that the target protein is predominantly bound to the phage peptide displayed on the phage pIII protein. Supporting this scenario Reynolds and coworkers have also set the fact that the surfaces of both the phage particle and the cell are negatively charged. The electrostatic repulsion only favors the union between the peptide ligands with high affinity to the specific targets. In their experiments the results have shown that different phage clones crosslink to just one or a few surface proteins and these proteins differ from one clone to another (**Reynolds et al., 2011**).

When we have compared both experiments, two proteins appear as candidates to be recognized by the clone 48 during IL-1β stimulation of hCMEC/D3: Fascin and galectin-1. Although both proteins could be considered as potential targets of this clone, we have concentrated the discussion around the galectin-1 because of its expression on BBB surface and its possible function in cell-cell adhesion. In contrast, fascin protein is a protein with cytoplasmic localization under the plasma membrane, which makes it difficult to be bound to the phage clone.

It should be noted that the results obtained from mass spectrometry analysis have shown a big quantity of cytoplasmic proteins, nuclear proteins and submembrane proteins that technically could not be recognized by the phage clones in the experimental conditions. Whereby we have expected to find proteins targets cross-linked with the phages clones at extracellular surface. According with that most of the proteins found correspond to background obtained during proteins targets purification after cellular lysis.

Galectins are a family of carbohydrate-binding proteins; they contain a conserved carbohydrate recognition domain (CRD) to O or N-linked glycoproteins. These are secreted and active as monomers but some of them require dimerization

for biological function on cell surface (**Cedeno-Laurent and Dimitroff, 2012**; **Garner and Baum, 2008**).

In addition galectins can form lattices that cluster glycolipids or glycoproteins into lipid raft micro-domains. The formation of this micro-domains are involved in the transmission of signals relevant to cell function. Thus galectins are expressed and upregulated by all immune cells, and have a role as immunomodulators by inducing apoptosis of leukocytes. However, in some cases galectins act as proinflammatory enhancers mediated by T-cell activation, cytokine secretion, and neutrophil activation leading to phagocytosis (**Rabinovich et al., 2002**).

Thus, for example galectin -1 participates in acute and allergic inflammation and displays anti-inflammatory activities by blocking or attenuating signaling events that lead to leukocyte infiltration, migration, and recruitment (**Rabinovich et al., 2007**).

The galectins can be expressed by endothelial cells, and are found through the cell, in nucleus, cytoplasm and cell membrane. It enables galectins to regulate several cell functions. At the level of cell surface galectins participate in protein-protein interactions to mediate cell-cell interaction; galectin-1 is required for the attachment of endothelial cells. Thus are also involved in angiogenesis, by interaction with neuropilin-1 promoting signaling via VEGF receptor-2 and modulates endothelial cell (EC) migration (**D'Haene et al., 2013**).

Galectin-1 expression can be induced by several cytokines, including IL-1beta, IFNgamma and TNF-alpha, then galectin-1 is translocated to the outer cell membrane, what is identified as an early marker of endothelial cell activation (**Thijssen et al., 2008**). Galectin-1 on the endothelium surface has an inhibitory and anti-inflammatory effect on T-cell migration through the extracellular matrix (**He and Baum, 2006**).

Galectin-1 plays an anti-inflammatory role in EAE and early stages of MS, however it is also associated with pathogenesis in advanced stages of MS. Moreover it has been shown that the expression of galectins 1, 3, 8 and 9 is increased in MS on microglia/macrophages, endothelial cells and astrocytes (**Stancic et al., 2011**).

Here we have shown the high affinity of the phage clone 48 (EAE specific) on HMEC/D3 brain IL-1beta stimulated endothelial cells Then after target purification and mass spectrometry analysis, galectin-1 is presented as a possible target. However, according with structural and functional properties of the galectin-1, the interaction with phage clone 48 has to be mediated by a different region from the CRD motif, because each phage clone displays peptide ligands but not carbohydrates motifs recognize each specific target.

Nevertheless, it has been reported that galectin-3 and galectin-8 are also functional by interaction with not glycosylated proteins (**Li et al., 2013**). In addition hydrophobic amino acids bound to cytosolic galectin-1 bind to Ras-GTP, enhancing the induced extracellular signal pathway (**Rotblat et al., 2004**).

9. CONCLUSIONS

We have improved the EAE specific phage peptide selection by means of the development of a DNA subtraction between EAE minus Healthy, which presents a satisfactory efficiency of 97 %.

This has allowed to obtain an enriched list of EAE specific peptide sequences, from which we have synthesized four of them to be used as potential biomarkers in neuroinflammatory conditions. According to that the four peptides were that selected and tested are good binders of brain ECs activated with IL-1β or VEGF.

Although the assays for target identification of selected phage clones do not show strongly conclusive results, the differences of intensity between proteins appearing in mass spectrometry analysis to the hCMEC/D3 cells stimulated *vs* controls are congruent with the results obtained by immunohistochemistry.

Thus, it is important to highlight that the phage clone 88 selected in this project from EAE repertoire and Subtraction repertoire is a potential binder to brain ECs in neuroinflammatory conditions.

We have reached the goal of this project by getting the identification of some EAE specific peptide ligands that can be used a potential biomarkers for neuroinflammation.

10. PERSPECTIVES

The clones 48 and 88 have been identified as strong binders in neuroinflammatory conditions, which was already proved by *in vitro* assays. Thus, they should be chemically synthesized and then conjugated with magnetofluorescent nanoparticles or fluorocromes for testing by fluorescence microscopy their biological application as biomarkers *in vitro* on IL-1β stimulated HMEC/D3.

To allow *in vivo* monitoring of the peptides, focal brain acute inflammation could be induced in Lewis rats by injection of IL-1β into one side of the brain and then for a next step the peptides conjugated to MPIO or radiotracers could be administered by intravenous injection for subsequent MRI or SPECT analysis.

In addition, as neuroinflammatory processes are observed in other brain pathologies, these biomarkers should be tested *in vitro* and *in vivo* in other neuroinflammatory disease models, for example AD, PD or brain tumor.

In the next steps it will be necessary to continue the attempts to identify the targets for the phage clones and peptide ligands selected as a potential biomarkers. This experiment should be done again directly with peptides conjugated with biotin or any other linker, which enable these to be bound with Sulfo-SBED or streptavidin to improve the target separation and purification procedure. Then these will be identified by mass spectrometry.

Once the targets-peptides interaction will be confirmed, I propose to perform *in vitro* experiments on HMEC/D3 IL-1β stimulated, with the peptides synthesized from the clone 88 and 48 and the four peptides NGS-EAE-05, 06, 23 and 24 already selected as ~~a~~ potential biomarkers in neuroinflammation, where monoclonal antibodies will be directed against different supposed targets and different regions exposed to the cell surface for these targets. Thus, if that is the case the antibodies will compete with the peptides, to block peptide-target interactions, which probably will allow identifying the possible ligands proteins and peptide target-interaction.

Besides, it would be pertinent to develop *in vivo* assays in rats with IL-1β brain focal induced neuroinflammation, in which will be administered conjugated peptides-MPIO and control monoclonal antibodies-MPIO to block peptide-target interaction. Thus, it will confirm the peptide molecular specificity for the diagnosis of neuroinflammatory episodes. Then the peptides-MPIO could be applied for *in vivo* MRI detection in EAE rats.

On the other hand, considering the around 4000 peptide sequences potentially EAE specifics obtained from subtraction, and which were identified by bioinformatics analysis to mimic not only ligand proteins on endothelial cell surfaces, but even probably intracellular ligands, then it would be also pertinent for future studies to chemically synthesize additional selected candidates, with the perspective of applications in the diagnosis of neuroinflammatory conditions.

In addition to the peptides selected for their affinity with inflammatory lesions, we propose that “Healthy specific” peptides could also be of great interest. Indeed, in the EAE CNS, many regions do not show any detectable inflammation (what is described as "normal appearing white matter (NAWM)" in multiple sclerosis. When CNS was recovered during the EAE selection process, non-inflammatory tissue regions were also recovered and could be, in a first approximation, considered as Normal Appearing White Matter and Normal Appearing Grey Matter (NAGM). Therefore, if peptides that were efficiently selected in Healthy rat CNS and not in the EAE rat CNS are real binders of healthy tissue and not of the NAWM-like and NAGM-like tissues of EAE rats, these molecules could be very sensible imaging biomarkers to discard the hypothesis of a neuroinflammatory event.

Finally, in the future, once the targets of the selected peptide biomarkers will be identified, they could be applied in the field of drug carrier and delivery into the brain, and more specifically in inflammatory regions. Thus the high specificity of peptides ligands for targets, which can internalize the ligand, could ease the delivery of specific drug attached to the peptide-nanovector vehicle. Thereby these peptide ligands are promising for controlled and safety spatiotemporal drug delivery in the therapy of several brain neuroinflammatory diseases.

ANNEXES

1. Phage amplification

1.1. Solutions for phage amplification and purification

LB Medium:

Per liter: 10 g Bacto-Tryptone, 5 g yeast extract, 5 g NaCl. Autoclaved and stored at room temperature.

LB-Tet Plates:

LB medium + 15 g/L agar. Autoclaved and then cool to < 60°C, added 1/1000 of tetracycline stock and then pour in plates to use.

Tetracycline Stock:

20 mg/mL in ethanol. Stored at -20°C in the dark. And vortex before use.

LB/IPTG/Xgal Plates:

LB medium + 15 g/L agar. Autoclaved and then cool to < 60°C, added 1/1000 of IPTG/Xgal stock. Pour in the plates and stored at 4°C in the dark.

IPTG/Xgal:

Mix 1.25 g IPTG (isopropyl β-D-thiogalactoside) and 1 g Xgal (5-Bromo-4-chloro-3-indolyl-β-D-galactoside) in 25 mL dimethyl formamide. The solution can be stored at -20°C in the dark with a glass bottle.

Top Agarose:

Per liter: 10 g Bacto-Tryptone, 5 g yeast extract, 1 g $MgCl_2.6H_20$, 7 g agarose. Autoclaved and stored at room temperature, melted in microwave as needed.

TBS:

50 mM Tris-HCl (pH 7.5), 150 mM NaCl. Autoclaved and stored at room temperature.

PEG/NaCl:

20 % (w/v) polyethylene glycol-8000. 2.5 M NaCl. Autoclaved and stored at room temperature.

1.2. Petri dishes of bacteria ER2738

From the original vial of bacteria ER2738 stored at -70°C was taken an aliquot with a glass handle previously sterilized on fire. Then the bacteria were spread in four quadrants on the LB-Tet plates, and finally were incubated to grow at 37°C. The petri-dish was change each 3 weeks.

1.3. Bacteria ER2738 culture

Previously to infection and amplification of phages, one colony of the bacteria ER2738 was taken from the LB-Tet plates and put in 10mL of LB Broth medium to grow overnight. The next day a 1/100 dilution was made in LB Broth medium and grown for 2 h until the log growth phase was obtained ($O.D_{600nm}$ 0.5) to be used in phage infection.

1.4. Phage titration

3 mL of Top-Agarose previously melted and maintained to 48°C was mixed with 300 µL of Bacteria ER2738 culture at log growth phase ($O.D_{600nm}$ 0.5) and then the suspension was spread on the petri dishes with LB-agar/IPTG/Xgal and allowed to solidify.

Serial phage dilutions were prepared in TBS within 10^2 and 10^{12} and then spread as spots on the petri dish pre-cover with bacteria and incubated overnight at 37°C. The next day the number of colonies for each dilution was counted.

2. PCR

Master mix PCR (PROMEGA): Taq DNA polymerase, 400 µM dATP, 400 µM dGTP, 400 µM dCTP, 400 µM dTTP, 3 mM $MgCl_2$ and reaction buffer (pH 8.5). Stored in aliquots at -20°C.

Primers:
+18 pIII sequencing primer: 5'-TCGCAATTCCTTTAGTGGTA-3' (1 µM),
-28 pIII sequencing primer: 5'-GTATGGGATTTTGCTAAACAAC-3' (1 µM),
-96 pIII sequencing primer: 5'-CCCTCATAGTTAGCGTAACG-3' (1 µM)

2.1. PCR program:

Denaturation

2 minutes initial denaturation step at 95°C.

Subsequent denaturation steps 30 seconds.

Annealing

The annealing step at 55 °C, 30 seconds.

Extension

The extension reaction at 72°C 30 seconds

A final extension of 5 minutes at 72°C.

Refrigeration

Programmed to end by holding the tubes at 4°C for several hours.

Cycle Number

25–30 cycles.

Note:

The asymmetric PCR was performed during 50 cycles with the primers +18 (0,1 µM) and -28 (1 µM).

3. Subtraction

3.1. Phage DNA extractions

Iodide Buffer: 10 mM Tris-HCl (pH 8.0), 1 mM EDTA, 4 M NaI. Stored at RT in the dark.

3.2. Digestion

FastDigest KpnI (Thermo Scientific): KpnI (~800U) stored at -20°C

Buffer KpnI: 25 mM Tris-Acetate, pH 7.5, 100mM potassium acetate, 10mM magnesium acetate, 1 mM DTT.

5.2. Transformation

RapidTransit Kit (Sigma, R2653): RapidTransit Transformation Buffer, 2.5 mL

4. Immunostaining Solutions

PBS 10x:

1L solution stock pH 7.2: Na_2HPO_4: (141.9 g/mol), 11.36g, 0.08 M; KH_2PO_4: (136.08 g/mol), 2.27 g, 0.02 M; NaCl: (58.44 g/mol), 87.60 g, 1.5 M.

Tris-HCl: 0.05 M, pH 7.5

5. Human brain ECs culture hCMEC/D3

5.1. Preparation of petri dishes/flasks/labteck for cell culture

Collagen solution: 150 µg/ml

- 5 mL of collagen in flasks and petri dishes 100 mm and incubation 1h at 37ºC
- Add 200 µl of collagen in wells on lab-tek and incubation at 37ºC.

The non-attached collagen was removed by washing once with PBS 1x and 10 mL of growth medium was added.

5.2. Preparation of medium

To prepare complete medium	500mL
Fetal Calf serum 5%	25mL
Penicillin- streptomycin (1%)	5mL
Hydrocortisone* (1.4 μM)	250μL (2.8 mM)
Ascorbic Acid (5 μg/mL)	2.5mL (1 mg/mL)
Chemically defined lipid Concentrate (1/100)	5mL
HEPES (10 mM)	5mL (1 M)
bFGF* (1 ng/mL)	2.5mL (200 ng/mL)
EBM-2	To a final volume of 500mL

For each flask 10ml of medium were added.

*bFGF was added just before use, 50 µL/10 mL of medium

*To prepare hydrocortisone, it was dissolved in 1ml of absolute ethanol.

Note: The stimulation of hCMEC/D3 cells was performed with 20 ng/mL IL-1β (ImmunoTools 11340013).

6. Dot blot:

Non-denaturating lysis buffer: 50 mM Tris HCl pH 7.5, 150 mM NaCl, 1% Triton X-100, 5 mM EDTA containing protease inhibitors.

Protease Inhibitor (SIGMA): DMSO solution containing: AEBSF, 104 mM, Aprotinin, 80 µM, Bestatin, 4 mM, E-64, 1.4 mM, Leupeptin, 2 mM, Pepstatin A, 1.5 mM. 1:100 working dilution.

BCA protein assay (Thermo scientific): Colorimetric assay containing reagent A: Solution cupric with sodium-potassium tartrate and reagent B: Bincinchoninic acid solution (BCA). Measure with spectrophotometer at 562 nm. Linear working range of BSA equals 20 to 2000 µg/ml.

Hybond-C Extra membrane (Amersham, RPN137E): (137 mm), capacity of 80 to 100 µg/cm^2. The membrane was cut to 12 cm by 8 cm in each assay.

Solution of revelation: 4-chloro-1 naphtol stock solution 3 mg/mL in methanol and work solution: 1 mL of stock solution in 10 mL of PBS. Immediately before used, added 0.1 mL of 3% hydrogen peroxide.

Dot Blot apparatus: Sci-Plas's dot, DHM-96 - for 7.5 x 11.3cm, 96-well Dot Blot, http://www.alphametrix.de/electrophoresis/index.php?pageid=62.

7. Crosslinking

Sulfo-SBED: Crosslinker reagent (Thermo Scientific, ref 33073)

Tween 20: Sigma ref p22B7 0.1% was used as a gentle surfactant agent that don't affect protein activity and help in removing unbound moieties.

Glycine solution: 0.1M pH 2.5. Stored at 4°C before use.

TCEP: Reductor agent (Thermo Scientific, ref 20490), 50 mM. Stored at 4°C

Dynal M-280 (Invitrogen): Streptavidin magnetic beads in suspension, Iron content 12%, 2.8 µm, concentration 10 mg/mL.

DYNAL MPC-1(Invitrogen): The Dynal MPC-1 has been designed to hold one single tube with variable diameters (up to 30 mm) and volumes (5-50 mL).

Denaturating loading buffer: Tris-HCl 1 M pH 6.8, SDS 20%, glycerol, blue bromophenol.

BIBLIOGRAPHY

Abbott, N.J. (2005). Dynamics of CNS barriers: evolution, differentiation, and modulation. Cell. Mol. Neurobiol. *25*, 5–23.

Abbott, N.J., Rönnbäck, L., and Hansson, E. (2006). Astrocyte-endothelial interactions at the blood-brain barrier. Nat. Rev. Neurosci. *7*, 41–53.

Abbott, N.J., Patabendige, A.A.K., Dolman, D.E.M., Yusof, S.R., and Begley, D.J. (2010). Structure and function of the blood-brain barrier. Neurobiol. Dis. *37*, 13–25.

Agrawal, S., Anderson, P., Durbeej, M., van Rooijen, N., Ivars, F., Opdenakker, G., and Sorokin, L.M. (2006). Dystroglycan is selectively cleaved at the parenchymal basement membrane at sites of leukocyte extravasation in experimental autoimmune encephalomyelitis. J. Exp. Med. *203*, 1007–1019.

Alt, C., Laschinger, M., and Engelhardt, B. (2002). Functional expression of the lymphoid chemokines CCL19 (ELC) and CCL 21 (SLC) at the blood-brain barrier suggests their involvement in G-protein-dependent lymphocyte recruitment into the central nervous system during experimental autoimmune encephalomyelitis. Eur. J. Immunol. *32*, 2133–2144.

Arap, M.A. (2005). Phage display technology: applications and innovations. Genet. Mol. Biol. *28*, 1–9.

Armulik, A., Genové, G., Mäe, M., Nisancioglu, M.H., Wallgard, E., Niaudet, C., He, L., Norlin, J., Lindblom, P., Strittmatter, K., et al. (2010). Pericytes regulate the blood-brain barrier. Nature *468*, 557–561.

Bábíčková, J., Tóthová, Ľ., Boor, P., and Celec, P. (2013). *In vivo* phage display--a discovery tool in molecular biomedicine. Biotechnol. Adv. *31*, 1247–1259.

Barber, P.A. (2013). Magnetic resonance imaging of ischemia viability thresholds and the neurovascular unit. Sensors *13*, 6981–7003.

Bates, D.O., Cui, T.-G., Doughty, J.M., Winkler, M., Sugiono, M., Shields, J.D., Peat, D., Gillatt, D., and Harper, S.J. (2002). VEGF165b, an inhibitory splice variant

of vascular endothelial growth factor, is down-regulated in renal cell carcinoma. Cancer Res. *62*, 4123–4131.

Becher, B., Bechmann, I., and Greter, M. (2006). Antigen presentation in autoimmunity and CNS inflammation: how T lymphocytes recognize the brain. J. Mol. Med. Berl. Ger. *84*, 532–543.

Bechmann, I., Priller, J., Kovac, A., Böntert, M., Wehner, T., Klett, F.F., Bohsung, J., Stuschke, M., Dirnagl, U., and Nitsch, R. (2001). Immune surveillance of mouse brain perivascular spaces by blood-borne macrophages. Eur. J. Neurosci. *14*, 1651–1658.

Blamire, A.M., Anthony, D.C., Rajagopalan, B., Sibson, N.R., Perry, V.H., and Styles, P. (2000). Interleukin-1beta -induced changes in blood-brain barrier permeability, apparent diffusion coefficient, and cerebral blood volume in the rat brain: a magnetic resonance study. J. Neurosci. Off. J. Soc. Neurosci. *20*, 8153–8159.

Bomprezzi, R., Schafer, R., Reese, V., Misra, A., Vollmer, T.L., and Kala, M. (2011). Glatiramer acetate-specific antibody titres in patients with relapsing/remitting multiple sclerosis and in experimental autoimmune encephalomyelitis. Scand. J. Immunol. *74*, 219–226.

Borst, P., and Elferink, R.O. (2002). Mammalian ABC transporters in health and disease. Annu. Rev. Biochem. *71*, 537–592.

Brockmann, E.-C. (2010). Evolution of Bioaffinity Reagents by Phage Display.

Brucklacher-Waldert, V., Stuerner, K., Kolster, M., Wolthausen, J., and Tolosa, E. (2009). Phenotypical and functional characterization of T helper 17 cells in multiple sclerosis. Brain J. Neurol. *132*, 3329–3341.

Carman, C.V., and Springer, T.A. (2008). Trans-cellular migration: cell-cell contacts get intimate. Curr. Opin. Cell Biol. *20*, 533–540.

Cedeno-Laurent, F., and Dimitroff, C.J. (2012). Galectin-1 research in T cell immunity: past, present and future. Clin. Immunol. Orlando Fla *142*, 107–116.

Charil, A., and Filippi, M. (2007). Inflammatory demyelination and neurodegeneration in early multiple sclerosis. J. Neurol. Sci. *259*, 7–15.

Chen, Y., and Liu, L. (2012). Modern methods for delivery of drugs across the blood-brain barrier. Adv. Drug Deliv. Rev. *64*, 640–665.

Clarkson, B.D., Héninger, E., Harris, M.G., Lee, J., Sandor, M., and Fabry, Z. (2012). Innate-adaptive crosstalk: how dendritic cells shape immune responses in the CNS. Adv. Exp. Med. Biol. *946*, 309–333.

Cross, A.K., Haddock, G., Surr, J., Plumb, J., Bunning, R.A.D., Buttle, D.J., and Woodroofe, M.N. (2006). Differential expression of ADAMTS-1, -4, -5 and TIMP-3 in rat spinal cord at different stages of acute experimental autoimmune encephalomyelitis. J. Autoimmun. *26*, 16–23.

Croxford, A.L., Kurschus, F.C., and Waisman, A. (2011). Mouse models for multiple sclerosis: historical facts and future implications. Biochim. Biophys. Acta *1812*, 177–183.

Cucullo, L., Couraud, P.-O., Weksler, B., Romero, I.-A., Hossain, M., Rapp, E., and Janigro, D. (2008). Immortalized human brain endothelial cells and flow-based vascular modeling: a marriage of convenience for rational neurovascular studies. J. Cereb. Blood Flow Metab. Off. J. Int. Soc. Cereb. Blood Flow Metab. *28*, 312–328.

D'Haene, N., Sauvage, S., Maris, C., Adanja, I., Le Mercier, M., Decaestecker, C., Baum, L., and Salmon, I. (2013). VEGFR1 and VEGFR2 involvement in extracellular galectin-1- and galectin-3-induced angiogenesis. PloS One *8*, e67029.

Dalkara, T., Gursoy-Ozdemir, Y., and Yemisci, M. (2011). Brain microvascular pericytes in health and disease. Acta Neuropathol. (Berl.) *122*, 1–9.

Daneman, R., Zhou, L., Kebede, A.A., and Barres, B.A. (2010). Pericytes are required for blood-brain barrier integrity during embryogenesis. Nature *468*, 562–566.

Dean, M., Rzhetsky, A., and Allikmets, R. (2001). The human ATP-binding cassette (ABC) transporter superfamily. Genome Res. *11*, 1156–1166.

Deloire, M.S.A., Touil, T., Brochet, B., Dousset, V., Caillé, J.-M., and Petry, K.G. (2004). Macrophage brain infiltration in experimental autoimmune encephalomyelitis is not completely compromised by suppressed T-cell invasion: in vivo magnetic resonance imaging illustration in effective anti-VLA-4 antibody treatment. Mult. Scler. Houndmills Basingstoke Engl. *10*, 540–548.

Dheen, S.T., Kaur, C., and Ling, E.-A. (2007). Microglial activation and its implications in the brain diseases. Curr. Med. Chem. *14*, 1189–1197.

Dijkhuizen, R.M. (2011). Advances in MRI-Based Detection of Cerebrovascular Changes after Experimental Traumatic Brain Injury. Transl. Stroke Res. *2*, 524–532.

Dore-Duffy, P., and Cleary, K. (2011). Morphology and properties of pericytes. Methods Mol. Biol. Clifton NJ *686*, 49–68.

Dousset, V., Brochet, B., Deloire, M.S.A., Lagoarde, L., Barroso, B., Caille, J.-M., and Petry, K.G. (2006). MR imaging of relapsing multiple sclerosis patients using ultra-small-particle iron oxide and compared with gadolinium. AJNR Am. J. Neuroradiol. *27*, 1000–1005.

Drin, G., Rousselle, C., Scherrmann, J.-M., Rees, A.R., and Temsamani, J. (2002). Peptide delivery to the brain via adsorptive-mediated endocytosis: advances with SynB vectors. AAPS PharmSci *4*, E26.

Duan, H., Luo, Y., Hao, H., Feng, L., Zhang, Y., Lu, D., Xing, S., Feng, J., Yang, D., Song, L., et al. (2013). Soluble CD146 in cerebrospinal fluid of active multiple sclerosis. Neuroscience *235*, 16–26.

Ebnet, K., Aurrand-Lions, M., Kuhn, A., Kiefer, F., Butz, S., Zander, K., Meyer zu Brickwedde, M.-K., Suzuki, A., Imhof, B.A., and Vestweber, D. (2003). The junctional adhesion molecule (JAM) family members JAM-2 and JAM-3 associate with the cell polarity protein PAR-3: a possible role for JAMs in endothelial cell polarity. J. Cell Sci. *116*, 3879–3891.

El-behi, M., Rostami, A., and Ciric, B. (2010). Current views on the roles of Th1 and Th17 cells in experimental autoimmune encephalomyelitis. J. Neuroimmune Pharmacol. Off. J. Soc. NeuroImmune Pharmacol. *5*, 189–197.

Engelhardt, B. (2011). β1-integrin/matrix interactions support blood-brain barrier integrity. J. Cereb. Blood Flow Metab. Off. J. Int. Soc. Cereb. Blood Flow Metab. *31*, 1969–1971.

Engelhardt, B., and Coisne, C. (2011). Fluids and barriers of the CNS establish immune privilege by confining immune surveillance to a two-walled castle moat surrounding the CNS castle. Fluids Barriers CNS *8*, 4.

Engelhardt, B., and Ransohoff, R.M. (2012). Capture, crawl, cross: the T cell code to breach the blood-brain barriers. Trends Immunol. *33*, 579–589.

Engelhardt, B., and Sorokin, L. (2009). The blood-brain and the blood-cerebrospinal fluid barriers: function and dysfunction. Semin. Immunopathol. *31*, 497–511.

Engelhardt, B., and Wolburg, H. (2004). Mini-review: Transendothelial migration of leukocytes: through the front door or around the side of the house? Eur. J. Immunol. *34*, 2955–2963.

Esposito, P., Chandler, N., Kandere, K., Basu, S., Jacobson, S., Connolly, R., Tutor, D., and Theoharides, T.C. (2002). Corticotropin-releasing hormone and brain mast cells regulate blood-brain-barrier permeability induced by acute stress. J. Pharmacol. Exp. Ther. *303*, 1061–1066.

Fabriek, B.O., Van Haastert, E.S., Galea, I., Polfliet, M.M.J., Döpp, E.D., Van Den Heuvel, M.M., Van Den Berg, T.K., De Groot, C.J.A., Van Der Valk, P., and Dijkstra, C.D. (2005). CD163-positive perivascular macrophages in the human CNS express molecules for antigen recognition and presentation. Glia *51*, 297–305.

Fasler-Kan, E., Suenderhauf, C., Barteneva, N., Poller, B., Gygax, D., and Huwyler, J. (2010). Cytokine signaling in the human brain capillary endothelial cell line hCMEC/D3. Brain Res. *1354*, 15–22.

Faulkner, J.R., Herrmann, J.E., Woo, M.J., Tansey, K.E., Doan, N.B., and Sofroniew, M.V. (2004). Reactive astrocytes protect tissue and preserve function after spinal cord injury. J. Neurosci. Off. J. Soc. Neurosci. *24*, 2143–2155.

Fleming, T.J., Sachdeva, M., Delic, M., Beltzer, J., Wescott, C.R., Devlin, M., Lander, R.C., Nixon, A.E., Roschke, V., Hilbert, D.M., et al. (2005). Discovery of

high-affinity peptide binders to BLyS by phage display. J. Mol. Recognit. JMR *18*, 94–102.

Floris, S., Blezer, E.L.A., Schreibelt, G., Döpp, E., van der Pol, S.M.A., Schadee-Eestermans, I.L., Nicolay, K., Dijkstra, C.D., and de Vries, H.E. (2004). Blood-brain barrier permeability and monocyte infiltration in experimental allergic encephalomyelitis: a quantitative MRI study. Brain J. Neurol. *127*, 616–627.

Fujimori, J., Nakashima, I., Fujihara, K., Misu, T., Sato, S., and Itoyama, Y. (2011). Epitope analysis of cerebrospinal fluid IgG in Japanese multiple sclerosis patients using phage display method. Mult. Scler. Int. *2011*, 353417.

Gao, B., Hagenbuch, B., Kullak-Ublick, G.A., Benke, D., Aguzzi, A., and Meier, P.J. (2000). Organic anion-transporting polypeptides mediate transport of opioid peptides across blood-brain barrier. J. Pharmacol. Exp. Ther. *294*, 73–79.

Garner, O.B., and Baum, L.G. (2008). Galectin-glycan lattices regulate cell-surface glycoprotein organization and signalling. Biochem. Soc. Trans. *36*, 1472–1477.

Geurts, J.J.G., Bö, L., Roosendaal, S.D., Hazes, T., Daniëls, R., Barkhof, F., Witter, M.P., Huitinga, I., and van der Valk, P. (2007). Extensive hippocampal demyelination in multiple sclerosis. J. Neuropathol. Exp. Neurol. *66*, 819–827.

Godula, K., and Bertozzi, C.R. (2012). Density variant glycan microarray for evaluating cross-linking of mucin-like glycoconjugates by lectins. J. Am. Chem. Soc. *134*, 15732–15742.

Gordon, G.R.J., Mulligan, S.J., and MacVicar, B.A. (2007). Astrocyte control of the cerebrovasculature. Glia *55*, 1214–1221.

Greenwood, J., Heasman, S.J., Alvarez, J.I., Prat, A., Lyck, R., and Engelhardt, B. (2011). Review: leucocyte-endothelial cell crosstalk at the blood-brain barrier: a prerequisite for successful immune cell entry to the brain. Neuropathol. Appl. Neurobiol. *37*, 24–39.

Greter, M., Heppner, F.L., Lemos, M.P., Odermatt, B.M., Goebels, N., Laufer, T., Noelle, R.J., and Becher, B. (2005). Dendritic cells permit immune invasion of the CNS in an animal model of multiple sclerosis. Nat. Med. *11*, 328–334.

Gumbleton, M., Abulrob, A.G., and Campbell, L. (2000). Caveolae: an alternative membrane transport compartment. Pharm. Res. *17*, 1035–1048.

Hanisch, U.-K., and Kettenmann, H. (2007). Microglia: active sensor and versatile effector cells in the normal and pathologic brain. Nat. Neurosci. *10*, 1387–1394.

Harkness, K.A., Sussman, J.D., Davies-Jones, G.A.B., Greenwood, J., and Woodroofe, M.N. (2003). Cytokine regulation of MCP-1 expression in brain and retinal microvascular endothelial cells. J. Neuroimmunol. *142*, 1–9.

He, J., and Baum, L.G. (2006). Endothelial cell expression of galectin-1 induced by prostate cancer cells inhibits T-cell transendothelial migration. Lab. Investig. J. Tech. Methods Pathol. *86*, 578–590.

Hediger, M.A., Romero, M.F., Peng, J.-B., Rolfs, A., Takanaga, H., and Bruford, E.A. (2004). The ABCs of solute carriers: physiological, pathological and therapeutic implications of human membrane transport proteinsIntroduction. Pflüg. Arch. Eur. J. Physiol. *447*, 465–468.

Heyn, C., Ronald, J.A., Ramadan, S.S., Snir, J.A., Barry, A.M., MacKenzie, L.T., Mikulis, D.J., Palmieri, D., Bronder, J.L., Steeg, P.S., et al. (2006). *In vivo* MRI of cancer cell fate at the single-cell level in a mouse model of breast cancer metastasis to the brain. Magn. Reson. Med. Off. J. Soc. Magn. Reson. Med. Soc. Magn. Reson. Med. *56*, 1001–1010.

Hossann, M., Wang, T., Syunyaeva, Z., Wiggenhorn, M., Zengerle, A., Issels, R.D., Reiser, M., Lindner, L.H., and Peller, M. (2013). Non-ionic Gd-based MRI contrast agents are optimal for encapsulation into phosphatidyldiglycerol-based thermosensitive liposomes. J. Control. Release Off. J. Control. Release Soc. *166*, 22–29.

Huber, J.D., Egleton, R.D., and Davis, T.P. (2001). Molecular physiology and pathophysiology of tight junctions in the blood-brain barrier. Trends Neurosci. *24*, 719–725.

Iadecola, C., and Nedergaard, M. (2007). Glial regulation of the cerebral microvasculature. Nat. Neurosci. *10*, 1369–1376.

Ifergan, I., Kébir, H., Bernard, M., Wosik, K., Dodelet-Devillers, A., Cayrol, R., Arbour, N., and Prat, A. (2008). The blood-brain barrier induces differentiation of migrating monocytes into Th17-polarizing dendritic cells. Brain J. Neurol. *131*, 785–799.

Inglese, M. (2006). Multiple sclerosis: new insights and trends. AJNR Am. J. Neuroradiol. *27*, 954–957.

Inglis, H.R., Greer, J.M., and McCombe, P.A. (2012). Gene expression in the spinal cord in female lewis rats with experimental autoimmune encephalomyelitis induced with myelin basic protein. PloS One *7*, e48555.

Jadidi-Niaragh, F., and Mirshafiey, A. (2011). Th17 cell, the new player of neuroinflammatory process in multiple sclerosis. Scand. J. Immunol. *74*, 1–13.

Ji, K., and Tsirka, S.E. (2012). Inflammation modulates expression of laminin in the central nervous system following ischemic injury. J. Neuroinflammation *9*, 159.

Jodoin, J., Demeule, M., Fenart, L., Cecchelli, R., Farmer, S., Linton, K.J., Higgins, C.F., and Béliveau, R. (2003). P-glycoprotein in blood-brain barrier endothelial cells: interaction and oligomerization with caveolins. J. Neurochem. *87*, 1010–1023.

Jouve, N., Despoix, N., Espeli, M., Gauthier, L., Cypowyj, S., Fallague, K., Schiff, C., Dignat-George, F., Vély, F., and Leroyer, A.S. (2013). The involvement of CD146 and its novel ligand Galectin-1 in apoptotic regulation of endothelial cells. J. Biol. Chem. *288*, 2571–2579.

Karlsson, F. (2004). The biology of filamentous phage infection - implications for display technology.

Karman, J., Chu, H.H., Co, D.O., Seroogy, C.M., Sandor, M., and Fabry, Z. (2006). Dendritic cells amplify T cell-mediated immune responses in the central nervous system. J. Immunol. Baltim. Md 1950 *177*, 7750–7760.

Kelly, K.A., Allport, J.R., Tsourkas, A., Shinde-Patil, V.R., Josephson, L., and Weissleder, R. (2005). Detection of vascular adhesion molecule-1 expression using a novel multimodal nanoparticle. Circ. Res. *96*, 327–336.

Kierdorf, K., and Prinz, M. (2013). Factors regulating microglia activation. Front. Cell. Neurosci. *7*, 44.

Kim, M.-H., and Hersh, L.B. (2004). The vesicular acetylcholine transporter interacts with clathrin-associated adaptor complexes AP-1 and AP-2. J. Biol. Chem. *279*, 12580–12587.

Kitagawa, M., Goto, D., Mamura, M., Matsumoto, I., Ito, S., Tsutsumi, A., and Sumida, T. (2005). Identification of three novel peptides that inhibit CD40-CD154 interaction. Mod. Rheumatol. Jpn. Rheum. Assoc. *15*, 423–426.

Kivisäkk, P., Imitola, J., Rasmussen, S., Elyaman, W., Zhu, B., Ransohoff, R.M., and Khoury, S.J. (2009). Localizing central nervous system immune surveillance: meningeal antigen-presenting cells activate T cells during experimental autoimmune encephalomyelitis. Ann. Neurol. *65*, 457–469.

Kleine, T.O., and Benes, L. (2006). Immune surveillance of the human central nervous system (CNS): different migration pathways of immune cells through the blood-brain barrier and blood-cerebrospinal fluid barrier in healthy persons. Cytom. Part J. Int. Soc. Anal. Cytol. *69*, 147–151.

Koffie, R.M., Farrar, C.T., Saidi, L.-J., William, C.M., Hyman, B.T., and Spires-Jones, T.L. (2011). Nanoparticles enhance brain delivery of blood-brain barrier-impermeable probes for in vivo optical and magnetic resonance imaging. Proc. Natl. Acad. Sci. U. S. A. *108*, 18837–18842.

Konsman, J.P., Drukarch, B., and Van Dam, A.-M. (2007). (Peri)vascular production and action of pro-inflammatory cytokines in brain pathology. Clin. Sci. Lond. Engl. 1979 *112*, 1–25.

Kruegel, J., and Miosge, N. (2010). Basement membrane components are key players in specialized extracellular matrices. Cell. Mol. Life Sci. CMLS *67*, 2879–2895.

Krueger, M., and Bechmann, I. (2010). CNS pericytes: concepts, misconceptions, and a way out. Glia *58*, 1–10.

Kurkowska-Jastrzębska, I., Swiątkiewicz, M., Zaremba, M., Cudna, A., Piechal, A., Pyrzanowska, J., Widy-Tyszkiewicz, E., and Członkowska, A. (2013). Neurodegeneration and inflammation in hippocampus in experimental autoimmune encephalomyelitis induced in rats by one--time administration of encephalitogenic T cells. Neuroscience *248*, 690–698.

Kusuhara, H., and Sugiyama, Y. (2005). Active efflux across the blood-brain barrier: role of the solute carrier family. NeuroRx J. Am. Soc. Exp. Neurother. *2*, 73–85.

Kutzelnigg, A., Lucchinetti, C.F., Stadelmann, C., Brück, W., Rauschka, H., Bergmann, M., Schmidbauer, M., Parisi, J.E., and Lassmann, H. (2005). Cortical demyelination and diffuse white matter injury in multiple sclerosis. Brain J. Neurol. *128*, 2705–2712.

Kutzelnigg, A., Faber-Rod, J.C., Bauer, J., Lucchinetti, C.F., Sorensen, P.S., Laursen, H., Stadelmann, C., Brück, W., Rauschka, H., Schmidbauer, M., et al. (2007). Widespread demyelination in the cerebellar cortex in multiple sclerosis. Brain Pathol. Zurich Switz. *17*, 38–44.

Ley, K., Laudanna, C., Cybulsky, M.I., and Nourshargh, S. (2007). Getting to the site of inflammation: the leukocyte adhesion cascade updated. Nat. Rev. Immunol. *7*, 678–689.

Li, S., Wandel, M.P., Li, F., Liu, Z., He, C., Wu, J., Shi, Y., and Randow, F. (2013). Sterical hindrance promotes selectivity of the autophagy cargo receptor NDP52 for the danger receptor galectin-8 in antibacterial autophagy. Sci. Signal. *6*, ra9.

Liebner, S., Czupalla, C.J., and Wolburg, H. (2011). Current concepts of blood-brain barrier development. Int. J. Dev. Biol. *55*, 467–476.

Liew, H.-K., Pang, C.-Y., Hsu, C.-W., Wang, M.-J., Li, T.-Y., Peng, H.-F., Kuo, J.-S., and Wang, J.-Y. (2012). Systemic administration of urocortin after intracerebral hemorrhage reduces neurological deficits and neuroinflammation in rats. J. Neuroinflammation *9*, 13.

Linnartz, B., and Neumann, H. (2013). Microglial activatory (immunoreceptor tyrosine-based activation motif)- and inhibitory (immunoreceptor tyrosine-based

inhibition motif)-signaling receptors for recognition of the neuronal glycocalyx. Glia *61*, 37–46.

Loeffler, C., Dietz, K., Schleich, A., Schlaszus, H., Stoll, M., Meyermann, R., and Mittelbronn, M. (2011). Immune surveillance of the normal human CNS takes place in dependence of the locoregional blood-brain barrier configuration and is mainly performed by CD3(+)/CD8(+) lymphocytes. Neuropathol. Off. J. Jpn. Soc. Neuropathol. *31*, 230–238.

Löscher, W., and Potschka, H. (2005). Blood-brain barrier active efflux transporters: ATP-binding cassette gene family. NeuroRx J. Am. Soc. Exp. Neurother. *2*, 86–98.

Lossinsky, A.S., and Shivers, R.R. (2004). Structural pathways for macromolecular and cellular transport across the blood-brain barrier during inflammatory conditions. Review. Histol. Histopathol. *19*, 535–564.

Luissint, A.-C., Artus, C., Glacial, F., Ganeshamoorthy, K., and Couraud, P.-O. (2012). Tight junctions at the blood brain barrier: physiological architecture and disease-associated dysregulation. Fluids Barriers CNS *9*, 23.

McAteer, M.A., and Choudhury, R.P. (2013). Targeted molecular imaging of vascular inflammation in cardiovascular disease using nano- and micro-sized agents. Vascul. Pharmacol. *58*, 31–38.

McAteer, M.A., Sibson, N.R., von Zur Muhlen, C., Schneider, J.E., Lowe, A.S., Warrick, N., Channon, K.M., Anthony, D.C., and Choudhury, R.P. (2007). *In vivo* magnetic resonance imaging of acute brain inflammation using microparticles of iron oxide. Nat. Med. *13*, 1253–1258.

McAteer, M.A., Schneider, J.E., Ali, Z.A., Warrick, N., Bursill, C.A., von zur Muhlen, C., Greaves, D.R., Neubauer, S., Channon, K.M., and Choudhury, R.P. (2008). Magnetic resonance imaging of endothelial adhesion molecules in mouse atherosclerosis using dual-targeted microparticles of iron oxide. Arterioscler. Thromb. Vasc. Biol. *28*, 77–83.

McAteer, M.A., von Zur Muhlen, C., Anthony, D.C., Sibson, N.R., and Choudhury, R.P. (2011). Magnetic resonance imaging of brain inflammation using microparticles of iron oxide. Methods Mol. Biol. Clifton NJ *680*, 103–115.

Miller, S.D., McMahon, E.J., Schreiner, B., and Bailey, S.L. (2007). Antigen presentation in the CNS by myeloid dendritic cells drives progression of relapsing experimental autoimmune encephalomyelitis. Ann. N. Y. Acad. Sci. *1103*, 179–191.

Modo, M., Hoehn, M., and Bulte, J.W.M. (2005). Cellular MR imaging. Mol. Imaging *4*, 143–164.

Murakami, T., Felinski, E.A., and Antonetti, D.A. (2009). Occludin phosphorylation and ubiquitination regulate tight junction trafficking and vascular endothelial growth factor-induced permeability. J. Biol. Chem. *284*, 21036–21046.

Myer, D.J., Gurkoff, G.G., Lee, S.M., Hovda, D.A., and Sofroniew, M.V. (2006). Essential protective roles of reactive astrocytes in traumatic brain injury. Brain J. Neurol. *129*, 2761–2772.

Neumann, J., Sauerzweig, S., Rönicke, R., Gunzer, F., Dinkel, K., Ullrich, O., Gunzer, M., and Reymann, K.G. (2008). Microglia cells protect neurons by direct engulfment of invading neutrophil granulocytes: a new mechanism of CNS immune privilege. J. Neurosci. Off. J. Soc. Neurosci. *28*, 5965–5975.

Neuwelt, E., Abbott, N.J., Abrey, L., Banks, W.A., Blakley, B., Davis, T., Engelhardt, B., Grammas, P., Nedergaard, M., Nutt, J., et al. (2008). Strategies to advance translational research into brain barriers. Lancet Neurol. *7*, 84–96.

Nicole Hildebrandt, D.H. Superparamagnetic iron oxide nanoparticles functionalized with peptides by electrostatic interactions. ARKIVOC *2007*.

Nies, A.T. (2007). The role of membrane transporters in drug delivery to brain tumors. Cancer Lett. *254*, 11–29.

Nitta, T., Hata, M., Gotoh, S., Seo, Y., Sasaki, H., Hashimoto, N., Furuse, M., and Tsukita, S. (2003). Size-selective loosening of the blood-brain barrier in claudin-5-deficient mice. J. Cell Biol. *161*, 653–660.

Nowacka, M.M., and Obuchowicz, E. (2012). Vascular endothelial growth factor (VEGF) and its role in the central nervous system: a new element in the neurotrophic hypothesis of antidepressant drug action. Neuropeptides *46*, 1–10.

Ohtsuki, S., Sato, S., Yamaguchi, H., Kamoi, M., Asashima, T., and Terasaki, T. (2007). Exogenous expression of claudin-5 induces barrier properties in cultured rat brain capillary endothelial cells. J. Cell. Physiol. *210*, 81–86.

Osada, T., Gu, Y.-H., Kanazawa, M., Tsubota, Y., Hawkins, B.T., Spatz, M., Milner, R., and del Zoppo, G.J. (2011). Interendothelial claudin-5 expression depends on cerebral endothelial cell-matrix adhesion by β(1)-integrins. J. Cereb. Blood Flow Metab. Off. J. Int. Soc. Cereb. Blood Flow Metab. *31*, 1972–1985.

Parkinson, F.E., Damaraju, V.L., Graham, K., Yao, S.Y.M., Baldwin, S.A., Cass, C.E., and Young, J.D. (2011). Molecular biology of nucleoside transporters and their distributions and functions in the brain. Curr. Top. Med. Chem. *11*, 948–972.

Pasqualini, R., and Ruoslahti, E. (1996). Organ targeting *in vivo* using phage display peptide libraries. Nature *380*, 364–366.

Pasqualini, R., Arap, W., and McDonald, D.M. (2002). Probing the structural and molecular diversity of tumor vasculature. Trends Mol. Med. *8*, 563–571.

Peluffo, H., Alí-Ruiz, D., Ejarque-Ortíz, A., Heras-Alvarez, V., Comas-Casellas, E., Martínez-Barriocanal, A., Kamaid, A., Alvarez-Errico, D., Negro, M.L., Lago, N., et al. (2012). Overexpression of the immunoreceptor CD300f has a neuroprotective role in a model of acute brain injury. Brain Pathol. Zurich Switz. *22*, 318–328.

Petry, K.G., Boiziau, C., Dousset, V., and Brochet, B. (2007). Magnetic resonance imaging of human brain macrophage infiltration. Neurother. J. Am. Soc. Exp. Neurother. *4*, 434–442.

Pierson, E., Simmons, S.B., Castelli, L., and Goverman, J.M. (2012). Mechanisms regulating regional localization of inflammation during CNS autoimmunity. Immunol. Rev. *248*, 205–215.

Rabinovich, G.A., Rubinstein, N., and Toscano, M.A. (2002). Role of galectins in inflammatory and immunomodulatory processes. Biochim. Biophys. Acta *1572*, 274–284.

Rabinovich, G.A., Toscano, M.A., Jackson, S.S., and Vasta, G.R. (2007). Functions of cell surface galectin-glycoprotein lattices. Curr. Opin. Struct. Biol. *17*, 513–520.

Rahn, J.J., Chow, J.W., Horne, G.J., Mah, B.K., Emerman, J.T., Hoffman, P., and Hugh, J.C. (2005). MUC1 mediates transendothelial migration *in vitro* by ligating endothelial cell ICAM-1. Clin. Exp. Metastasis *22*, 475–483.

Ransohoff, R.M., and Perry, V.H. (2009). Microglial physiology: unique stimuli, specialized responses. Annu. Rev. Immunol. *27*, 119–145.

Reynolds, F., Panneer, N., Tutino, C.M., Wu, M., Skrabal, W.R., Moskaluk, C., and Kelly, K.A. (2011). A functional proteomic method for biomarker discovery. PloS One *6*, e22471.

Roberts, J., Kahle, M.P., and Bix, G.J. (2012). Perlecan and the blood-brain barrier: beneficial proteolysis? Front. Pharmacol. *3*, 155.

Romo-González, T., Chavarría, A., and Pérez-H, J. (2012). Central nervous system: a modified immune surveillance circuit? Brain. Behav. Immun. *26*, 823–829.

Van Rooy, I., Cakir-Tascioglu, S., Couraud, P.-O., Romero, I.A., Weksler, B., Storm, G., Hennink, W.E., Schiffelers, R.M., and Mastrobattista, E. (2010). Identification of peptide ligands for targeting to the blood-brain barrier. Pharm. Res. *27*, 673–682.

Rosenberg, G.A. (2009). Matrix metalloproteinases and their multiple roles in neurodegenerative diseases. Lancet Neurol. *8*, 205–216.

Rotblat, B., Niv, H., André, S., Kaltner, H., Gabius, H.-J., and Kloog, Y. (2004). Galectin-1(L11A) predicted from a computed galectin-1 farnesyl-binding pocket selectively inhibits Ras-GTP. Cancer Res. *64*, 3112–3118.

Saijo, K., and Glass, C.K. (2011). Microglial cell origin and phenotypes in health and disease. Nat. Rev. Immunol. *11*, 775–787.

Salmaggi, A., Gelati, M., Dufour, A., Corsini, E., Pagano, S., Baccalini, R., Ferrero, E., Scabini, S., Silei, V., Ciusani, E., et al. (2002). Expression and modulation of IFN-gamma-inducible chemokines (IP-10, Mig, and I-TAC) in human brain endothelium and astrocytes: possible relevance for the immune invasion of the central nervous system and the pathogenesis of multiple sclerosis. J. Interferon Cytokine Res. Off. J. Int. Soc. Interferon Cytokine Res. *22*, 631–640.

Sathe, P., Pooley, J., Vremec, D., Mintern, J., Jin, J.-O., Wu, L., Kwak, J.-Y., Villadangos, J.A., and Shortman, K. (2011). The acquisition of antigen cross-presentation function by newly formed dendritic cells. J. Immunol. Baltim. Md 1950 *186*, 5184–5192.

Schinkel, A.H., and Jonker, J.W. (2003). Mammalian drug efflux transporters of the ATP binding cassette (ABC) family: an overview. Adv. Drug Deliv. Rev. *55*, 3–29.

Scott, J.K., and Smith, G.P. (1990). Searching for peptide ligands with an epitope library. Science *249*, 386–390.

Senapati, S., Das, S., and Batra, S.K. (2010). Mucin-interacting proteins: from function to therapeutics. Trends Biochem. Sci. *35*, 236–245.

Serres, S., Mardiguian, S., Campbell, S.J., McAteer, M.A., Akhtar, A., Krapitchev, A., Choudhury, R.P., Anthony, D.C., and Sibson, N.R. (2011). VCAM-1-targeted magnetic resonance imaging reveals subclinical disease in a mouse model of multiple sclerosis. FASEB J. Off. Publ. Fed. Am. Soc. Exp. Biol. *25*, 4415–4422.

Shapiro, E.M., Skrtic, S., and Koretsky, A.P. (2005). Sizing it up: cellular MRI using micron-sized iron oxide particles. Magn. Reson. Med. Off. J. Soc. Magn. Reson. Med. Soc. Magn. Reson. Med. *53*, 329–338.

Shibata, M., Yamada, S., Kumar, S.R., Calero, M., Bading, J., Frangione, B., Holtzman, D.M., Miller, C.A., Strickland, D.K., Ghiso, J., et al. (2000). Clearance of Alzheimer's amyloid-ss(1-40) peptide from brain by LDL receptor-related protein-1 at the blood-brain barrier. J. Clin. Invest. *106*, 1489–1499.

Shin, T., Ahn, M., and Matsumoto, Y. (2012). Mechanism of experimental autoimmune encephalomyelitis in Lewis rats: recent insights from macrophages. Anat. Cell Biol. *45*, 141–148.

Sicotte, N.L. (2011). Neuroimaging in multiple sclerosis: neurotherapeutic implications. Neurother. J. Am. Soc. Exp. Neurother. *8*, 54–62.

Sixt, M., Engelhardt, B., Pausch, F., Hallmann, R., Wendler, O., and Sorokin, L.M. (2001). Endothelial cell laminin isoforms, laminins 8 and 10, play decisive roles in T

cell recruitment across the blood-brain barrier in experimental autoimmune encephalomyelitis. J. Cell Biol. *153*, 933–946.

Smith, M.W., Al-Jayyoussi, G., and Gumbleton, M. (2012). Peptide sequences mediating tropism to intact blood-brain barrier: an *in vivo* biodistribution study using phage display. Peptides *38*, 172–180.

Sofroniew, M.V., and Vinters, H.V. (2010). Astrocytes: biology and pathology. Acta Neuropathol. (Berl.) *119*, 7–35.

Stancic, M., van Horssen, J., Thijssen, V.L., Gabius, H.-J., van der Valk, P., Hoekstra, D., and Baron, W. (2011). Increased expression of distinct galectins in multiple sclerosis lesions. Neuropathol. Appl. Neurobiol. *37*, 654–671.

Steiner, D., Forrer, P., Stumpp, M.T., and Plückthun, A. (2006). Signal sequences directing cotranslational translocation expand the range of proteins amenable to phage display. Nat. Biotechnol. *24*, 823–831.

Steiner, O., Coisne, C., Cecchelli, R., Boscacci, R., Deutsch, U., Engelhardt, B., and Lyck, R. (2010). Differential roles for endothelial ICAM-1, ICAM-2, and VCAM-1 in shear-resistant T cell arrest, polarization, and directed crawling on blood-brain barrier endothelium. J. Immunol. Baltim. Md 1950 *185*, 4846–4855.

Stepaniak, J.A., Gould, K.E., Sun, D., and Swanborg, R.H. (1995). A comparative study of experimental autoimmune encephalomyelitis in Lewis and DA rats. J. Immunol. Baltim. Md 1950 *155*, 2762–2769.

Stoll, G., and Bendszus, M. (2009). Imaging of inflammation in the peripheral and central nervous system by magnetic resonance imaging. Neuroscience *158*, 1151–1160.

Stoll, G., and Bendszus, M. (2010). New approaches to neuroimaging of central nervous system inflammation. Curr. Opin. Neurol. *23*, 282–286.

Stosic-Grujicic, S., Ramic, Z., Bumbasirevic, V., Harhaji, L., and Mostarica-Stojkovic, M. (2004). Induction of experimental autoimmune encephalomyelitis in Dark Agouti rats without adjuvant. Clin. Exp. Immunol. *136*, 49–55.

Strecker, J.-K., Minnerup, J., Schütte-Nütgen, K., Gess, B., Schäbitz, W.-R., and Schilling, M. (2013). Monocyte chemoattractant protein-1-deficiency results in altered blood-brain barrier breakdown after experimental stroke. Stroke J. Cereb. Circ. *44*, 2536–2544.

Tang, Z., Gan, Y., Liu, Q., Yin, J.-X., Liu, Q., Shi, J., and Shi, F.-D. (2014). CX3CR1 deficiency suppresses activation and neurotoxicity of microglia/macrophage in experimental ischemic stroke. J. Neuroinflammation *11*, 26.

Tarang, S., Kumar, S., and Batra, S.K. (2012). Mucins and toll-like receptors: kith and kin in infection and cancer. Cancer Lett. *321*, 110–119.

Thijssen, V.L., Hulsmans, S., and Griffioen, A.W. (2008). The galectin profile of the endothelium: altered expression and localization in activated and tumor endothelial cells. Am. J. Pathol. *172*, 545–553.

Tipps, M.E., Lawshe, J.E., Ellington, A.D., and Mihic, S.J. (2010). Identification of novel specific allosteric modulators of the glycine receptor using phage display. J. Biol. Chem. *285*, 22840–22845.

Traub, L.M. (2003). Sorting it out: AP-2 and alternate clathrin adaptors in endocytic cargo selection. J. Cell Biol. *163*, 203–208.

Vellinga, M.M., Oude Engberink, R.D., Seewann, A., Pouwels, P.J.W., Wattjes, M.P., van der Pol, S.M.A., Pering, C., Polman, C.H., de Vries, H.E., Geurts, J.J.G., et al. (2008). Pluriformity of inflammation in multiple sclerosis shown by ultra-small iron oxide particle enhancement. Brain J. Neurol. *131*, 800–807.

Virgintino, D., Robertson, D., Errede, M., Benagiano, V., Tauer, U., Roncali, L., and Bertossi, M. (2002). Expression of caveolin-1 in human brain microvessels. Neuroscience *115*, 145–152.

Wang, K., Purushotham, S., Lee, J.-Y., Na, M.-H., Park, H., Oh, S.-J., Park, R.-W., Park, J.Y., Lee, E., Cho, B.C., et al. (2010). *In vivo* imaging of tumor apoptosis using histone H1-targeting peptide. J. Control. Release Off. J. Control. Release Soc. *148*, 283–291.

Weksler, B., Romero, I.A., and Couraud, P.-O. (2013). The hCMEC/D3 cell line as a model of the human blood brain barrier. Fluids Barriers CNS *10*, 16.

Weksler, B.B., Subileau, E.A., Perrière, N., Charneau, P., Holloway, K., Leveque, M., Tricoire-Leignel, H., Nicotra, A., Bourdoulous, S., Turowski, P., et al. (2005). Blood-brain barrier-specific properties of a human adult brain endothelial cell line. FASEB J. Off. Publ. Fed. Am. Soc. Exp. Biol. *19*, 1872–1874.

Winkler, E.A., Bell, R.D., and Zlokovic, B.V. (2011). Central nervous system pericytes in health and disease. Nat. Neurosci. *14*, 1398–1405.

Wolburg, H., and Lippoldt, A. (2002). Tight junctions of the blood-brain barrier: development, composition and regulation. Vascul. Pharmacol. *38*, 323–337.

Wolburg, H., Wolburg-Buchholz, K., Fallier-Becker, P., Noell, S., and Mack, A.F. (2011). Structure and functions of aquaporin-4-based orthogonal arrays of particles. Int. Rev. Cell Mol. Biol. *287*, 1–41.

Wong, H.L., Wu, X.Y., and Bendayan, R. (2012). Nanotechnological advances for the delivery of CNS therapeutics. Adv. Drug Deliv. Rev. *64*, 686–700.

Wu, C., Ivars, F., Anderson, P., Hallmann, R., Vestweber, D., Nilsson, P., Robenek, H., Tryggvason, K., Song, J., Korpos, E., et al. (2009). Endothelial basement membrane laminin alpha5 selectively inhibits T lymphocyte extravasation into the brain. Nat. Med. *15*, 519–527.

Xiao, G., and Gan, L.-S. (2013). Receptor-mediated endocytosis and brain delivery of therapeutic biologics. Int. J. Cell Biol. *2013*, 703545.

Yang, Y., Yang, Y., Yanasak, N., Schumacher, A., and Hu, T.C.-C. (2010). Temporal and noninvasive monitoring of inflammatory-cell infiltration to myocardial infarction sites using micrometer-sized iron oxide particles. Magn. Reson. Med. Off. J. Soc. Magn. Reson. Med. Soc. Magn. Reson. Med. *63*, 33–40.

Ye, Q., Wu, Y.L., Foley, L.M., Hitchens, T.K., Eytan, D.F., Shirwan, H., and Ho, C. (2008). Longitudinal tracking of recipient macrophages in a rat chronic cardiac allograft rejection model with noninvasive magnetic resonance imaging using micrometer-sized paramagnetic iron oxide particles. Circulation *118*, 149–156.

Yen, J.-H., Xu, S., Park, Y.S., Ganea, D., and Kim, K.C. (2013). Higher susceptibility to experimental autoimmune encephalomyelitis in Muc1-deficient mice is associated with increased Th1/Th17 responses. Brain. Behav. Immun. *29*, 70–81.

Yurchenco, P.D., and Patton, B.L. (2009). Developmental and pathogenic mechanisms of basement membrane assembly. Curr. Pharm. Des. *15*, 1277–1294.

Zaharchuk, G. (2007). Theoretical basis of hemodynamic MR imaging techniques to measure cerebral blood volume, cerebral blood flow, and permeability. AJNR Am. J. Neuroradiol. *28*, 1850–1858.

Zheng, H., Jiang, Y., Wang, J., Gong, X., and Guo, B. (2011). Mimic peptides bonding specifically with the first and second extracellular loops of the CC chemokine receptor 5 derived from a phage display peptide library are potent inhibitors of experimental autoimmune encephalomyelitis. Inflamm. Res. Off. J. Eur. Histamine Res. Soc. Al *60*, 759–767.

Zhou, C., Kang, J., Wang, X., Nie, M., and Jiang, W. (2013). [Screening of short peptides that bind specifically to ovarian cancer cell line through whole-cell subtraction biopanning]. Xi Bao Yu Fen Zi Mian Yi Xue Za Zhi Chin. J. Cell. Mol. Immunol. *29*, 1098–1101.

Zlokovic, B.V. (2008). The blood-brain barrier in health and chronic neurodegenerative disorders. Neuron *57*, 178–201.

Del Zoppo, G.J., Milner, R., Mabuchi, T., Hung, S., Wang, X., and Koziol, J.A. (2006). Vascular matrix adhesion and the blood-brain barrier. Biochem. Soc. Trans. *34*, 1261–1266.

Zozulya, A.L., Clarkson, B.D., Ortler, S., Fabry, Z., and Wiendl, H. (2010). The role of dendritic cells in CNS autoimmunity. J. Mol. Med. Berl. Ger. *88*, 535–544.